Tensile Strength and Performance of the INDUO®-Heavy-Timber Connector in Combination with Structural Composite Lumber and Douglas Fir

by

MARKUS STEINIGER

Diplom-Ingenieur (FH) *Holzbau und Ausbau,* [B.A.Sc.]
Fachhochschule Rosenheim, 2001

A thesis submitted in partial fulfillment of the
requirements for the degree of

Master of Science

in

FACULTY OF GRADUATE STUDIES
Department of Wood Science

We accept this thesis as conforming to the
required standard

THE UNIVERSITY OF BRITISH COLUMBIA

July, 2003

© Markus Steiniger, 2003

In presenting this thesis in partial fulfilment of the requirements for an advanced degree at the University of British Columbia, I agree that the Library shall make it freely available for reference and study. I further agree that permission for extensive copying of this thesis for scholarly purposes may be granted by the head of my department or by his or her representatives. It is understood that copying or publication of this thesis for financial gain shall not be allowed without my written permission.

Department of WOOD SCIENCE

The University of British Columbia
Vancouver, Canada

Date 7/7/2003

DE-6 (2/88)

Abstract

The INDUO-connection is a new steel-to-wood joint for highly loaded heavy-timber structures. Embedded in the end-grain of laminated timber beams, the special INDUO-connector is designed to transfer axial and transverse loads. Due to the weaker strength properties of solid wood perpendicular to the grain direction, the connection's capacity under transverse loading is comparatively small. Parallel to the grain, however, the connection is capable to transfer loads of up to 180kN and is thus predominantly suited for tension applications. Since the introduction to the European market in the Mid-90s, the INDUO-connection system has been mainly deployed in Post-and-Beam structures using softwood timber and Glulam as beam material.

This thesis investigates the tensile strength and performance of the INDUO-connector in combination with different beam materials. Static tension tests were performed in two separate test series with a total of 99 specimens of different member cross-sections (100x100mm and 120x120mm), connector types (A and B) and beam materials (Microllam®LVL, Parallam®PSL, TimberStrand®LSL, thick Douglas-Fir plywood and Douglas-Fir lumber).

In test series 1 all possible combinations of beam material, connector type and member cross-section were tested with a sample size of up to three, providing trends on strength properties and failure performance. For test series 2 it was decided to focus on fewer combinations with a larger sample size to create statistically more significant results on ultimate tensile strength and connection stiffness for the most advantageous setups.

By modeling and calculating the INDUO-connection according to different international timber codes (German DIN1052-2000, European EC5, Canadian CSA 086.1 and US ASCE 16-95) as a bolted or tight-fitting dowel connection, characteristic tensile strength data was computed and compared with the characteristic values derived from the results of series 2.

In terms of tensile strength and performance, TimberStrand®LSL presented the best test results, outperforming Microllam®LVL, Parallam®PSL and Douglas-Fir lumber, which showed significantly lower tensile strengths accompanied by brittle failure modes. Thick Douglas-Fir plywood was only examined in test series 1, presenting high tensile strength for larger beam-cross-sections, whereas smaller cross-sections failed brittely.

The comparison of different design approaches for the INDUO-connection showed that based on the same connection model (dowel-type fasteners with inside steel plate) the Canadian timber code provided by far the most conservative design values, whereas all other codes presented significantly higher numbers relative to the Canadian code . The comparison of characteristic tensile strength properties generated from the test results and values derived from the different design strengths indicate all four timber codes have more or less similar results.

Table of Contents

Abstract ii

Table of Contents iv

List of Figures vii

List of Tables xi

Dedication xii

Acknowledgements xiii

1 Introduction 1

1.1 Research Objective 5

1.2 Scope 6

2 Non-visible heavy-timber joints 7

2.1 Non-visible mechanical connections 7

2.1.1 The BSB-system (Tight-fitting dowels) 7

2.1.2 The SpikeTec-system (Embedded nail plate) 9

2.2 Non-visible composite connections 10

2.2.1 Glued-in steel rods 11

2.2.2 The TiSCo®-system 14

2.2.3 The BVD®-system 15

3 Materials and Methods 19

3.1 Materials 19

3.1.1 Microllam®LVL 19

3.1.2 Parallam®PSL 21

3.1.3 TimberStrand®LSL 23

3.1.4 Douglas-Fir plywood 24

3.1.5 Douglas-Fir lumber 26

3.1.6 INDUO-connector (type A) 27

3.1.7 INDUO-connector (type B) 28

3.2 Methods 29
3.2.1 Scope of the test series 29
3.2.2 Connection design 31
3.2.3 Fabrication of test specimens 34
3.2.4 Experimental setup 37
3.2.5 Test procedure 39

4 Results 40
4.1 Test series I 41
4.1.1 Group I (TimberStrand®LSL & Douglas-Fir plywood) 43
4.1.2 Group II (Douglas Fir & Microllam®LVL) 47
4.1.3 Group III (Parallam® PSL) 50
4.2 Test series II 52
4.2.1 Performance 54
4.2.1.1 TimberStrand®LSL 54
4.2.1.2 Douglas Fir 56
4.2.1.3 Parallam®PSL 58
4.2.1.4 Microllam®LVL 60
4.2.2 Strength and stiffness 62

5 Discussion 68
5.1 Evaluation of test results 68
5.2 Comparison of characteristic strength values 71
5.2.1 Connection Model 71
5.2.2 Determination of code design values 72
5.2.2.1 DIN 1052-2000 (draft) 75
5.2.2.2 EC5 (Eurocode 5) 76
5.2.2.3 CSA 086.1 77
5.2.2.4 ASCE 16-95 78
5.2.3 Characteristic strength values 79

5.3 Evaluation of connection stiffness with structural model 83

6 Conclusion and Recommendations 86

7 List of References 88

8 Appendices 92

8.1 Photographic documentation 92

8.1.1 Manufacturing steps of test specimen 92

8.1.2 Test procedure 95

8.1.3 Failure modes 100

8.2 Calculations 110

List of Figures

Figure 1: Plan of connection 2
Figures 2 & 3: Assembly of a single-family house constructed with the INDUO-system 2
Figure 4: 3-dimensional roof truss 3
Figure 5: INDUO-system applied in 3-dimensional truss system 3
Figure 6: INDUO-connector and timber halves before assembly 3
Figure 7: Embedded connector; beam ready to be pressed in hydraulic press 3
Figure 8: INDUO-connector type A 4
Figure 9: INDUO-connector type B 4
Figure 10: Manufacture of INDUO-Quarter Logs 4
Figure 11: BSB-joints in heavy timber truss 8
Figure 12: Scheme of BSB-connection 8
Figure 13: BSB-system applied in a roof structure of a spa 8
Figure 14: Footbridge constructed with BSB-connection 8
Figure 15: Close-up of SpikeTec-connection 9
Figure 16: Nail plates are set in place 9
Figure 15: SpikeTec-system applied in the roof structure of a supermarket 10
Figure 16: Roof truss system constructed with SpikeTec-connection 10
Figure 17: Glued-in steel rod connection (Madsen) 12
Figure 18: Applications for glued-in steel rod connections (Madsen) 12
Figure 19: Research conducted on glued-in steel rod connections 13
Figure 20: Sketch of test specimens (before grouting) 13
Figure 21: TiSCo-connector: Sandblasted and grooved version 14
Figure 22: TiSCo-connector inserted in end grain 14
Figure 23: Manufacturing steps of the TiSCo-connection 15
Figure 24a: Components of the BVD-system 16
Figure 24b: Different hanger sizes in various length configuration 16
Figure 25: Manufacturing the BVD-connection 16
Figure 26: Knee joint with BVD-connection 17
Figure 27: Tower column with BVD-connection to foundation 18
Figure 28: EXPO-Roof with towers supporting the roof structure 18
Figure 29: Manufacture of LVL 20
Figure 30: Close-up of LVL 20
Figure 31: Manufacture of PSL 21
Figure 32: Close-up of PSL 22
Figure 33: PSL applied in heavy-timber structure (Forestry building, UBC) 22

Figure 34: Manufacture of LSL 23
Figure 35: Close-up of LSL 24
Figure 36: Manufacture of plywood 25
Figure 37: Close-up of thick Douglas Fir plywood 25
Figure 38: Close-up of Douglas Fir 26
Figure 39: Manufacture of sawn lumber 26
Figure 40: Connector type A 27
Figure 41: Connector type B 28
Figure 42: Components of lower support 33
Figure 43: Lower support assembled 33
Figure 44: Ring Side Plate 33
Figure 45: Upper support 34
Figure 46: Plan of timber halves:
a) type A –100 combination; b) type A – 120 combination 36
Figure 47: Plan of timber halves:
a) type B –100 combination, screw-bond; b) type B – 120 combination 36
Figure 48: Experimental setup: MTS 810 with control system and test member 37
Figure 49: Test member 38
Figure 50: Upper support featuring a DCDT measuring device 38
Figure 51: Connection failure modes 40
Figure 52: Group I: No failure for connector type B combinations 43
Figure 53: Group I: Severe bearing; a typical failure mode for connector type A combinations 43
Figure 54: Load-displacement curves of TB-combinations 45
Figure 55: Load-displacement curves of TA-combinations 45
Figure 56: Load-displacement curves of XB-combinations 46
Figure 57: Load-displacement curves of XA-combinations 46
Figure 58: Group II: Splitting along the rows of holes; a typical failure mechanism of connector type B combinations 47
Figure 59: Group II: Bearing and relatively large displacements due to shear failure of connector type A combinations 47
Figure 60: Load-displacement curves of DB-combinations 48
Figure 61: Load-displacement curves of DA-combinations 48
Figure 62: Load-displacement curves of MB-combinations 49
Figure 63: Load-displacement curves of MA-combinations 49
Figure 64: Group III: Bearing and tear-out of connector type A combinations 50
Figure 65: Group III: Connector type B combinations witness severe pin deformations or fracture 50
Figure 66: Load-displacement curves of PB-combinations 51

Figure 67: Load-displacement curves of PA-combinations 51
Figure 68: LSL: No damage observed at the pin holes 54
Figure 69: LSL: No deformations of the connector 54
Figure 70: Load-displacement curves of TB-combinations 55
Figure 71: Load-displacement curves of S-TB-combinations 55
Figure 72: DG fir: Splitting along rows of holes 56
Figure 73: DG fir: Shear failure in the plane of the pins 56
Figure 74: Load-displacement curves of DB-combinations 57
Figure 75: Load-displacement curves of S-DB-combinations 57
Figure 76: PSL: Splitting along the rows of holes 58
Figure 77: PSL: Deformation of the connector pins 58
Figure 78: Load-displacement curves of PB-combinations 59
Figure 79: Load-displacement curves of S-PB-combinations 59
Figure 80: LVL: Splitting along rows of holes 60
Figure 81: LVL: Ripped-off pins 60
Figure 82: Load-displacement curves of MB-combinations 60
Figure 83: Load-displacement curves of S-MB-combinations 61
Figure 84: Different approaches to determine the connection stiffness 63
Figure 85: Classification of member setups according to tensile performance 69
Figure 86: Close-up of end grain: a) PSL; b) LVL; c) Douglas Fir; d) LSL 70
Figure 87: Connection model 71
Figure 88: Plan of connection 73
Figure 89: Failure modes according to European Yield Model 74
Figure 90: Different test procedures to determine the embedding strength of wood and wood-based material; a), DIN EN 383-1993 b) ASTM D5764a-1997 80
Figure 91: Thalkirchen Bridge, Munich, Germany 83
Figure 92: Support with node and connected beams 83
Figure 93: Node in the truss system 83
Figure 94: Connection setup of INDUO-connector in 3D-space truss beam 84
Figure 95: Cutting timber members to rough dimensions (Sliding Table Saw) 92
Figure 96: Planing of timber members to final width and thickness (4-Sided Planer) 92
Figure 97: Machining of rows of holes and V-groove by means of CNC-router 92
Figure 98: Machining of circular grooves (CNC-router) 92
Figure 99: INDUO-connector ready to be embedded in machined timber halves 93
Figure 100: Circular grooves to accommodate Steel Side Plates 93
Figure 101: Applying PVA-construction glue to both inside faces of the timber halves 93
Figure 102: Inserting the connector in V-groove 93
Figure 103: Joining of both timber halves enclosing the connector 94

Figure 104: Inserting the composite member into hydraulic press; Pressing time: 30 minutes 94
Figure 105: Alternative connection of timber halves with regular wood-screws 6x10 94
Figure 106: Setup of screws 94
Figure 107: Tapering of the test member to squared cross-section 100x100 and 120x120mm respectively (NC-shaper) 94
Figure 108: Specimen ready to be tested 95
Figure 109: Stacked members of different connector-material setups before testing 95
Figure 110: Specimen connected to upper machine support 95
Figure 111: Steel Side Plates transfer applied load from the lower machine support to test member 95
Figure 112: Assembly of Steel Side Plates with 7/8-inch bolts 96
Figure 113: Close-up of steel rings sliding into circular groove 96
Figure 114: Steel Side Plates are pressed into grooves by means of regular clamps 96
Figure 115: Components of lower coupling: Distance plates and two 1-inch bolts 96
Figure 116: Lower coupling fastened 97
Figure 117: Specimen connected to test apparatus, ready to be tested 97
Figure 118: Test apparatus consisting of test machine, control unit and PC 98
Figure 119: Unloading of heavy test member by means of a "mobile gallow" 98
Figure 120: Gallow in place to support the test member after being uncoupled 98
Figure 121: Disassembling of upper and lower couplings 98
Figure 122: Tested type A and B specimens, 120x120mm, test series 1 99
Figure 123: Tested type A and B specimens, 100x100mm, test series 1 99
Figure 124: Tested connector-type-B specimens, 100x100mm, test series 2 99
Figures125a-e: No failure observed with TB-member setups 100
Figures126a-b: Failure modes observed with TA-member setups 101
Figures 127a-f: Failure modes observed with XB-member setups 102
Figures 128a-c: Failure modes observed with XA-member setups 103
Figures 129a-g: Failure modes observed with DB-member setups 104
Figures 130a-c: Failure modes observed with DA-member setups 105
Figures 131a-g: Failure modes observed with MB-member setups 106
Figures 132a-d: Failure modes observed with MA-member setups 107
Figures 133a-f: Failure modes observed with PB-member setups 108
Figures 134a-c: Failure modes observed with PA-member setups 109

List of Tables

Table 1: Test variables 29
Table 2: Moisture content and density of tested specimens 40
Table 3: Analyzed data of test series 1 41
Table 4: Analyzed data of test series 2 52
Table 5: Statistics on ultimate load 62
Table 6: Statistics on displacement at ultimate load 62
Table 7: Statistics on different 10/40- and 30/70-connection stiffness 64
Table 8: 5th percentile strengths of respective distributions 66
Table 9: Characteristic values of maximum tensile capacity 67
Table 10: 5th percentile of 10/40-stiffness 67
Table 11: 5th percentile of 30/70-stiffness 67
Table 12: Example showing a step-by-step approach to determine characteristic values for tensile capacity 81
Table 13: Comparison of characteristic connection strength values 81
Table 14: Calculation example on stiffness and displacement of INDUO-connector in 3D-truss beam 85
Table 15: RELAN data fitting of strength data set 110
Table 16: RELAN data fitting of stiffness data set 110
Table 17: Calculation of characteristic strength values; PSL 111
Table 18: Calculation of characteristic strength values; Douglas Fir 112
Table 19: Calculation of characteristic strength values; LVL 113
Table 20: Calculation of characteristic strength values; LSL 114

dedicated to my mother

Anne

Acknowledgements

I would like to express my greatest thanks to my supervisors **Dr. Helmut Prion** and **Dr. Frank Lam** for their advice and guidance during my Master's program and this research. Their comments and constant support meant a great help to me and contributed very much to the successful completion of the project.

I also would like to thank **Robert Fürst, Tom Wray, Robert Myronuk, George Lee** and **Emmanuel Sackey** of the Department of Wood Science and **Harald Schrempp** of the Department of Civil Engineering for their great practical help in the preparation process of the test series. Their dedication helped to carry out the research in a very smooth and effective manner.

I would like to thank especially **Bruce Craig** of **TrusJoist,** a Weyerhaeuser Business and **Gordon White** of **Ainsworth Lumber Co.** for providing the Microllam®LVL, Parallam®PSL, TimberStrand®LSL and Douglas-Fir plywood, respectively. Without their generous donations of material and their technical support, the research would have been a lot more difficult.

For comprehensively supporting the research and supplying the INDUO-connectors, I would like to express my special gratitude to **Paul Reichartz and his team** of **INDUO.**

1 Introduction

Carpentry in Europe looks back on a very long tradition and history. Over centuries craftsman skills have been improved and passed on from one generation to the next. In the past a carpenter meant more than just manufacturing wooden structures; via their craftsmanship carpenters united the work of engineers, architects and contractors into one person. Until the end of the 18th century, being universal experts, they acted as general contractors.

The industrial revolution changed the traditional construction habits. Especially the Central European countries witnessed a substantial shift from wood to steel, concrete and brick as major building materials. This development caused a severe depreciation of the carpenter's craftsmanship. Despite their knowledge and skills, carpentry's time and cost intensive manual-labor could not compete with the upcoming industrialized and engineered construction technology. Carpentry lost its dominating role both in the design process and the construction. Since then, carpenters gradually limited their field of work to the manufacturing of roof and truss structures.

Until the 1980s, wood as construction material remained relatively dormant. In the last two decades, however, especially in Austria, Germany, and Switzerland, an increasing environmental consciousness changed people's attitude towards the 'established' and 'old' construction materials. Demanding a healthy and 'environmentally friendly' as well as a comfortable and cozy home, more and more willing homebuilders decided to use wood for the construction of their new houses. Furthermore, public authorities supported the use of wood for commercial as well as public projects. With the renaissance of wood as the most natural of all building materials, the old carpenter's skills were again in great demand. In addition, computer-controlled woodworking machinery enabled carpenters to manufacture complex and labor-intensive wooden structures at a competitive price level.

Compared to North America, building your own house in Europe is a very costly endeavor. Contributing with their own labor force, many homebuilders reduce construction costs by resorting to *do-it-yourself* (DIY) kits. For this reason, manufacturers of prefab houses or building components offer a variety of both hardware – structural components – and service - construction of the house up to various degrees of completion. Depending on the skills of the homebuilder, all the finishing work can be done by DIY style. Due to good workability, wood and wood products are widely used in this area.

In the early 1990s, Paul Reichartz, a German businessman and consultant, came up with the idea to provide both carpenters and DIY-homebuilders with a simple and affordable state-of-the-art construction system, while meeting all performance and code requirements and satisfying customers' demands. After years of development and adjustment, in 1995 the INDUO-connection and construction system was introduced in the homebuilding market.

INDUO® is a contemporary heavy-timber system. It consists of precisely prefabricated, easy-to-assemble wooden members of varying cross-section and length, connected to standardized steel nodes. These basic elements can be used to build up post-and-beam frames with varying configurations. These building elements are also well suited for highly loaded timber structures, such as 3-dimensional space trusses.

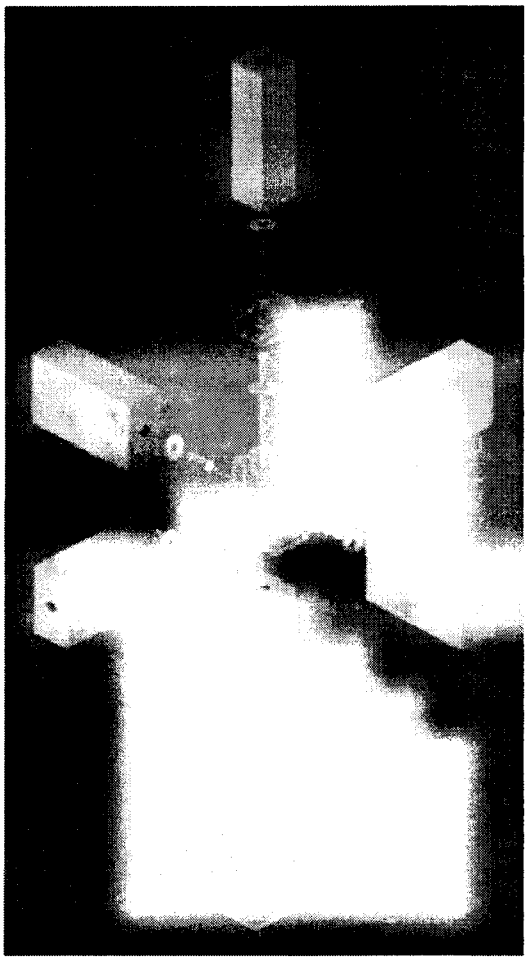

Figure 1: *Plan of connection*

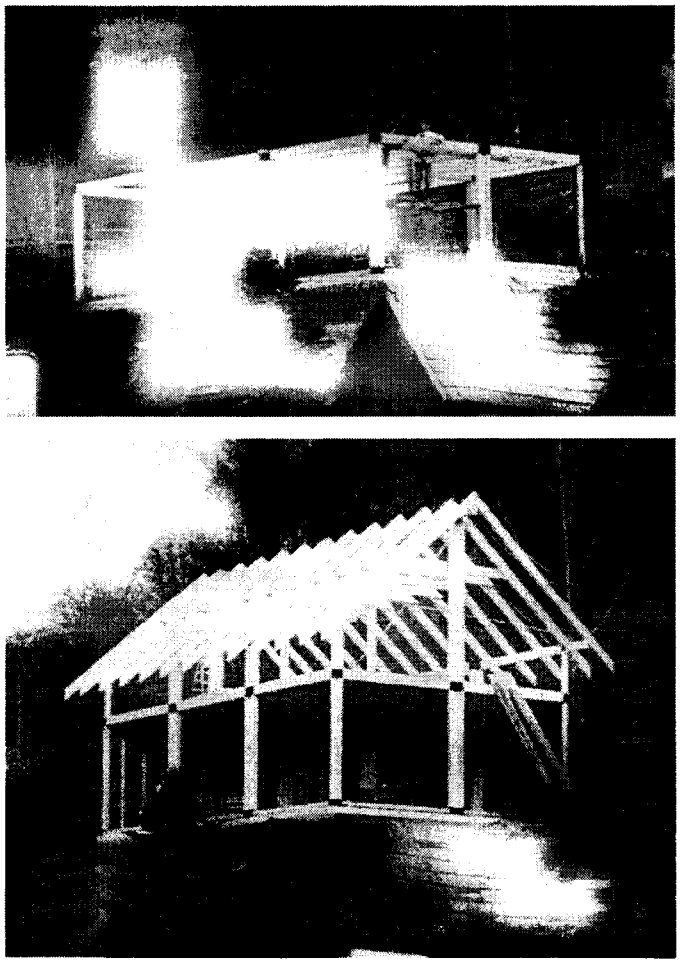

Figures 2 & 3: *Assembly of a single-family house constructed with the INDUO-system*

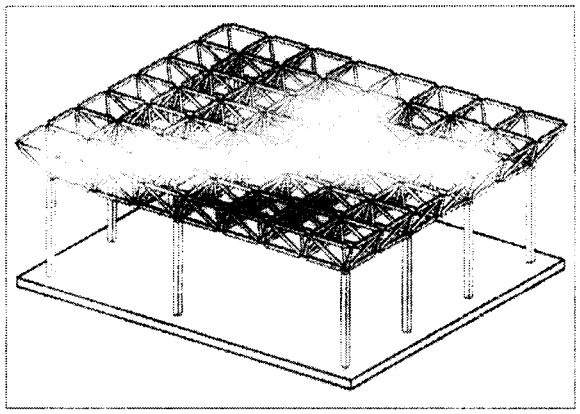

Figure 4: *3-dimensional roof truss*

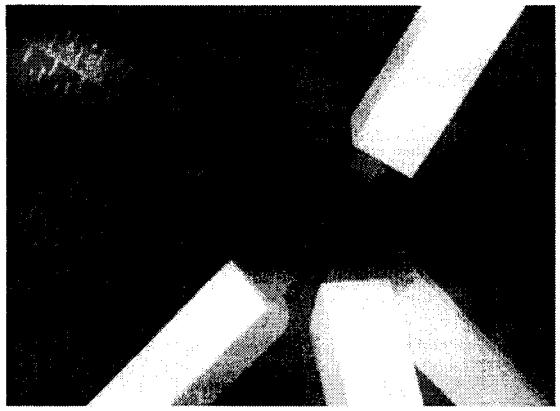

Figure 5: *INDUO-system applied in 3-dimensional truss system*

Consisting of two timber halves and two special wood connectors, the primary framing members can be considered as composite beams. Before gluing the wooden halves together, they are specially machined to accommodate the cast steel connector. The connector element itself features a set of tapered spikes and has a female thread connection at both ends, which can be bolted to a variety of nodes or brackets. Located along the center-line of the member, the connector is designed to transfer axial and transversal loads. A common wrench is the only tool necessary for the assembly. Thus, both simple and complex structures can be erected fast and precisely.

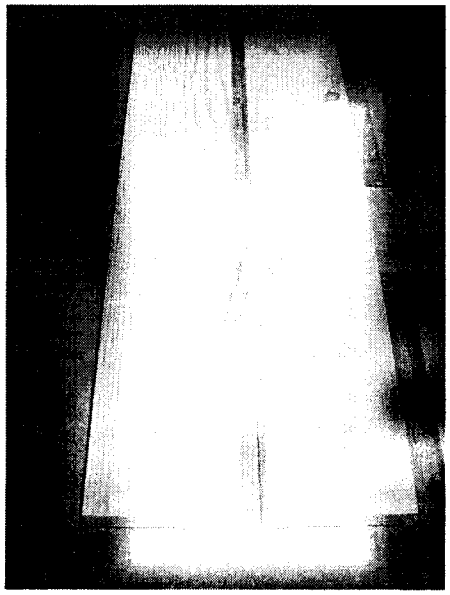

Figure 6: *INDUO-connector and timber halves before assembly*

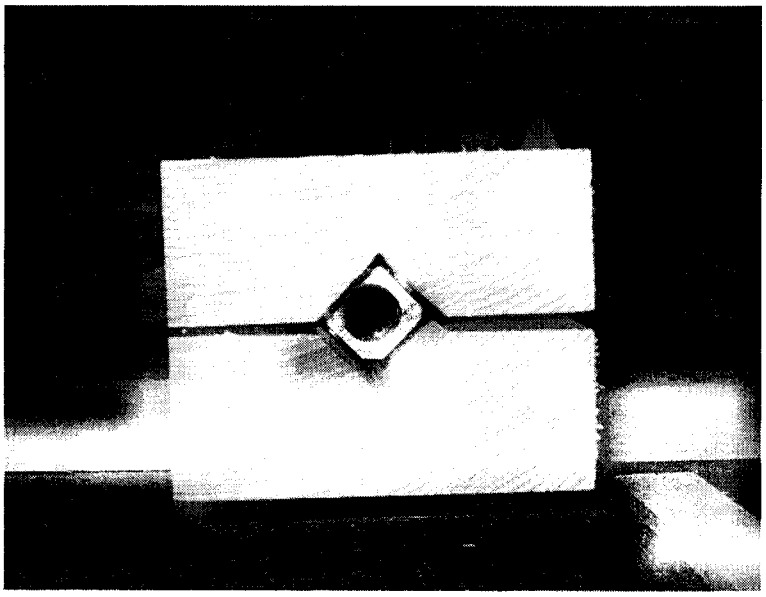

Figure 7: *Embedded connector; beam ready to be pressed in hydraulic press*

Since 1995 various research projects have focused on the manufacturing process of the joint with less emphasis on load carrying capacities (Führer 1997). In a small test series Güldenpfennig (1996) proofloaded 12 INDUO-connections with Spruce gluelam up to 100kN. Only one of the specimens failed. In 2001, the original connector (type A) was superceded by an advanced version. The modified shape of the new connector (type B) allowed the capacity of the connection to be calculated according to the German code DIN 1052-1988 as a Tight-Fitting-Dowel joint (Blaß 2001). Tests to verify this design and calculation model were not conducted.

***Figure 8:** INDUO-connector type A*

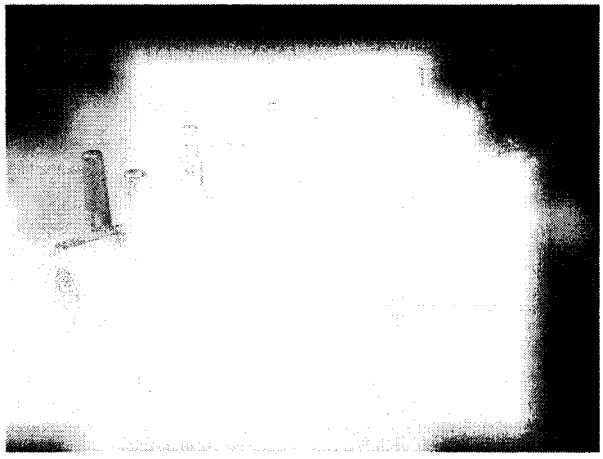

***Figure 9:** INDUO-connector type B*

In the past, the basic elements were made with solid softwood - mainly Spruce and Fir. Manufacturing the so-called "Quarter Logs" with exposed edge grain and pith forming the member corners allows the connector spikes to penetrate into the flat grain portion of the log. Visually more attractive, the Quarter Log can be made from small logs, possibly even peeler cores.

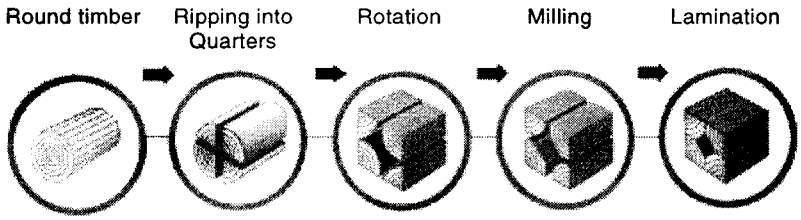

***Figure 10:** Manufacture of INDUO-Quarter Logs*

Being a high-performance connection method, the INDUO connector could be cost-effectively applied in heavy-timber construction with structural composite lumber. Since little is known about the connection's behavior in combination with such engineered wood products, composites like *Laminated Strand Lumber* (LSL), *Parallel Strand Lumber* (PSL) or *Laminated Veneer Lumber* (LVL) have so far not been considered as possible substitutes for solid wood.

The intention of this Master research project was to gain more specific information on the joint's tension behavior with emphasis on ultimate strength and failure mode. As this connector is primarily suited for tension application, it was decided that testing of the INDUO-member deployed as beam elements, where transverse shear will be the dominant load, would not be done.

1.1 Research objective

Officially introduced in Germany, the INDUO®-system has been successfully marketed in many European countries. The system has been gradually improved to respond to various customer demands. INDUO's future goal is to enter the North American marketplace. Considering different construction standards and techniques as well as a different set of priorities, it is essential to adjust the system to North American demands and requirements.

Concerning the adaptation of INDUO, the following issues are of substantial interest:

- Investigation of connector type B's tensile behavior:
  - Mechanical properties (strength and stiffness)
  - Failure mode
  - Calibration of rational calculation model (Blaß 2001)
- Influence of different member configurations on tensile behavior;
  Comparison of connector type A and type B with:
  - Beams built-up with different wood species (solid wood and wood composites)
  - Different methods of bonding the two member halves: screwed or glued
  - Members of different cross-sections

1.2 Scope

A comprehensive test program, considering all the above-mentioned parameters and providing a sufficient sample size to create statistically significant data, was deemed to be beyond the scope of a Master thesis. Therefore, it was agreed to split the project into two separate test series, each focusing on different aspects.

In series 1, beam members of all the possible combinations of material, connector type, member cross-section and lamination type were tested under tensile loading. Up to three specimen for each individual combination are meant to provide general information and performance trends.

Data assessment and experiences of series 1 then served as the basis for a detailed and more accurate investigation of one combination. With a sample size of up to 10, statistically more significant results for ultimate tensile strength were determined. This test series would then be used to calibrate an analytical model for calculating the tensile capacity of typical connections.

2 Non-visible heavy-timber joints

Comparing North American and European practices, the design approach of timber joints is significantly different. Since the 1970s, European architects and structural engineers have more and more tended to 'hide' or embed timber connections for esthetic and / or fire protection purposes, whereas contemporary North American heavy-timber design still prefers to expose the connection. Responding to the trend for non-visible joints, numerous new connection types have been developed in Europe. With improved mechanical properties and advanced performance, these innovative connections have been widely applied in various timber structures.

Being embedded in a composite beam member, the INDUO-connector, which is the focus of research in this Master thesis, represents one of the above-mentioned non-visible timber joints. The following sections give an overview of various other non-visible connector systems.

2.1 Non-visible mechanical connector systems

Most of the joints used in timber structures are mechanical connections. Being exposed, simple fasteners like nails, bolts, drift pins and lag screws, as well as advanced fastener types like shear plates, split rings, truss plates, sheet metal connectors and glulam rivets often present a problem with esthetic and fire protection demands. Embedded or hidden connectors, however, typically meet these requirements.

Mechanical connectors, when proportioned carefully, can meet demands for high ductility which is important for equal load distribution and energy absorption.

2.1.1 The BSB-system *(Tight-fitting dowel connection)*

Tight-fitting dowel connections consist of high-quality steel dowels and embedded steel plates. Driven into undersized pre-drilled holes, the dowels are kept in place by friction. In addition to being esthetically more pleasing, tight-fitting dowels are further distinguished from bolted connections by higher strength values and better failure performance. The dowel press fit prevents initial slip and guarantees a stiff connection as well as a more uniform load distribution.

Figure 11: *BSB-joints in heavy timber truss*

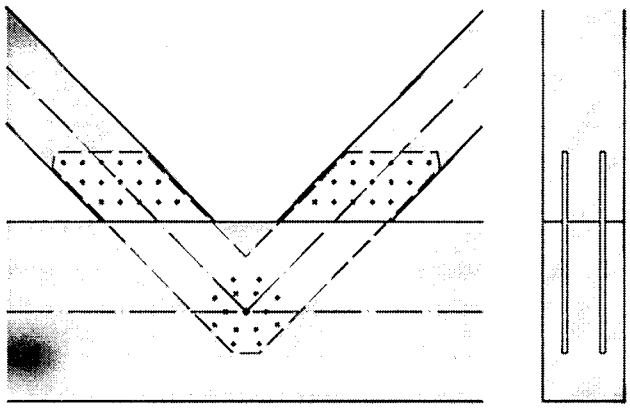

Figure 12: *Scheme of BSB-connection*

Requiring highly accurate fabrication, Computer Numerically Controlled-equipment more and more substitutes the time-consuming and difficult manual labor of precisely drilling the dowel holes and machining the slots for the steel plate. Manufacture and assembly of the joint is mostly done in the shop under controlled conditions. Depending on the size, smaller components of the structure are prefabricated, then brought to the construction site and finally completed by connecting a limited number of joints. During fabrication, transport and assembly, moisture fluctuations of the wood must be strictly avoided.

The BSB-connection is a highly optimized tight-fitting dowel connection that was developed in Switzerland (Mischler 2000). It is officially approved in many European countries and has been applied in many heavy-timber structures.

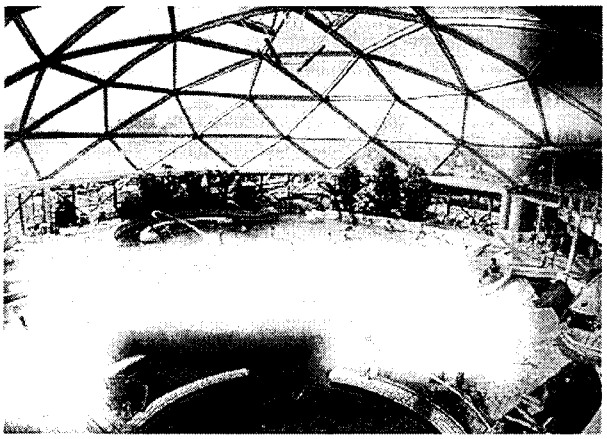

Figure 13: *BSB-system applied in a roof structure of a spa*

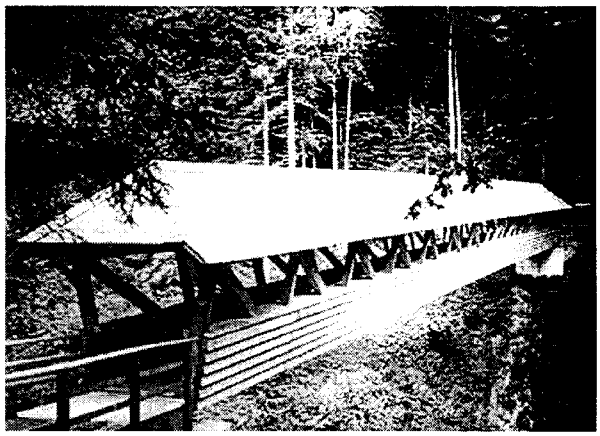

Figure 14: *Footbridge constructed with BSB-connection*

2.1.2 The SpikeTec-system *(Embedded nail plate)*

Invented by MERK[1] and officially approved in Germany (DIBt[2] 2002), the SpikeTec-system is a further development of the truss-plate connection. It is mainly applied for large trusses and is typically used with composite structural lumber. The connection consists of the SpikeTec-connector - a steel plate with a double-sided set of spikes welded perpendicular to its surface – sandwiched between a pair of timber members.

Figure 15: *Close-up of SpikeTec-connection*

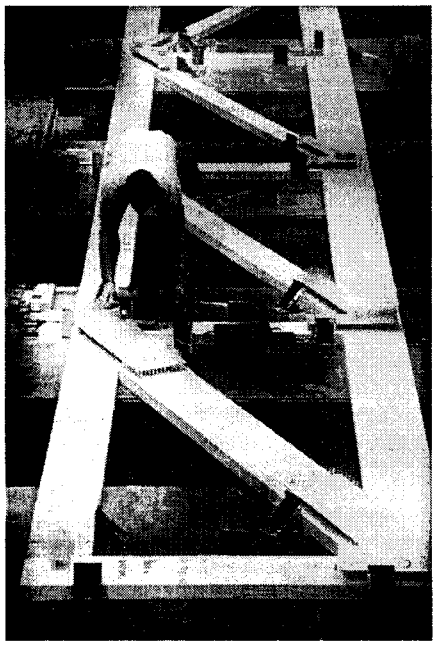

Figure 16: *Nail plates are set in place*

The steel plate is 10mm thick; the spikes have a length of 50mm and a diameter of 5mm. LVL and glued-laminated timber are commonly used for the truss members.

In the manufacturing process, the nail plate is pressed into the flanging side members. To meet higher fire protection requirements, both timbers have to be countersunk by 5mm in the nail plate area. The wood thus completely encloses the connector.

Optimized design enables the SpikeTec-connection to carry 50% more load parallel to grain than a conventionally bolted joint of the same size. Due to compact joint dimensions and reduced member cross-sections, the construction of large timber trusses has become competitive with structural steel.

---

[1] MERK Holzbau, Aichach, Germany. Leading contractor for heavy-timber constructions
[2] DIBT: Deustches Institut für Bautechnik *(German Institute for Construction Technology)*

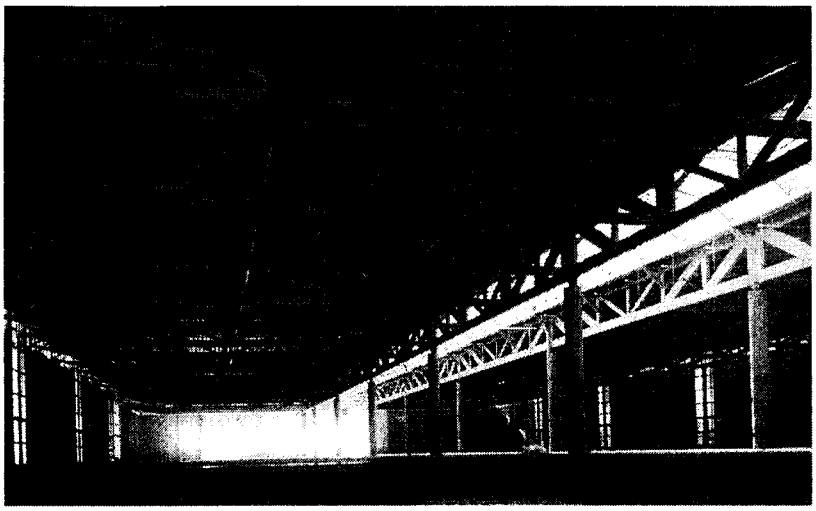

Figure 15: *SpikeTec-system applied in the roof structure of a supermarket*

Figure 16:
Roof truss system constructed with SpikeTec-connection

2.2 Non-visible composite connector systems

Unlike many mechanical connectors, composite joints with Epoxy, Resorcinol or non-shrink grout glued-in steel components, provide high stiffness and strength, low tolerances, easy fabrication, and for completely embedded connectors systems, good fire protection. The main disadvantages are brittle failure modes of the glued connection and deterioration of strength properties due to climate changes and poor quality of the glue bond.

While glued wood-to-wood connections are common in traditional joinery, larger structures have typically relied on mechanical fasteners. This is mainly to facilitate construction and / or assembly on site. The advantage of high-performance glued

connections can be combined with mechanical on-site connection methods by gluing metal connectors to the wood. Failure modes can then also be controlled by assuring a weak link in the steel element.

2.2.1 Glued-in steel rods

In the past 30 years several researchers have investigated means of transferring high loads from wood members to steel rod elements. In the 1960s and '70s Scandinavian engineers (Riberholt 1988) conducted initial research on inserting steel rods into predrilled and oversized holes filled with Epoxy or Resorcinol glue. Placed parallel to grain, this composite joint was the first successful application of gluing steel to timber. In Russia (Turkowskij 1991[3]) ribbed steel bars were glued perpendicular to the grain in places where the Glulam was subjected to excessive bearing forces. Later, reinforcement bars were inserted at a 30° angle to reinforce the timber members for high shear stresses. In the late 1980s, extensive research was conducted at UBC (Madsen 1998), to develop a reliable glued-in steel rod connection. Madsen phrased guidelines to meet state-of-the-art performance requirements. They are:

- High Strength
- High Stiffness
- Avoid brittle failure
- Tolerate reverse loading
- Loads transferred via specified path
- Simplicity of design
- Ease of manufacturing
- Construction friendly
- Attractive appearance
- No field gluing
- No field welding
- Provide for corrosive environment (if needed)
- Fire protection
- MC of wood members less than 15%
- Cost

[3] Research had begun already in 1975, however, remained unknown for the rest of the world till 1989, because publications were in Russian.

Investigating the performance of the wood to glued-in steel rod connection in general, in terms of strength, stiffness, different sizes and lengths of the rods, as well as the joint's behavior with rods perpendicular and at an angle to the grain, Madsen came up with a basic connection design suitable for various applications.

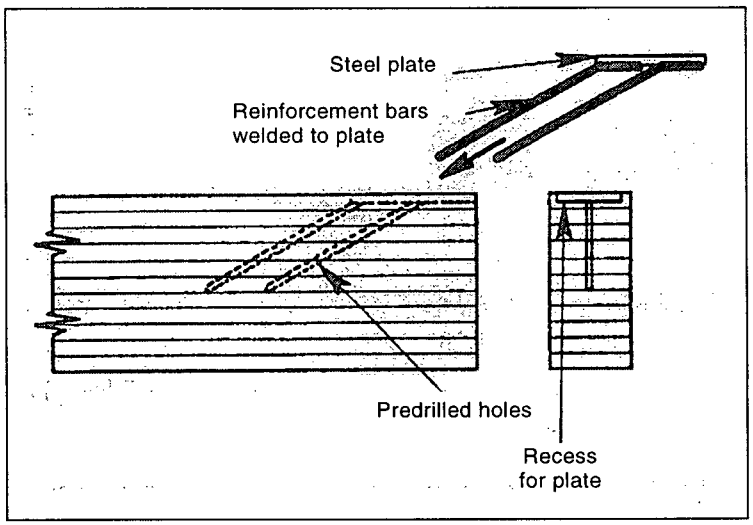

Figure 17: *Glued-in steel rod connection (Madsen)*

Anchor plates with pre-welded rods on one side are inserted in epoxy glue filled holes of the timber member. In the structure, these composite members are then connected to each other with bolts. Engaging a larger portion of the cross-section, the use of angular rods was found to increase load-bearing and shear capacities of the wood member.

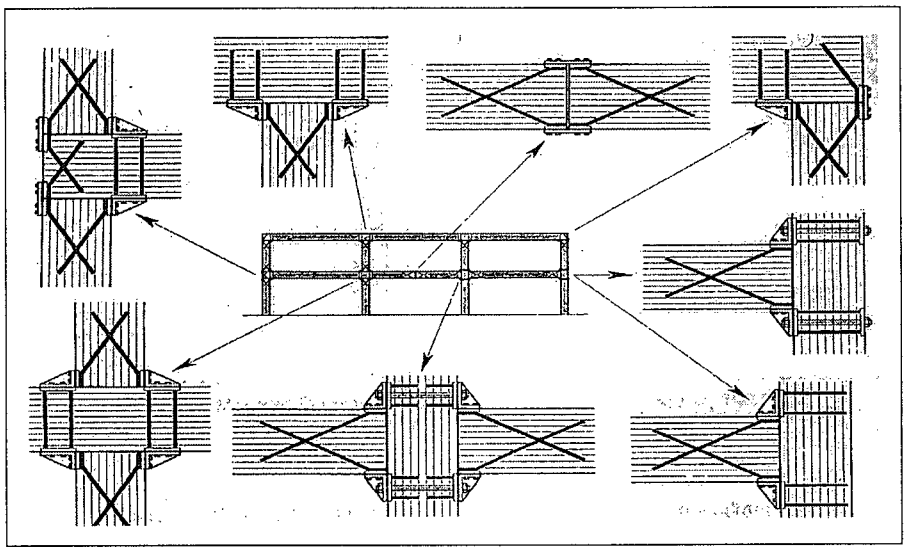

Figure 18: *Applications for glued-in steel rod connections (Madsen)*

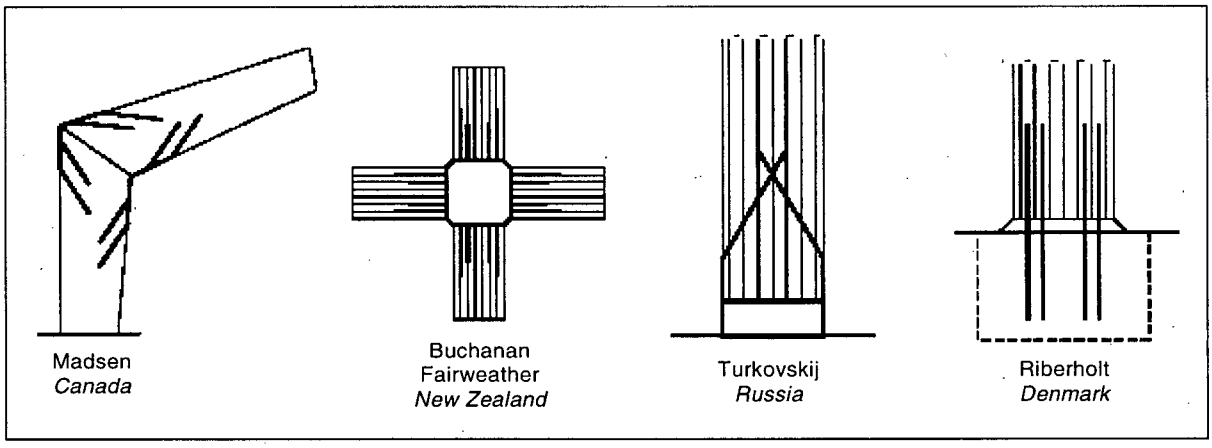

Figure 19: *Research conducted on glued-in steel rod connections*

Many researchers worldwide have raised concerns about the sensitivity of the epoxy glue joint to climatic changes. The loss of strength and stability due to changing moisture contents and temperatures, as well as a required minimum temperature for the adhesive reaction, limits the use of epoxy for outside applications or structures with strict fire protection requirements. Kangas (2000) conducted fire resistance tests of epoxy glued-in V-form steel rod connections. To avoid premature failure of the joint, he found that all fire exposed steel parts have to be covered with rock wool and steel sheets. Due to severe loss of strength when heated above 50°C, epoxy glue was substituted by cement grout (Buchanan and Eiststetter 2000). While easy to handle, inexpensive and fire resistant, however, cement grout's poor adhesion to the timber represents a major problem, therefore requiring a mechanical bond. Reinforcement with pins and screws, driven into to the wood member before grouting, is one way to create a strong connection with good fire resistance.

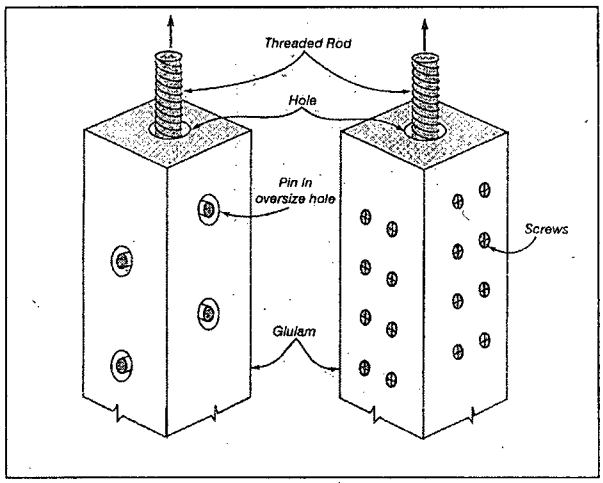

Figure 20: *Sketch of test specimens (before grouting) (Buchanan)*

The TiSCo®-system

Building on the knowledge of more than 30 years of research experience in the field of glued-in steel connections, the German TiSCo®-system (**Ti**mber-**S**teel-**Co**nnector) represents a new type of composite connector. The tubular shape of the connector, providing a larger surface area to carry load and the use of an easy-to-handle, strong and temperature-tolerant vinyl-ester based compound mortar distinguishes this connector system from most other glued composite connections.

The connector, which consists of a mild steel tube (125mm long, 48mm outer diameter and 3mm wall thickness) and a steel plate welded to one end, is inserted into the end grain of a wooden member. Featuring a threaded hole (M16), the steel plate acts as connector head, which can easily be connected to adjacent elements of the structure. To provide enhanced adhesion, the surface of the tube is sandblasted or ribbed. In addition, four longitudinal slots over most of the tube's length are meant to reduce residual stresses due to deformations of the wood.

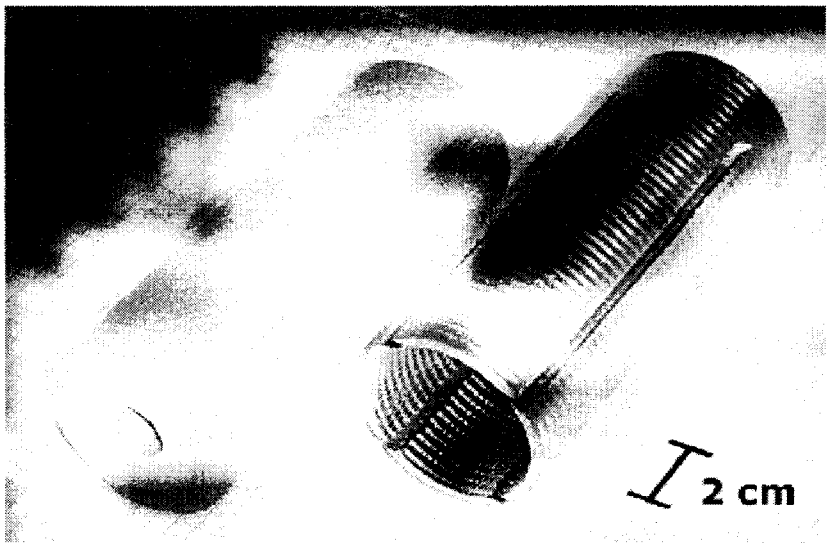

Figure 21: *TiSCo-connector: Sandblasted and grooved version (Schreyer)*

Figure 22: *TiSCo-connector inserted in end grain (Schreyer)*

The connection is manufactured in three steps:

1. Drill a circular hole, including a 20mm countersink to accommodate tube and head of the connector
2. Inject mortar into the hole and
3. Insert the connector with a twisting action, distributing the viscous mortar all over the glue splice.

After a short hardening time of approximately 10 minutes, the squeezed-out excess mortar can be removed; 1 hour later, loads can be applied.

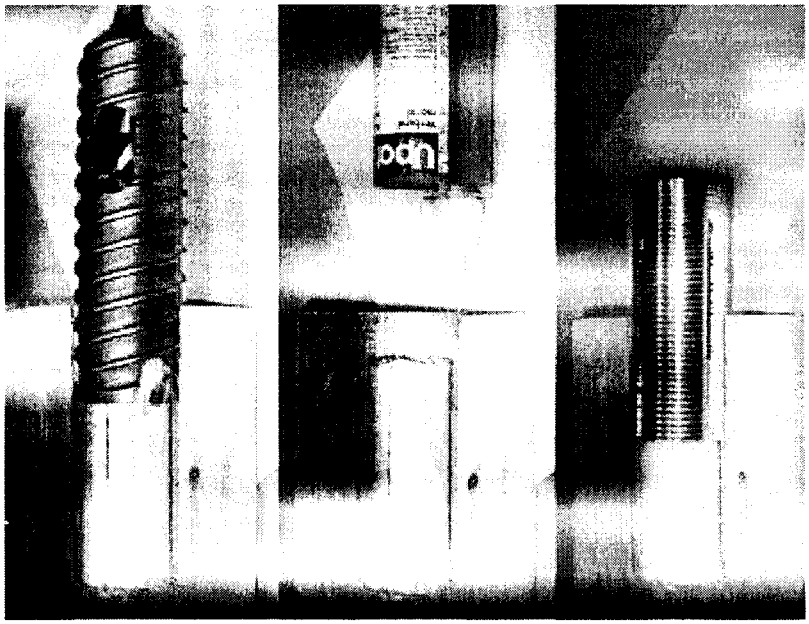

Figure 23: *Manufacturing steps of the TiSCo-connection (Schreyer)*

Bathon and Schreyer (2000) investigated strength and stiffness properties of the TiSCo-connector. Under tensile loading, the connection fails abruptly with a withdrawal of the connector along the mortar surface. Under compression, after a failure of the mortar bond, wood compression causes an increase of loading capacity with ductile failure characteristics. Preliminary research showed that exposure to changing climates may result in a reduction of the tensile load capacity of the connection.

Although, extensive research was conducted, TiSCo has never been tested and used in full-size timber structures, thus remaining a prototype.

2.2.2 The BVD®-system

Successfully utilized in numerous heavy-timber structures, the BVD-system, developed and marketed by German engineer Peter Bertsche, provides high connection strength and stiffness properties in the longitudinal direction of the loaded member. The BVD-system consists of a cylinder-shaped main connector hanger with inside thread inserted into the end grain of a member, a large number of drift pins located perpendicular to the connector's longitudinal axis and a non-shrink cement grout that compounds wood and

steel parts creating a composite joint. The recess for the main connector as well as the holes that accommodate the drift pins are predrilled and generously oversized to provide enough play for a uniform distribution of the cement grout poured into the voids between wood and steel parts.

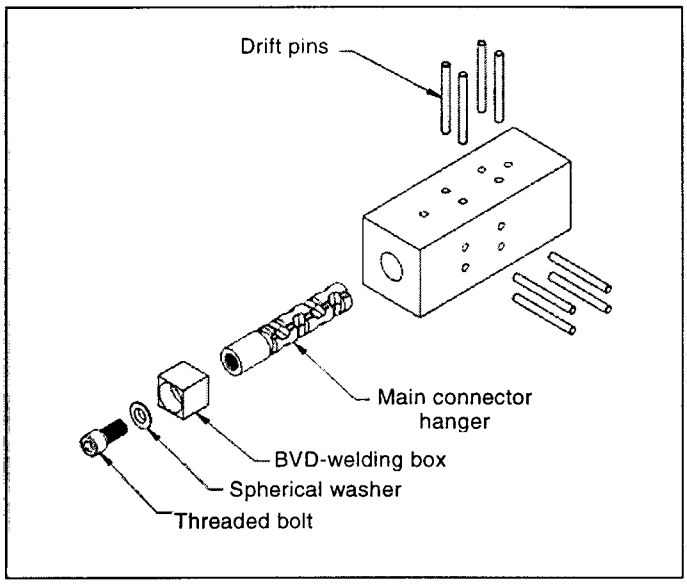

Figure 24a: *Components of the BVD-system (Bertsche)*

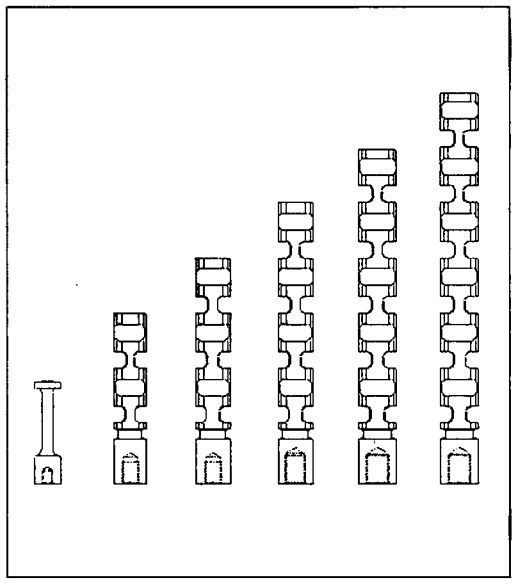

Figure 24b: *Different hanger sizes in various length configuration (Bertsche)*

The following set of pictures show the manufacture of the BVD-Joint:

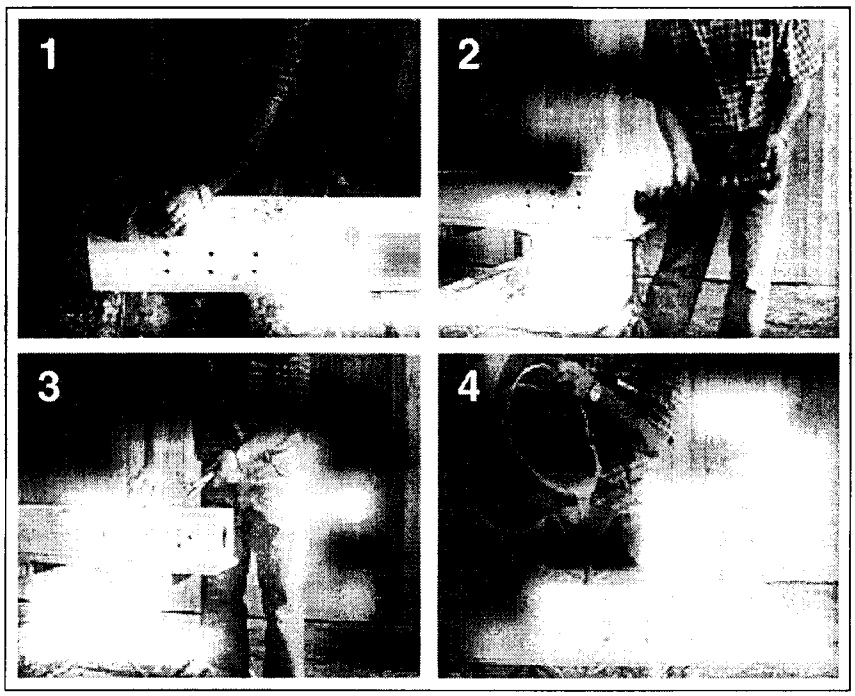

Figure 25: *Manufacturing the BVD-connection (Bertsche)*

The four steps of manufacturing and installing the BVD-joint are as follows:

1. Drill the pin holes.
2. Drill the large main connector hole in the end-grain of the member.
3. Insert connector hanger first, followed by the drift pins that interlock with the connector.

   Adjust and fix position of the connector.
4. Cover the surface of the member with plastic foil to protect the wood from being stained and pour cement grout into special feed openings.

The grout is cured after 12 hours. Ready to be installed in the structure, however, the member is not to be fully loaded for another 12 hours. After 28 days the grout is completely cured, providing the maximum strength.

The BVD-system has been widely applied in many heavy-timber structures all over the world. Over 250 major projects, including wooden bridges, large span roof structures and various custom timber constructions have been built using the high-strength BVD-connector. In addition, in the area of reconstruction and renovation of historic timber structures the system recently found a further field of application.

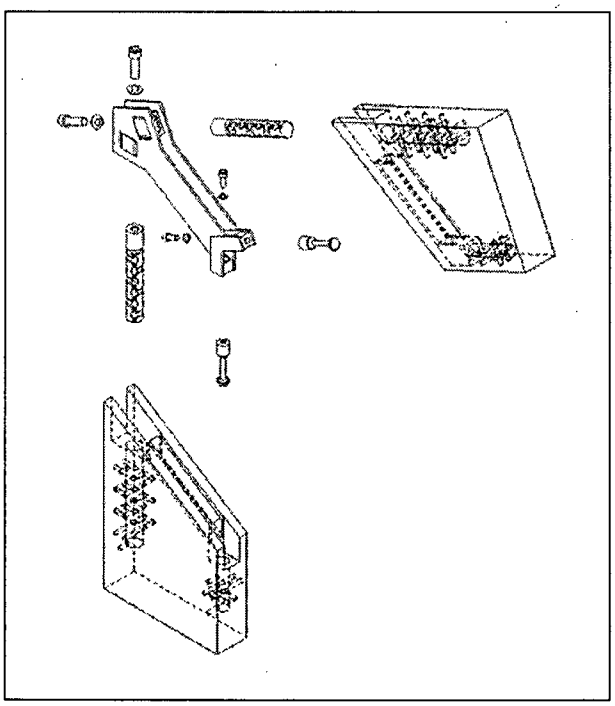

Figure 26: *Knee joint with BVD-connection (Bertsche)*

For the largest timber structure ever been designed and constructed, the EXPO-Roof built for the world exposition in Hannover, Germany in 2000, the BVD-system was applied in one of the main joints that connect the tower columns with the foundation of the structure. Due to the size and the number of the column members, the BVD-joints were processed on a CN-controlled machining center.

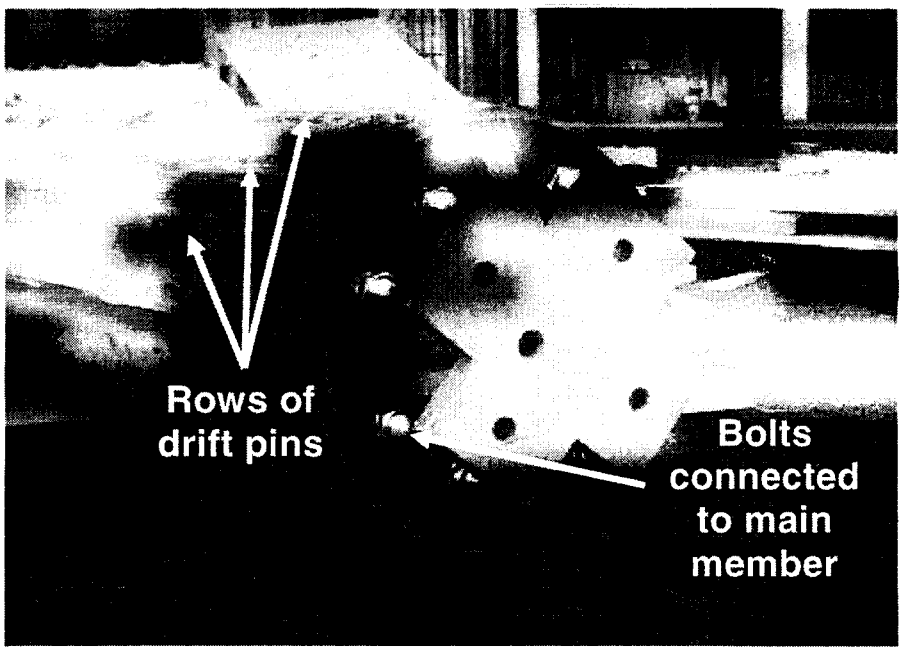

Figure 27: *Tower column with BVD-connection to foundation*

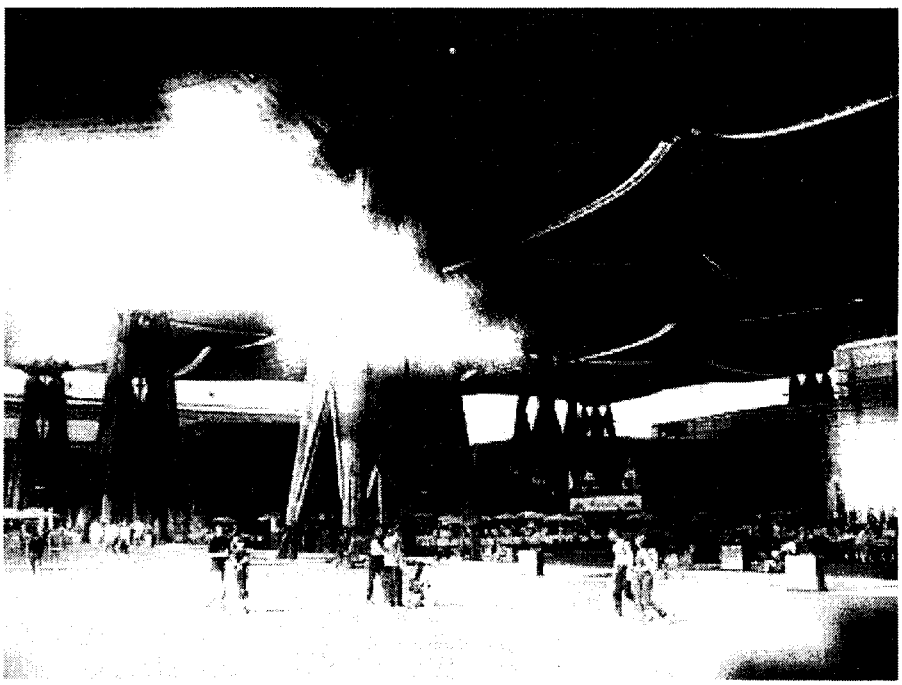

Figure 28: *EXPO-Roof with towers supporting the roof structure*

3 Materials and Methods

Chapter 3 describes the methodology of the research work on investigating the tensile performance of the INDUO-connector. As mentioned in the introductory chapter, limited knowledge on the strength and performance of both connector type A and type B and a set of various problems resulted in a subdivision of the practical research into two test series. Section 3.1 specifies the different wood materials used in the construction of the test members, including how these wood products are manufactured, and their material characteristics. Furthermore, section 3.1 introduces the different connector types. Section 3.2 describes in detail the scope of the research, the connection design, the fabrication of the test specimens and the set-up of the test apparatus.

3.1 Materials

Microllam®LVL, Parallam®PSL, TimberStrand®LSL, Douglas-Fir plywood and Douglas-Fir lumber are the different wood materials used in this research project.

3.1.1 Microllam®LVL

Laminated Veneer Lumber is an engineered wood product created by layering dried, graded and adhesive-coated wood veneers into blocks of material. Rotary-peeled on a lathe, the veneer is typically produced in thicknesses of 2.5, 3.2, and 4.2 mm. The adhesive used in Microllam®LVL is phenol formaldehyde, continuously applied to the veneer sheets by passing under a glue-curtain. Layered with the grain running in the lengthwise direction and specifically located in the veneer block to assure optimized strength properties, the laminations are cured in a heated press, fabricating a continuous billet. After exiting the press, the billet is sawn to standard dimensions, either 610 mm or 1220 mm wide and 19 mm to 89 mm thick and is finally stored to cool down. Dependent on customer orders, stocked LVL is ripped and cut to the required length in a separate line.

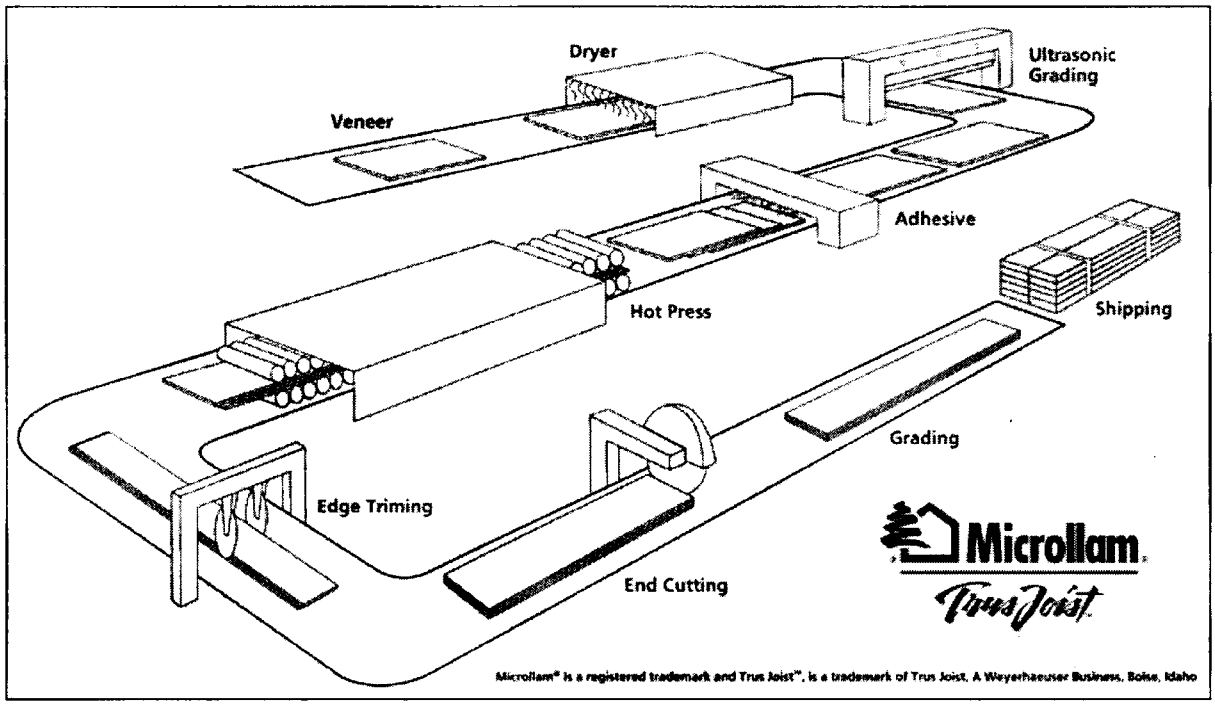

Figure 29: *Manufacture of LVL (TrusJoist)*

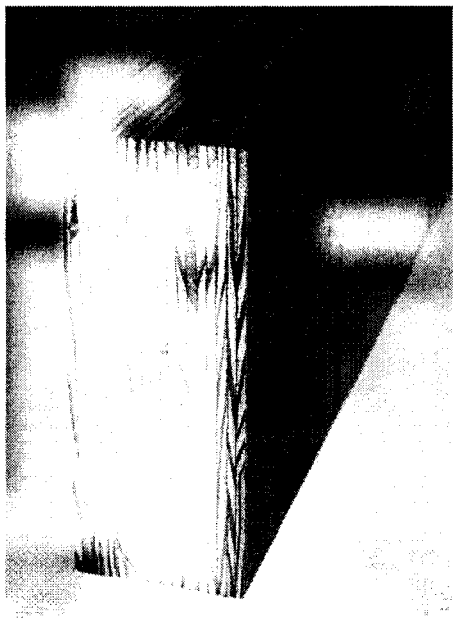

Figure 30: *Close-up of LVL*

With a consistent moisture content, LVL is virtually free from warping and splitting and can be easily worked using conventional woodworking tools.

Compared to common lumber products, due to defect removal and dispersal, LVL as a solid, highly predictable and uniform wood product offers higher reliability and lower variability. For the research project LVL of grade 1.9E was used.

One important benefit of LVL is that the veneering and gluing process creates large timbers from underutilized species of small trees. Besides the most common species Douglas Fir, Southern Pine and Spruce, in North America, Aspen and Yellow Poplar are increasingly being used.

3.1.2 Parallam®PSL

Representing a more recent development of structural composite lumber, Parallel Strand Lumber is another lengthwise oriented structural wood product, created by layering dried, adhesive-coated veneer strands parallel into blocks of material. Similar to the manufacture of LVL, the veneer is typically produced from Douglas Fir, Southern Pine or Yellow Poplar and either rotary-peeled to a veneer ribbon of 2.5 and 3.2mm thickness at the plant or purchased and delivered to the plant. The adhesive used in Parallam®PSL is resorcinol or phenol formaldehyde with a small admixture of wax to avoid moisture absorption of the composite.

In the manufacturing process veneer is clipped to strands between 12.5 to 25mm width and up to 2.4m length. In a sorting machine strands shorter than 300mm are removed. After being coated with adhesive in an immersion bath, the strands are dried and then passed through a distribution system, where density and strength of the finished product is set by controlling the mass flow. Being layered and aligned approximately parallel to the product axis, the strands are gathered in a conveyor hutch to form a continuous billet of required mass per length. The strand mat is slowly fed into the press, which applies pressure for densification and cures the adhesive using microwave energy.

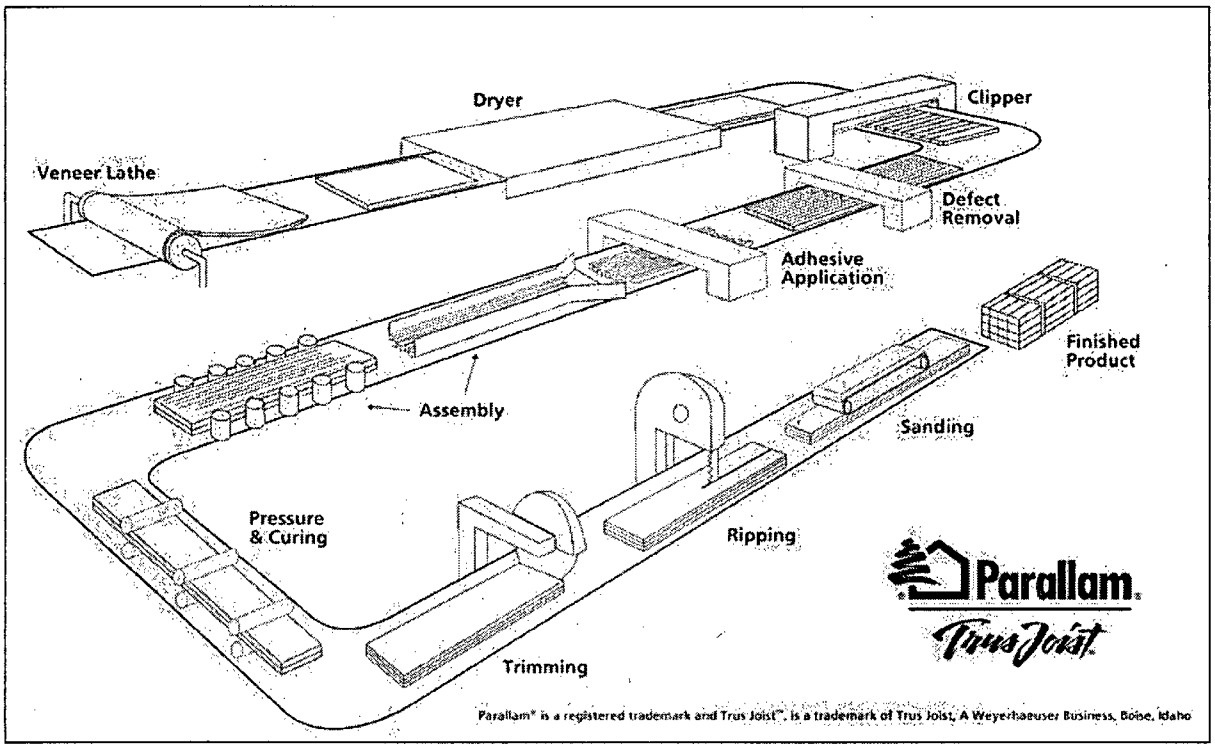

Figure 31: *Manufacture of PSL (TrusJoist)*

After cooling, finished billets of up to 279 x 483 mm in cross-section are ripped, cut and sanded to required dimensions. For handling reasons, the billet is cut to lengths of up to 22m. Because it is a continuous process any length is theoretically possible. Finally, the end grain of each finished member is treated with a sealant to avoid moisture absorption.

Figure 32: *Close-up of PSL*

Figure 33: *PSL applied in heavy-timber structure (Forestry building, UBC)*

Besides its good workability and high strength, the unique and appealing parallel grain structure of PSL satisfies esthetic demands and is often left exposed as a design element. Independent of the wood species of the strands, PSL is generally provided in a 2.0E grade. In terms of recovery and efficiency, the manufacture of Parallam®PSL utilizes 64 percent of a log, whereas traditional sawmilling processes convert only 40 percent of a log into lumber.

3.1.3 TimberStrand®LSL

Laminated Strand Lumber is one of the latest developments in engineered wood product technology. It is also a strand-based product with fiber orientation slightly more random than PSL. In the manufacturing process, around 75 percent of a log of low-density hardwood species such as Yellow Poplar, Aspen and Cucumbertree is utilized. The adhesive used in TimberStrand®LSL is polymeric diphenylmethane diisocyanate (MDI) with a small admixture of wax to avoid moisture absorption of the composite.

LSL is created by cutting the log into fine strands of 0.75 to 1.3mm thickness, roughly 25mm width and up to 300mm length. After drying and removing short pieces, the strands are conveyed to blenders where they are coated with adhesive and wax. Aligning the strands approximately parallel to the product axis, a 2.4 m wide continuous mat of specified mass is formed and cut to the appropriate pressing length. In the press the mat is densified and cured with injected steam, creating a composite with minimal density variation throughout its thickness. After exiting the press and cooling, the LSL billets with a rough size of up to 140mm thickness, 2.4m width and 11m length are sanded, ripped and cut to final dimensions, for structural material ranging from 32mm to approximately 100mm thickness.

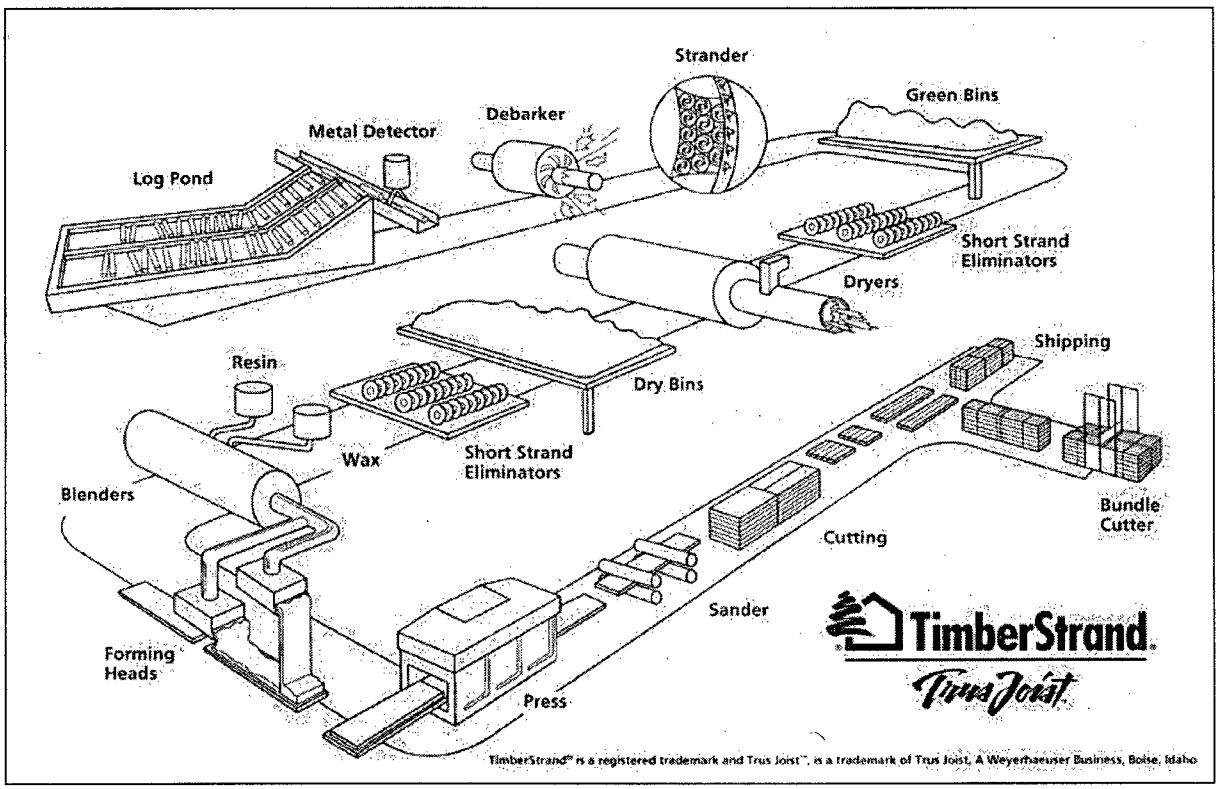

Figure 34: Manufacture of LSL (TrusJoist)

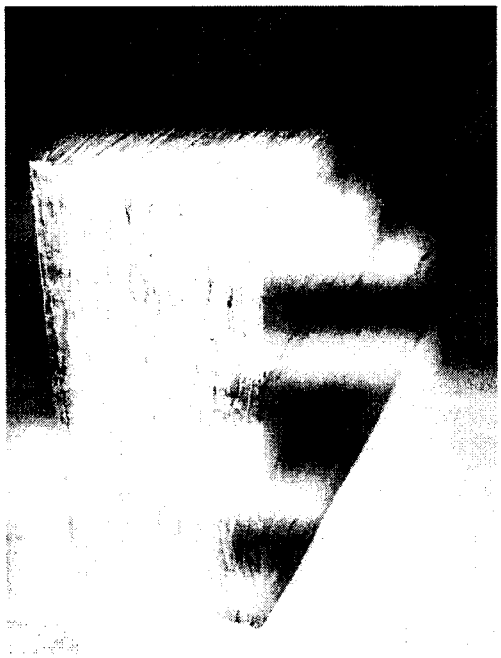

Although LSL is manufactured as panels, it is mainly used as linear elements, such as rimboards and studs.

In terms of manufacturing, LSL is similar to Oriented Strand Board (OSB), except that OSB is conventionally hot pressed and LSL strands are longer and more-or-less parallel aligned, thus enhancing bending and axial strengths in the main direction. LSL is available in 1.3E, 1.5E and 1.7E grades. 1.5E grade was used for the research project.

3.1.4 Douglas-Fir plywood

Plywood and LVL were originally developed in the 1930s for the manufacture of wooden airplane propellers and other high-strength aircraft parts. Since the 1950s as a substitute for solid wood sheathing, particularly in North America, plywood rapidly advanced to a highly deployed construction material. Although losing much of its market share to OSB, it remains one of the most important engineered wood products.

The fabrication of plywood is similar to LVL, except that the grain direction of sequential veneer sheets is alternated and the layer set-up is symmetrical to the centerline. Dependent on structural or non-structural, exterior or interior application, different plywood grades are available. Typically Douglas-Fir or other softwood veneers and waterproof formaldehyde adhesives are used to build up the panel. In the manufacture, plywood panels are produced to sizes of up to 6 x 12m, then ripped and cut to standard dimensions of 1.2 x 2.4m; thicknesses range from 12.5mm to 38mm.

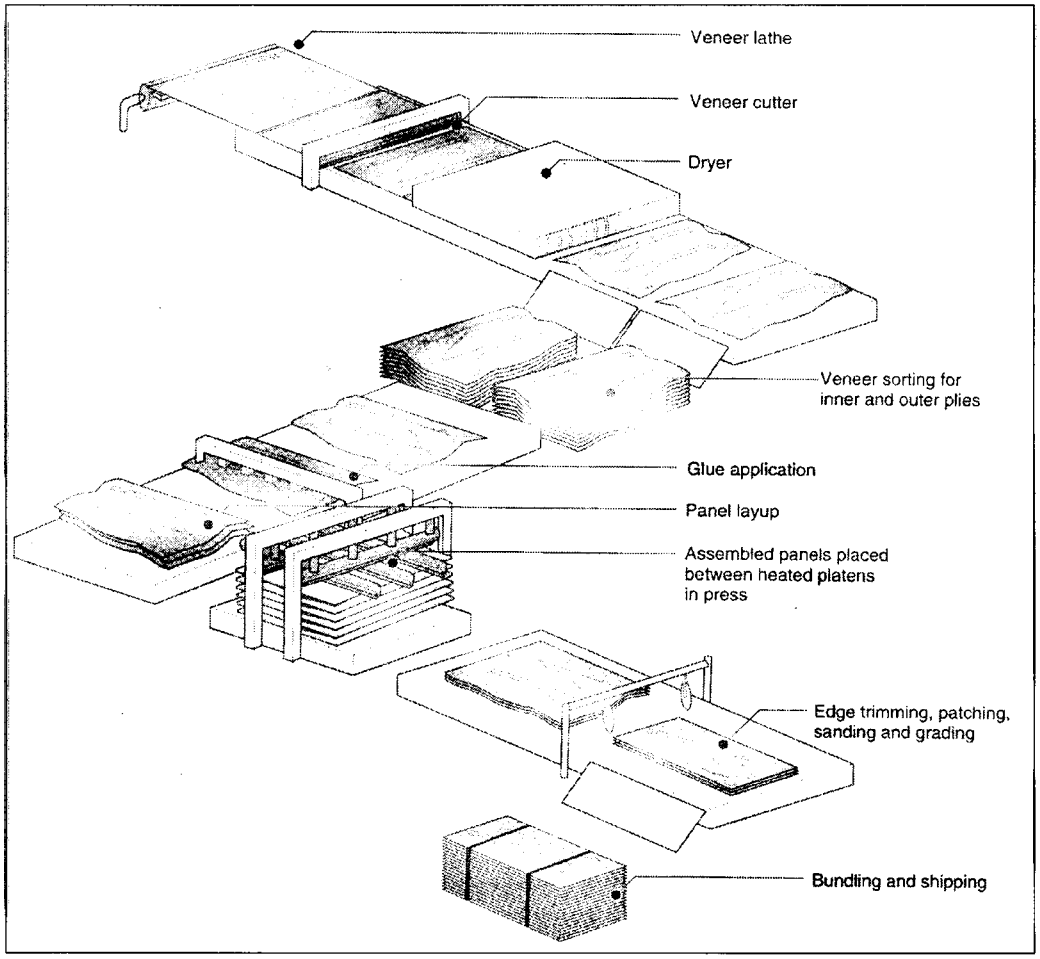

Figure 36: *Manufacture of plywood (CWC)*

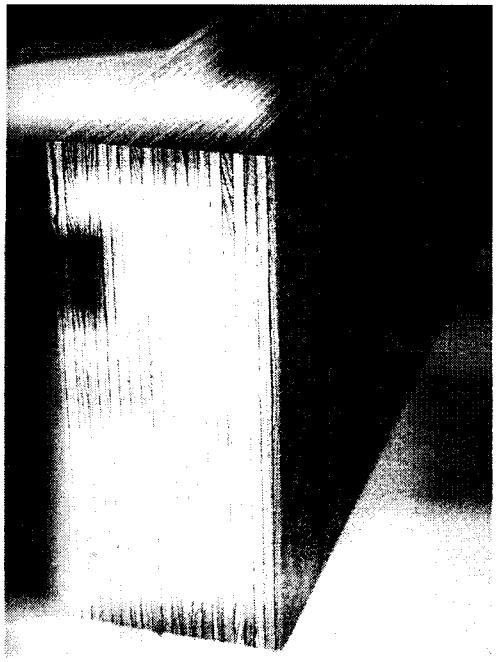

Figure 37: *Close-up of thick Douglas-Fir plywood*

For the research project plywood of 50 and 60mm thickness was needed. Since standard plywood is limited a maximum thickness of 25.4mm, a set of one 12.5mm and two 19mm as well as a pair of two 25.4mm thick panels respectively were glued-laminated in the shop to build up the required panel dimension. Providing grade A on both faces and grade C1 for all inner plies, the 12.5mm, 19mm and 25.4mm thick panels consisted of 5, 7 and 9 cross-plies, respectively.

3.1.5 Douglas-Fir lumber

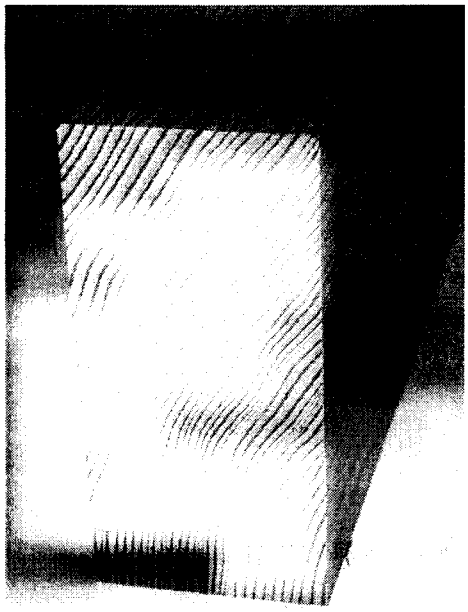

Figure 38: *Close-up of Douglas Fir*

Contrary to Europe, where timber is individually cut to customer demands, in North America sawmills mostly produce standard dimensions. In addition, dimension lumber sizes are expressed in nominal imperial units. A nominal 2x4 lumber member (pronounced 'two-by-four') for example has a cross-sectional area of 38 x 89mm.

For the test specimen manufacture nominal 3x6 Douglas-Fir lumber (64 x 140mm) was directly purchased from a sawmill, since building material suppliers do not carry larger lumber dimensions in stock. Internally specified as 'cross-arm grade' the rough-sawn lumber is considered to be of equal quality as 'No. 1 and better' grade. The lumber was delivered with an average moisture content of 26% and had to be conditioned to 13% MC in one of UBC's drying kilns.

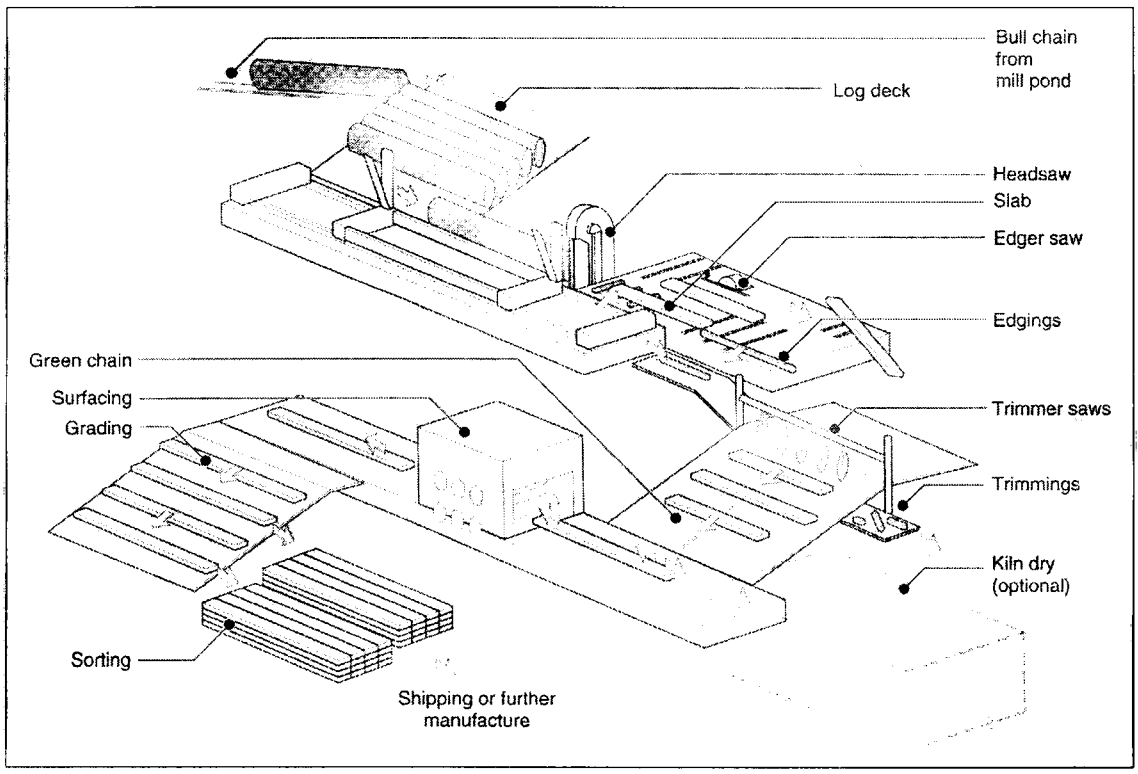

Figure 39: *Manufacture of sawn lumber (CWC)*

3.1.6 INDUO-connector type A

According to EN1562, connector type A consists of malleable cast iron of EN-GJMW-400-5 grade with a characteristic ultimate tensile strength $f_{u,k}$ = 360 N/mm^2 and a characteristic yield strength $f_{y,k}$ = 200 N/mm^2. The fabrication process is as followed:

1. Casting of connector according to standard methods
2. Unloading of casting mould and cooling of member
3. Brushing and deburring
4. Sandblasting
5. Tapping of inside-thread
6. Galvanizing

The solid connector body has a rhombic cross-section, featuring a set of 64 12mm long spikes, arranged in 4 rows of 8 spikes on either sides as well as two holes at both ends with an inside thread of 20mm in diameter (M20). The spike rows are offset by half the spike spacing in the longitudinal direction. With a total length of 213mm, the standard connector weighs approximately 1.3kg. According to technical specifications, dimension tolerances range around +/-0.5mm. In reality, longitudinal tolerances of up to 5mm were observed. This posed some challenges in the fabrication process of the beam element, as the precisely machined hole lines could not accommodate connectors with such large dimensional deviations. For this reason about 20% of the connectors could not be used.

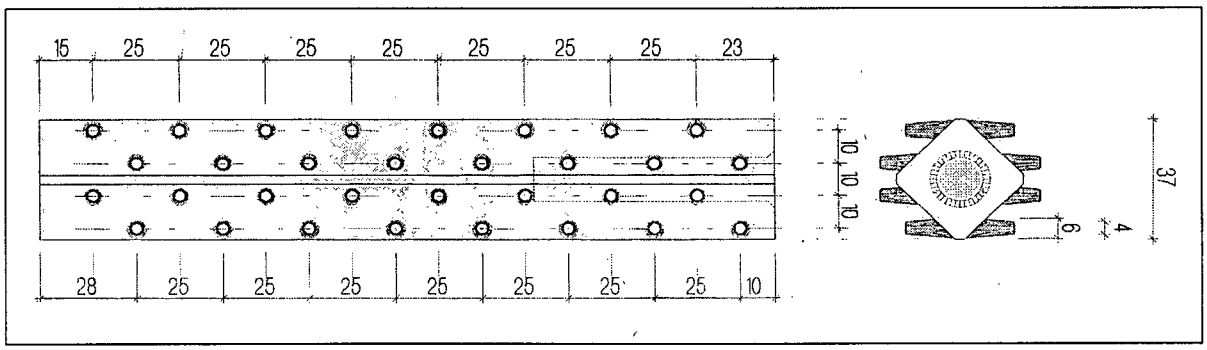

Figure 40: *Connector type A*

3.1.7 INDUO-connector type B

Being a further development, connector type B differs from type A in shape and material. Type B consists of spherical cast iron of EN-GIS-500-7 grade, defined in EN1563 with a characteristic ultimate tensile strength $f_{u,k}$ = 500 N/mm^2 and a characteristic yield strength $f_{y,k}$ = 320 N/mm^2. Weighing approximately 1.7kg, the standard connector has a total length of 247.8mm. The manufacturing process is the same as for type A.

Comparing both type A and B, the shape of the main body is similar, whereas form and number of the load-bearing spikes was significantly modified. The 64 small spikes were substituted by 2 rows of 6 33mm long dowel-like pins on both sides.

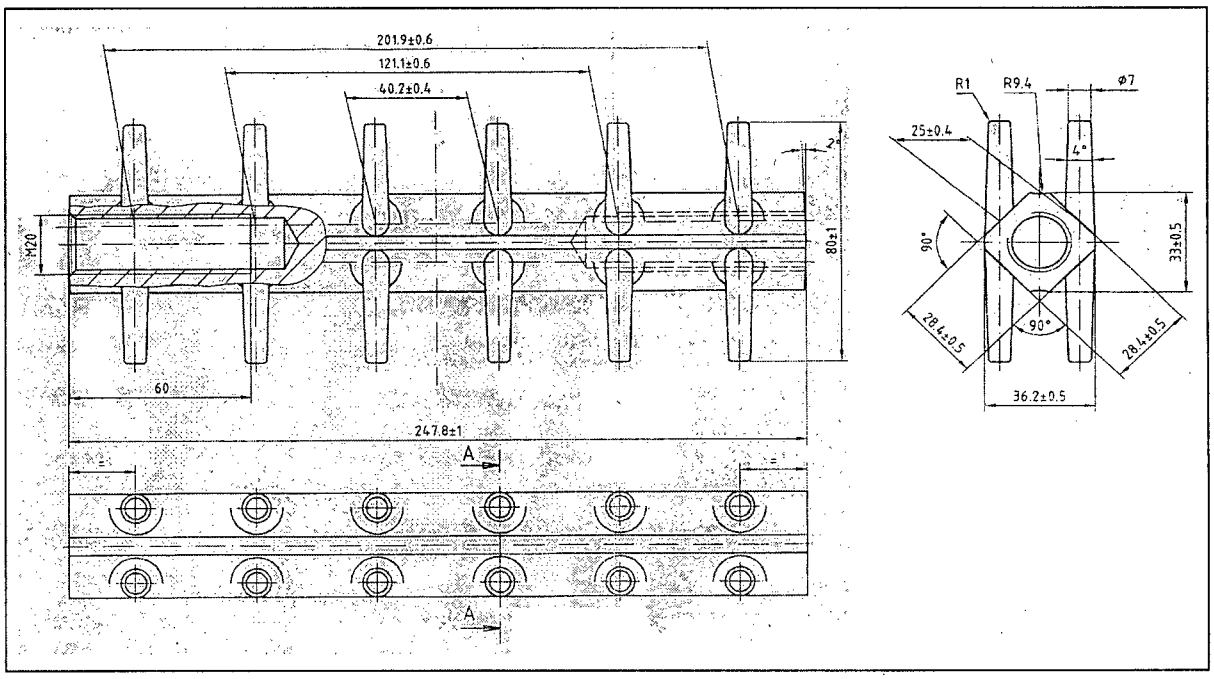

Figure 41: *Connector type B*

Based on a calculation model which classifies the INDUO-connection as 'tight-fitting dowel joint with embedded steel plate these refinements in shape and material assured the connector behavior commensurate with analytical models used for design equations. This provides design engineers with a rational calculation model and therefore permits the use of the connector without special certification testing.

3.2 Methods

3.2.1 Scope of the test series

To cover all the possible combinations of variables for the test specimens, considering two different connectors, as well as various dimension, lamination and material types, 40 different member types would be required (Table 1). To have a reasonable sample size of 10 per combination, 400 specimens would have to be tested.

Material	*Connector*	*Cross-section*	*Lamination*
Douglas Fir	Type A	100 x 100mm	glued-laminated
Douglas-Fir plywood	Type B	120 x 120mm	screw-bonded
Microllam®LVL			
Parallam®PSL			
TimberStrand®LSL			

Table 1: *Test variables*

To keep the testing program within the budgetary limitations, the total number of test specimens was set to 100 members. It was decided to investigate the different member combinations in two separate test series, gaining basic information on general connection behavior first and then focusing on one particular combination. To keep track of the various set-ups, a member code indicates important parameters:

(S-) MA1-100

The first character (**M**A1-100) specifies the material:

M	for	Microllam®LVL
P	for	Parallam®PSL
T	for	TimberStrand®LSL
D	for	Douglas-Fir
X	for	Douglas-Fir plywood (50 & 60mm)

The second character (M**A**1-100) indicates the connector type:

A	for	Type A
B	for	Type B

The last number (MA1-**100**) stands for the member cross-section:

100	for	100x100 mm
120	for	120x120 mm

The first numerical character (MA**1**-100) indicates the sequential numbering of the specific member combination. The prefix ***S*** (**S**-MA1-100) indicates that the specimens' timber halves are connected by screws; instead of glued.

In test series 1 only glued-laminated specimens were tested with a sample size (in brackets) of 2 and 3, respectively. These combinations are:

MA-100 *(2)*	***MA-120*** *(2)*	***MB-100*** *(2)*	***MB-120*** *(3)*
PA-100 *(2)*	***PA-120*** *(2)*	***PB-100*** *(2)*	***PB-120*** *(3)*
TA-100 *(2)*	***TA-120*** *(2)*	***TB-100*** *(2)*	***TB-120*** *(3)*
DA-100 *(2)*	***DA-120*** *(2)*	***DB-100*** *(2)*	***DB-120*** *(3)*
XA-100 *(2)*	***XA-120*** *(2)*	***XB-100*** *(2)*	***XB-120*** *(3)*

A small number of screw-laminated specimens were tested as a side study:
S-TA-100, ***S-TB-100***, 1 member each

The total number of specimens for test series 1 was 47.

Test series 1 was meant to point out performance trends of different member set-ups as well as to provide information for a better understanding of how individual parameters may influence the tensile strength and the failure mode.

Based on the data being assessed from series 1, further considerations in terms of gathering more applied results led to more focused research on one promising combination in series 2. Since the self-made thick plywood does not represent an officially approved construction material and the manufacture of connector type A was recently stopped, although providing interesting data in series 1, both components were

excluded from further research. In addition, it was agreed to focus on the smaller cross-sectional member dimension – 100x100mm.

In general, the manufacture of screw- or nail-laminated wood members does not require product certifications, such as glue permits. To facilitate the fabrication process, the use of screws to bond the timber halves is therefore a promising alternative to the traditional production of the INDUO-beam and was thus included in a side study in test series 2.

In conclusion, it was decided to examine the following combinations:

S-MB-100 *(5)*	***MB-100*** *(8+2)*
S-PB-100 *(5)*	***PB-100*** *(8+2)*
S-TB-100 *(5)*	***TB-100*** *(8+2)*
S-DB-100 *(5)*	***DB-100*** *(8+2)*

The total number of tests in series 2 was 52. Considering previously tested specimens from series 1, the sample sizes for glued-laminated and screw-bonded members were 8 and 5, respectively. In summary, for both series, 99 test specimens were built and tested with 78 type B and 21 type A members.

3.2.2 Connection Design

Performance and strength of wood-to-steel connections is significantly governed by the spacing and the end distances of fasteners, as well as the dimensions of connected members.

Embedded in the end grain of the composite member, the position of the INDUO-connector and its first pair of pins and spikes respectively was set to 10d from the loaded edge, resulting in 80mm end distance for connector type B and 50mm for type A. The pin spacing is predetermined by the geometry of the fastener itself.

<u>Connector type A:</u>

The connector body features four staggered rows of eight *spikes* on each side. The spacing of the spikes in the lengthwise direction is 25mm and 10mm in the transverse direction. Due to significant fabrication tolerances, the connector and its tapered spikes, 12mm long and 5mm in average diameter, require largely oversized holes (d = 7 - 8mm).

Initial slip of the connection is reduced in the assembly process by simply tightening the connecting bolt. The member cross-section is limited to a minimum of 80 x 80mm.

Connector type B:

Instead of a staggered alignment, the 33mm long *pins*, attached to both sides of the connector in two rows of six pins each, are arranged in an orthogonal matrix. The spacing in the lengthwise direction is 40.2mm and 25mm in the transverse direction. Precisely manufactured, type B's tapered pins (d_{avg} = 8mm) are designed to match accurately predrilled tapered holes, creating a press fit and thus eliminating initial slip.

To transfer applied loads, a standard metric bolt (M20) of steel grade 8.8 (640 N/mm^2 yield strength) is typically used to join the connector with other structural elements. In the research project M20-bolts of the best available grade 10.9 (900 N/mm^2 yield strength) were utilized, providing a maximum tensile load capacity of 176kN according to EuroCode3.

Due to various considerations, it was decided to install the INDUO-connector only at one end of the test member, thus requiring an appropriate support at the opposite end.

Since well-founded data on the connector's ultimate tensile strength is not available and preliminary information on performance and strength was needed to design the opposite support, a single tension test with two type B connectors installed at both ends of an LVL-member was conducted. Failure occurred in one joint at a load of 127kN. Considering a stronger material to fail at a higher load level and desiring the test member to fail around the INDUO-connection, an opposite support system had to be strong enough to resist at least 200kN.

Shear plate and split ring connections are known for high load capacities, but the tools required to manufacture the joint are very costly. For this reason a shear-plate-like connection with an estimated capacity of roughly 230kN was manufactured. Ring segments, cut from hydraulic tubing and welded to one face of a steel plate unite both components of a shear plate joint in one element, creating a strong and easy to assemble wood-to-steel connection, hereafter referred to as 'Ring Side Plates'.

Ring Side Plates and couplings needed to connect to the test apparatus represent the 'lower support', whereas the INDUO-connector and its related couplings are referred to as 'upper support'.

The lower support consisted of the following:

- A pairs of Ring Side Plates, mild steel of grade 300W
- Two 7/8inch bolts (d=22.2mm), washers and nuts
- Coupling block, mild steel of grade 300W
- Two 1inch bolts (d=25.4mm), washers and nuts
- Threaded coupling rod 1½ inch -12, (d=38.1mm)
- Spacer plates: 2 x 5mm and 2 x 10mm thick with a pair of holes (d=26.4mm)

Neither of the above mentioned materials were tested as these elements were over-designed and would thus be expected to remain linear elastic.

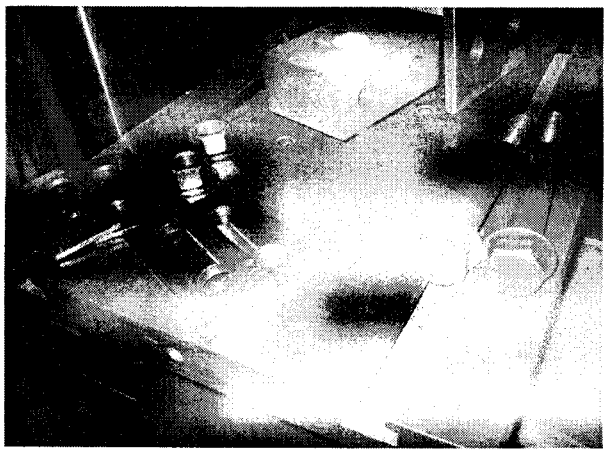

Figure 42: *Components of lower support*

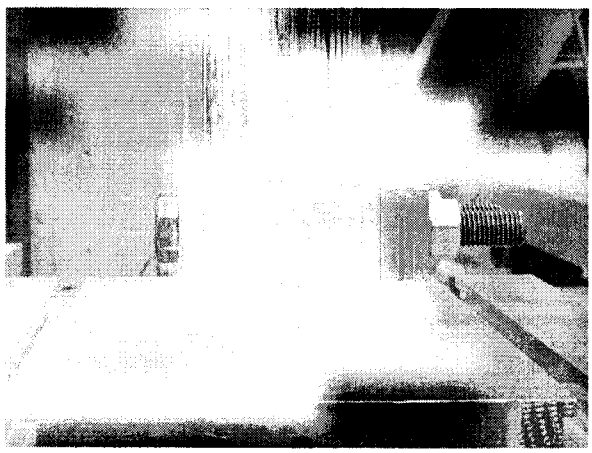

Figure 43: *Lower support assembled*

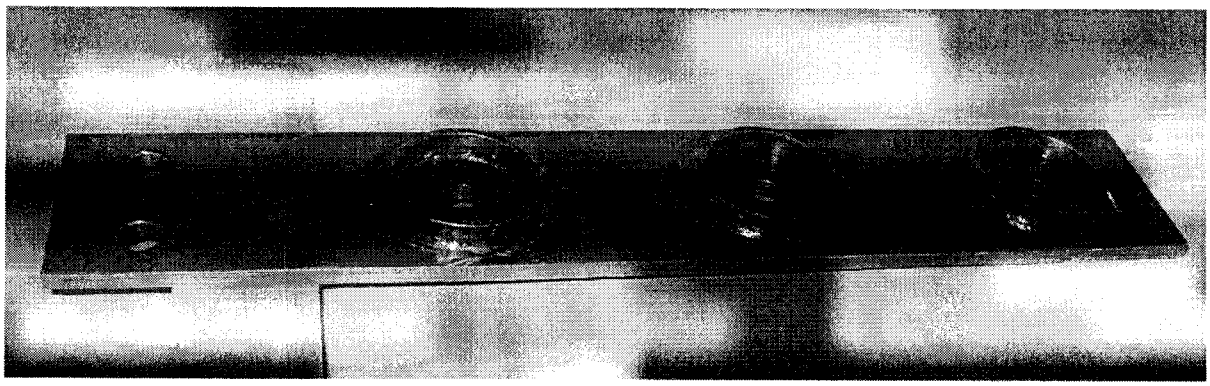

Figure 44: *Ring Side Plate*

The upper support consisted of the following:

- M20 steel rod, high-strength steel of grade 10.9 (EC3); washers and nuts
- Steel plate, fixed to steel rod
- Steel coupling, M20 and 1½ inch -12 (d=38.1mm) inside-threads on opposite sides
- DCDT measuring device to determine the displacement of the connection

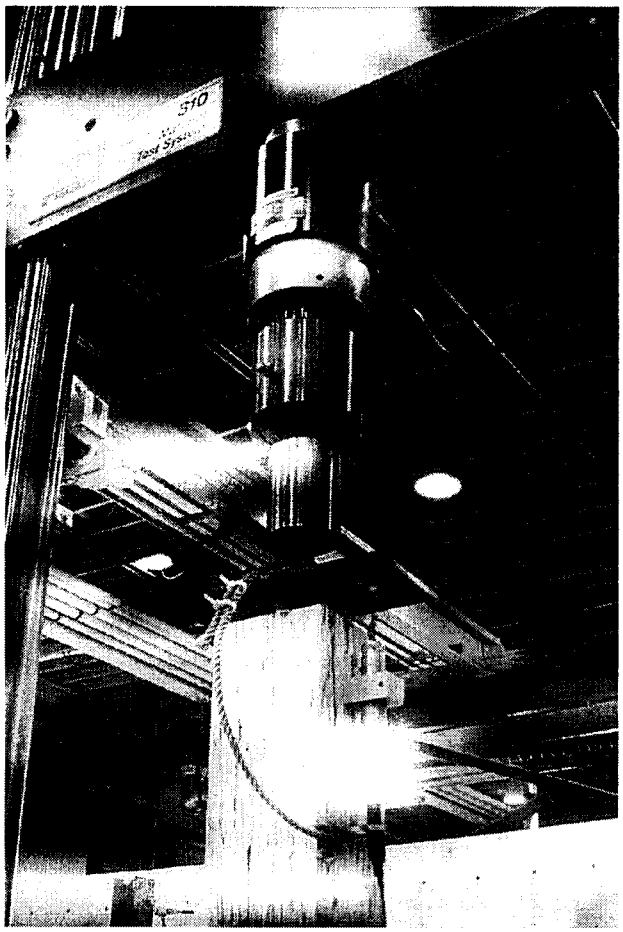

Figure 45: *Upper support*

3.2.3 Fabrication of test specimens

Typically an INDUO-element is built-up by two timber halves and the end-grain embedded connectors. The procedure is as follows:

1. ***Breakout*** *(table saw, four-sided planer):*
   - If necessary, lumber and wood products respectively are ripped, cut to length and planed to S4S-quality[4]

     Final dimension for a) 120x120mm test specimens: 1530 x 134 x 60mm

     b) 100x100mm test specimens: 1530 x 134 x 50mm

2. ***Secondary processing*** *(CNC-router):*

   Inside face of timber halves:
   - Drill rows of holes

     Type A: Four parallel rows of 8 holes, d = 8mm, staggered holes matrix, depth:19mm (outer row of holes) and 30mm (inner row of holes)

     Type B: Two parallel rows of 6 tapered holes, d = 7 to 9.5mm, depth: 40.4mm
   - Cut V-groove, depth: 20mm, length: 400mm

   Outside face of timber halves:
   - Mill three circular grooves, d = 101.6mm, width: 6mm, depth: 20mm, (for Ring Side Plates)
   - Drill two holes, d = 23mm, (for 7/8-inch bolts)

3a. ***Assembly*** *of glued-laminated members (hydraulic press):*
   - Apply adhesive on inside faces of timber halves
   - Sandwich connector between timber halves
   - Move composite member into veneer press and press for approximately 30 minutes until glue is cured.

3b. ***Assembly*** *of screw-bonded members:*
   - Sandwich connector between timber halves and clamp the setup to assure position
   - Pre-drill and countersink holes (d=4mm) to accommodate woodscrews (6x10)
   - Connect timber halves with a set of eight countersunk head woodscrews (for screw alignment see figure 47a)

4. ***Finish*** *(shaper):*
   - Taper end grain cross-section to desired 100x100mm and 120x120mm respectively (at the end where INDUO-connector is embedded)

The Appendix under section 8.1.1 shows a detailed photographic documentation of all manufacturing steps.

[4] Faces and edges are soundly planed to create a rectangular cross-section

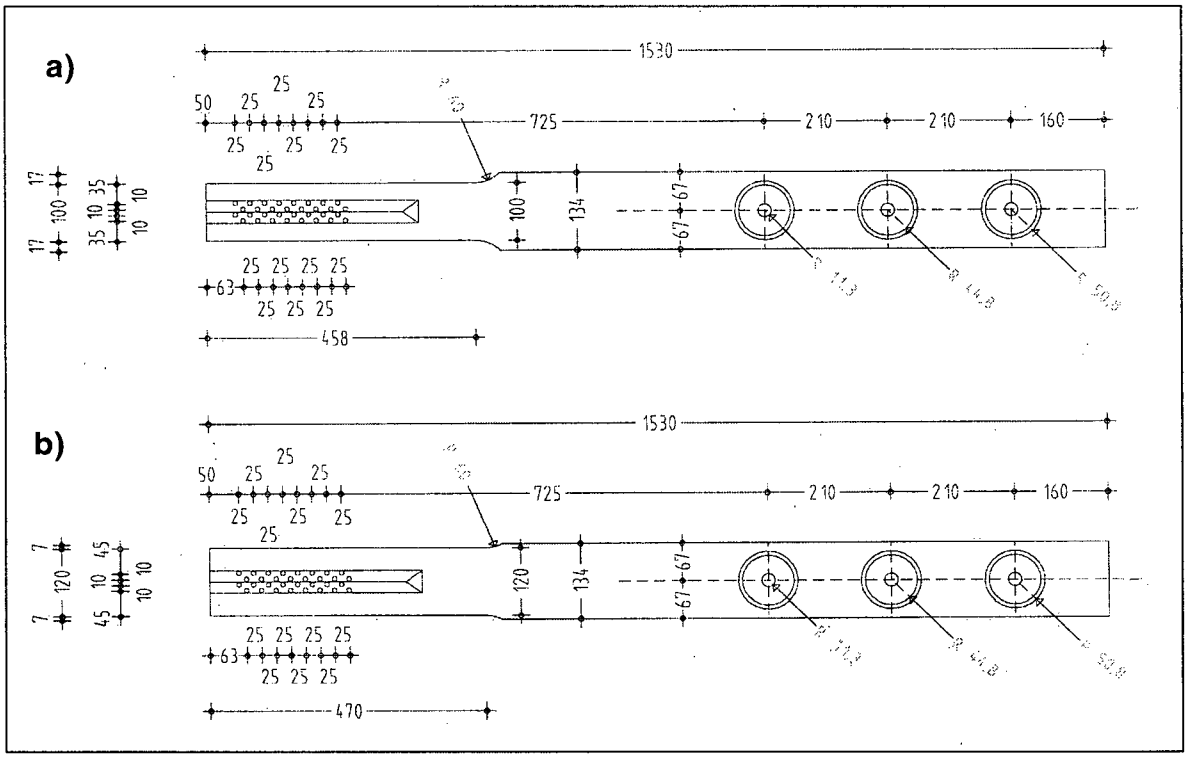

Figure 46: *Plan of timber halves:*
a) type A –100 combination; b) type A – 120 combination

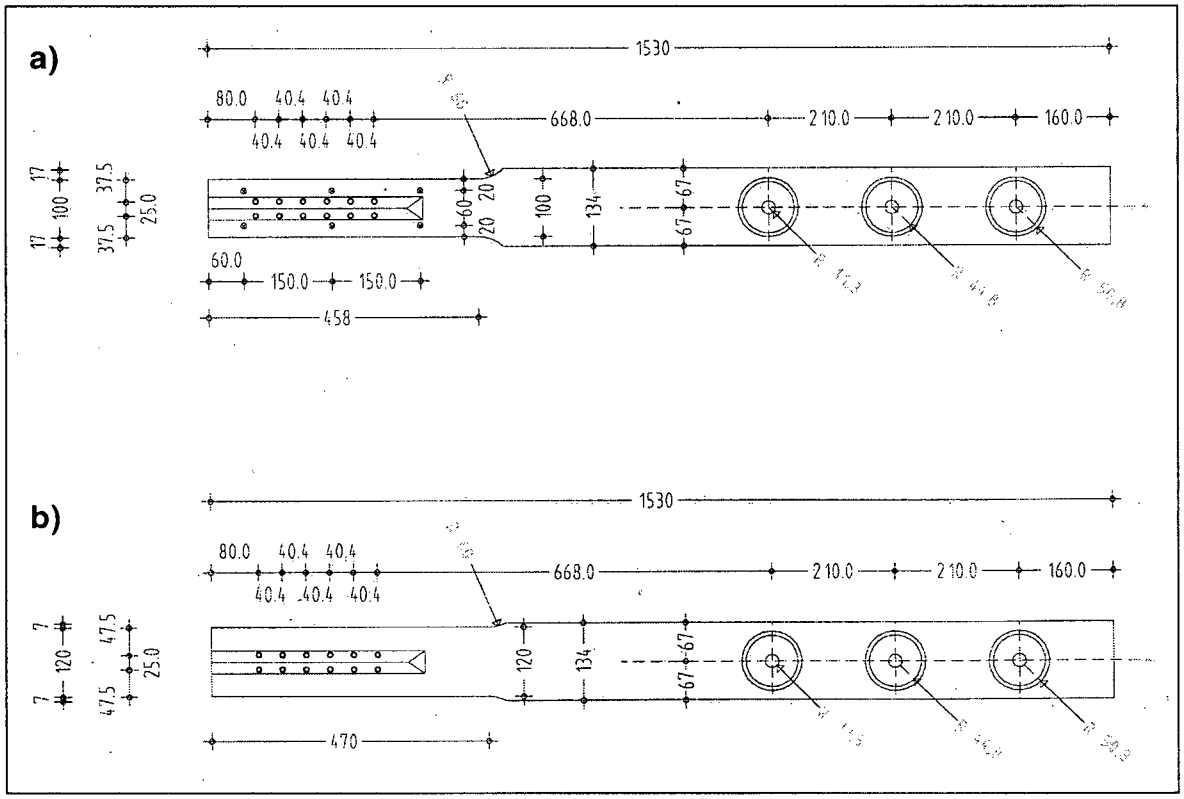

Figure 47: *Plan of timber halves:*
a) type B –100 combination, screw-bond; b) type B – 120 combination

3.2.4 Experimental setup

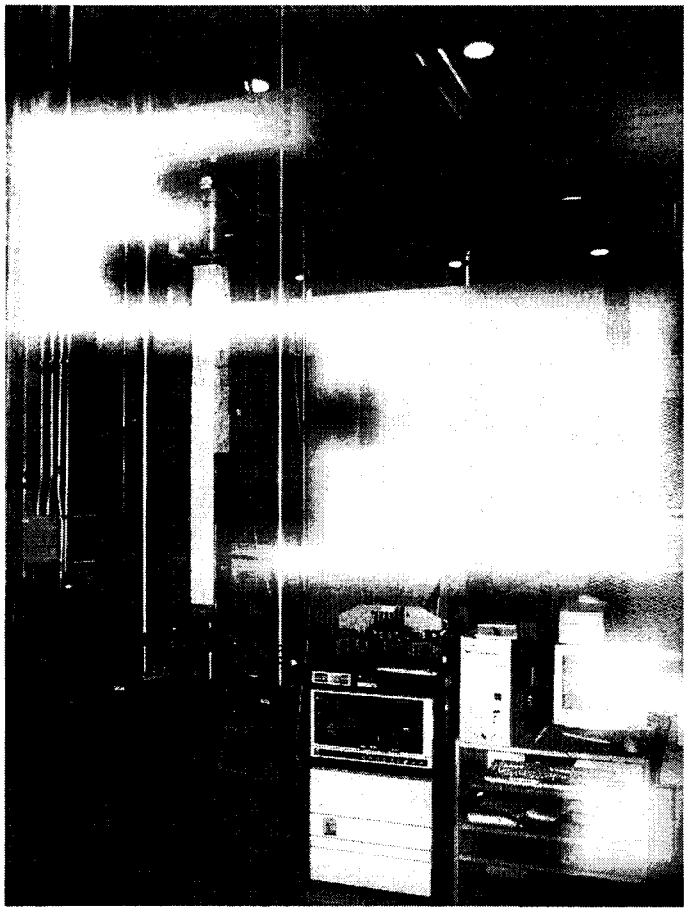

Figure 48: *Experimental setup: MTS 810 with control system and test member*

The experimental setup consists of 3 components:

1. ***Test apparatus***

   All tension tests were conducted in the Timber Engineering laboratory on a servo-controlled hydraulic testing machine (MTS 810), with a maximum capacity of 250kN. The main parts of the machine are:

   - Solid and heavy machine body
   - Two cylindrical guide rails, featuring a cross-head, adjustable in vertical direction and to be locked at a desired height
   - Load cell to be suspended from the center of the cross-head, accommodating a pivoted coupling device to provide axial alignment of the specimen setup
   - Movable machine table, operated by a hydraulic power unit
   - Hydraulic system

2. *Control system*

The control system is built up by a servo-controller and a personal computer. The servo-controller regulates the hydraulic system by controlling the stroke of the machine table. An integral data acquisition system processes all the electronic data input of displacement and load measurements. Running *LabTech Notebook pro software, version 10.1*, the computer controls the data recording and converts the information received from the servo-controller unit into an ASCII file. Load, stroke and displacement of the INDUO-connection were sampled and recorded at 2 Hertz. A monotonic loading rate of 1.2mm/min forced the specimens to fail in five to seven minutes.

3. *Test member*

Consisting of the specimen as well as the lower and upper support, the test member is the main component of the experimental setup. Figure 50 shows the standard setup of the upper support with a DCDT[5] measuring the displacement of the INDUO-connection. Couplings and fasteners at both ends of the member complete the setup of the test member.

Figure 49: *Test member*

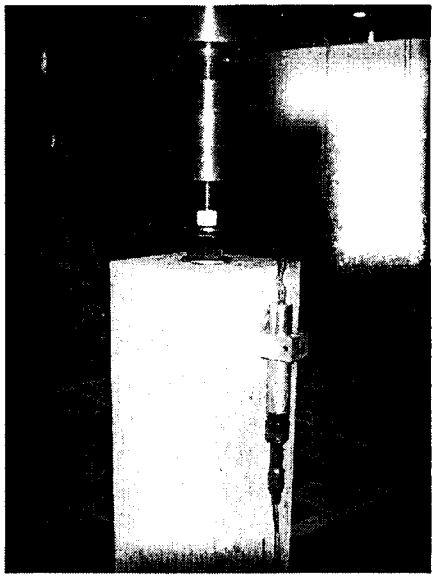

Figure 50: *Upper support featuring a DCDT measuring device*

[5] DCDT: Direct Current Displacement Transducer

3.2.5 Test procedure

Since length and basic member setup were kept the same for all specimens, all the tests were conducted on one schedule, which can be described as follows:

Mounting of test member

- Connect specimen with threaded rod and upper coupling
- Lift specimen onto machine table and screw coupling onto pivoted support of cross beam
- Screw DCDT attachment to specimen
- Install DCDT and adjust vertical position
- Mount Ring Side Plates by means of two clamps, pressing fasteners into the grooves of the specimen
- Fasten side plates with two 7/8inch bolts
- Connect side plates with coupling block, using spacer plates to accomodate different member dimensions
- Fasten lower coupling with two 1inch bolts

Test

- Start the test program
- Watch the control panel and take notes of incidents occurring during test, such as cracking noises or general performance of specimen being loaded
- In case of premature failure, stop data recording
- In case of surviving the 180kN load limit, stop loading and data recording
- Release residual load and disassemble test member in reverse order

Documentation (after completion of test series)

- Cut off 400mm long end grain piece from each specimen
- Disassemble screwed or rip glued-laminated members along glue line to separate timber halves
- Photograph damaged and deformed connection details
- Document in detail all significant information

The Appendix under section 8.1.2 provides detailed photographic information on the test procedure.

4 Results

Summarizing the experimental results of the research been conducted, the following sections present the analyzed data of test series 1 and 2. Each section will describe the behavior observed during load application and will present information on ultimate strength and displacement. In addition, section 4.2 will provide statistics on average ultimate strength and stiffness of test series 2 combinations (see section 8.2 for calculations).

Picturing the failure area of each member, section 8.1.3 presents detailed photographic information of occurred failure modes. In varying combinations all four known failure mechanisms were observed (Figure 51).

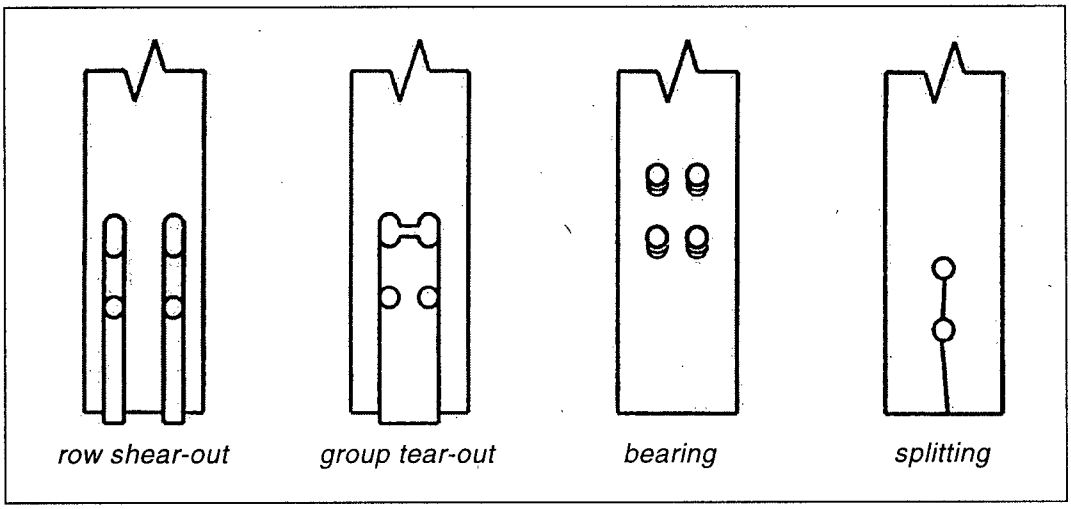

Figure 51: *Connection failure modes*

The moisture content and dry density of all tested specimens were determined according to ASTM D2395-93. The results are presented in the following table:

Moisture Content [%]

	LSL (24 spec.)	DG Fir (22 spec.)	PSL (22 spec.)	LVL (22 spec.)	X-LVL (9 spec.)
mean	6.2	13.6	8.8	7.3	8.0
std dev	0.1	2.7	0.3	0.2	0.2
COV	1.6%	19.6%	3.7%	2.1%	2.6%

Density [g/cm³]

	LSL	DG Fir	PSL	LVL	X-LVL
mean	0.68	0.53	0.66	0.58	0.52
std dev	0.02	0.05	0.01	0.01	0.01
COV	3.6%	9.7%	1.8%	1.4%	2.3%

Table 2: *Moisture content and density of tested specimens*

4.1 Test series I

The following member setups were tested under tensile loading:

MA-100	***MA-120***	***MB-100***	***MB-120***
PA-100	***PA-120***	***PB-100***	***PB-120***
TA-100	***TA-120***	***TB-100***	***TB-120***
DA-100	***DA-120***	***DB-100***	***DB-120***
XA-100	***XA-120***	***XB-100***	***XB-120***

and ***S-TA-100, S-TB-100***

Based on observations during the testing, it was decided to group the specimens according to general performance and failure mode. In doing so, TimberStrand®LSL and Douglas-Fir plywood, which exhibited superior and Douglas Fir and Microllam®LVL, with weaker properties, were configured in groups I and II, respectively. Due to inconsistent performance, Parallam®PSL was not assigned to either of the aforementioned groups and was separately analyzed.

Table 3 gives an overview of analyzed data collected in test series 1, showing the ultimate load, the load level where significant cracking noises were observed and in what manner the connection finally failed. Due to the test setup, the maximum load that could be applied was 180kN. For this reason test specimens that were not failed are indicated with a maximum load of >180kN.

LSL

Code	Max Load [kN]	cracking noises	failure	comments
TA1-100	124.1	> 60kN	ductile	bearing and splitting perp. to strands
TA2-100	112.7	> 50kN	ductile	bearing and splitting perp. to strands
TA1-120	132.7	> 80kN	ductile	bearing and splitting perp. to strands
TA2-120	130.9	> 70kN	ductile	bearing and splitting perp. to strands
TB1-100	177.6	> 120kN	brittle	failure of glueline
TB2-100	> 180.0	> 145kN	no	failure of glueline
TB1-120	> 180.0	no	no	
TB2-120	> 180.0	no	no	
TB3-120	> 180.0	> 160kN	no	

Table 3: *Analyzed data of test series 1*

X-LVL

Code	Max Load [kN]	cracking noises	failure	comments
XA1-100	104.2	> 45kN	ductile	bearing and splitting perp. to grain
XA2-100	108.2	> 60kN	ductile	bearing and splitting perp. to grain
XA1-120	127.2	> 50kN	ductile	bearing and splitting perp. to grain
XA2-120	119.1	> 40kN	ductile	bearing and splitting perp. to grain
XB1-100	174.2	> 125kN	brittle	net section failure at last pair of pins
XB2-100	163.8	> 130kN	brittle	net section failure at last pair of pins
XB1-120	> 180.0	no	no	
XB2-120	> 180.0	> 140kN	no	
XB3-120	> 180.0	no	no	

DG Fir

Code	Max Load [kN]	cracking noises	failure	comments
DA1-100	99.4	> 55kN	rather ductile	bearing and splitting
DA2-100	82.0	> 50kN	rather ductile	bearing, splitting and group tear-out
DA1-120	96.7	> 70kN	rather ductile	bearing and splitting
DA2-120	95.4	> 60kN	rather ductile	bearing and splitting
DB1-100	165.2	> 90kN	brittle	violent failure, row shear-out along rows of holes
DB2-100	165.8	> 105kN	brittle	violent failure, splitting, deformed pins
DB1-120	> 180.0	> 140kN	no	close to failure, heavy crack. noises
DB2-120	> 180.0	> 120kN	no	close to failure, heavy crack. noises
DB3-120	155.5	> 90kN	brittle	splitting along rows of holes

LVL

Code	Max Load [kN]	cracking noises	failure	comments
MA1-100	81.3	> 45kN	brittle	bearing, splitting and group tear-out
MA2-100	72.0	> 35kN	rather ductile	bearing, splitting and group tear-out
MA1-120	76.0	> 30kN	rather ductile	bearing and splitting
MA2-120	81.9	> 50kN	rather ductile	bearing and splitting
MB1-100	139.9	> 70kN	brittle	splitting along rows of holes
MB2-100	169.7	> 100kN	brittle	splitting with group tear out, deformed pins
MB1-120	145.0	> 105kN	brittle	splitting along hole line, deformed pins
MB2-120	167.6	> 120kN	brittle	splitting along hole line, ripped-off pins
MB3-120	163.9	> 110kN	brittle	splitting and group tear-out, deformed pins

Table 3 (continued): *Analyzed data of test series 1*

PSL

Code	Max Load [kN]	cracking noises	failure	comments
PA1-100	90.0	> 40kN	brittle	bearing, splitting and group tear-out
PA2-100	98.9	> 50kN	brittle	bearing, splitting and group tear-out
PA1-120	100.5	> 60kN	rather ductile	bearing, splitting and group tear-out
PA2-120	87.0	> 45kN	rather ductile	bearing, splitting and group tear-out
PB1-100	143.6	> 100kN	brittle	splitting, group tear-out, deformed pins
PB2-100	166.1	> 110kN	brittle	splitting, deformed pins
PB1-120	171.3	> 105kN	rather ductile	splitting along rows of holes, deformed off pins
PB2-120	157.5	> 90kN	brittle	splitting along rows of holes, ripped-off pins
PB3-120	151.0	> 110kN	rather ductile	splitting along rows of holes, deformed off pins

Table 3 (continued): *Analyzed data of test series 1*

4.1.1 Group I (TimberStrand®LSL & Douglas-Fir plywood)

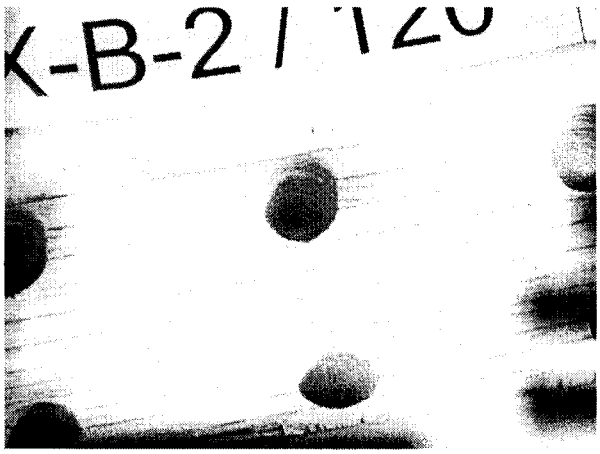

Figure 52: *Group I: No failure for connector type B combinations*

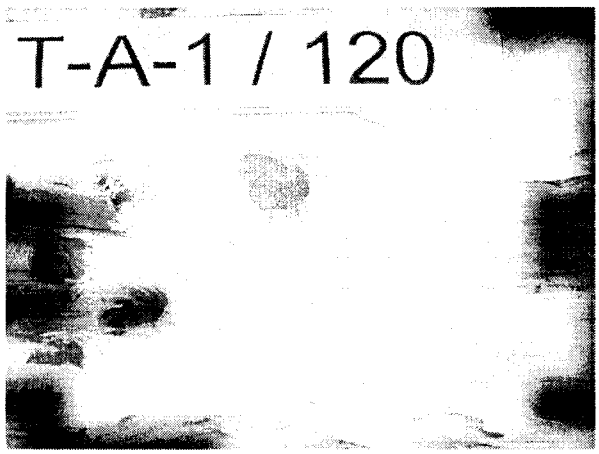

Figure 53: *Group I: Severe bearing; a typical failure mode for connector type A combinations*

In terms of strength and stiffness, combinations of connector type B and LSL or X-LVL outperformed all other specimens of the test series. None of the larger 120x120mm cross-sections could be failed at the maximum test load of 180kN. Damage to the fiber structure or deformation of the connector was not observed (Figure 52). While loading the test specimen, cracking noises indicating failure propagation, were rarely observed. Some of the smaller type B dimensions (100x100mm), however, failed. While both had a similar stiffness and high ultimate loads, LSL specimens typically failed due to a poorly

fabricated glue bond, whereas some X-LVL members experienced a sudden net section failure of the wood around the last pair of pins. In both cases failure was not governed by the connection itself.

All connector type A combinations failed before reaching the 180kN test limit. After linear-elastic behavior up to an average of 95kN, the connection showed a comparatively ductile performance, before most of the specimens finally failed in a brittle manner caused by splitting perpendicular to the strands and the veneer layers, respectively. Investigating the failure area, the wood structure of the spike holes was significantly damaged due to excessive bearing (Figure 53). Displacements of more than 150% of the spike diameter were measured. The average ultimate load determined for LSL specimen was 125kN and 115kN for X-LVL.

Interesting data was collected from the screw-laminated members S-TA1-100 and S-TB1-100. Compared to their glued-laminated counterparts, the screw-bonded specimens seemed to perform similarly or even better. Providing above average stiffness, S-TB-100 was not failed. The type A specimen presented the highest ultimate load of all TA combinations and remained on a high level before failing rapidly in splitting and shear (Figure 55).

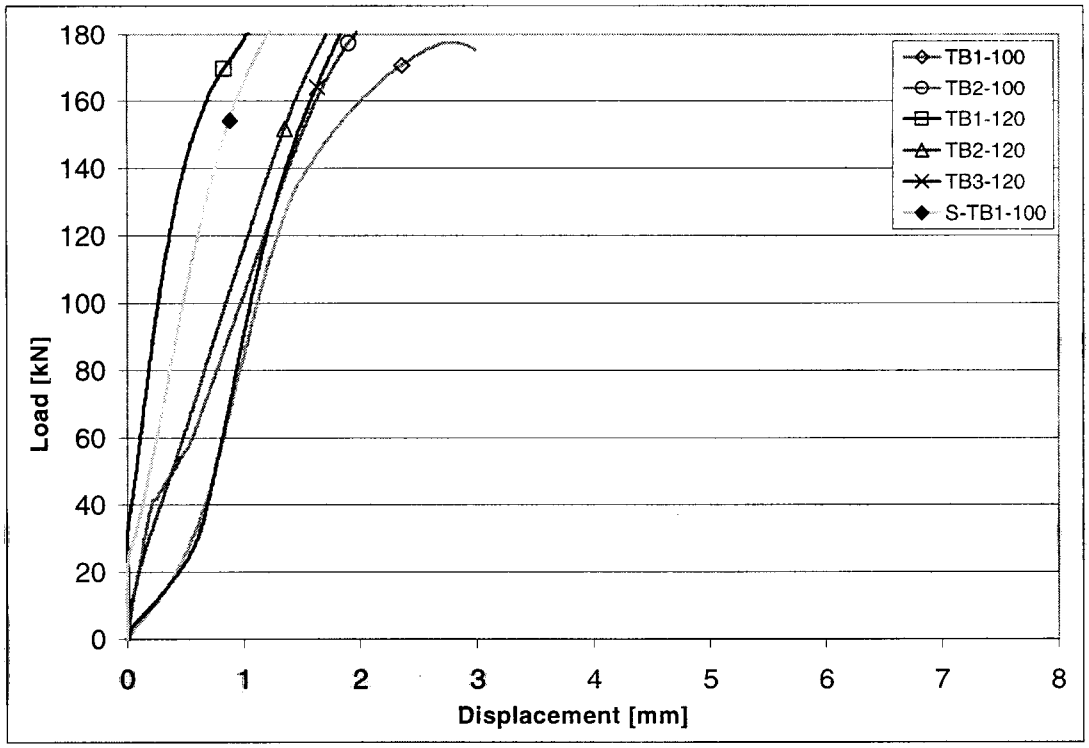

Figure 54: *Load-displacement curves of TB-combinations*

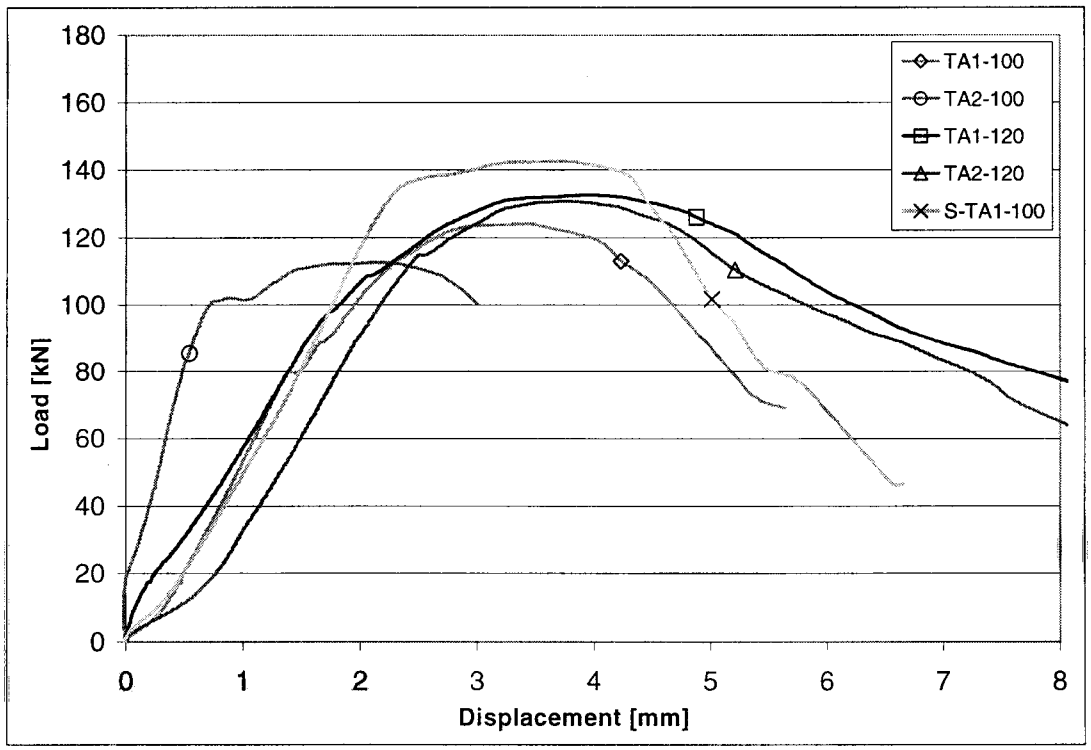

Figure 55: *Load-displacement curves of TA-combinations*

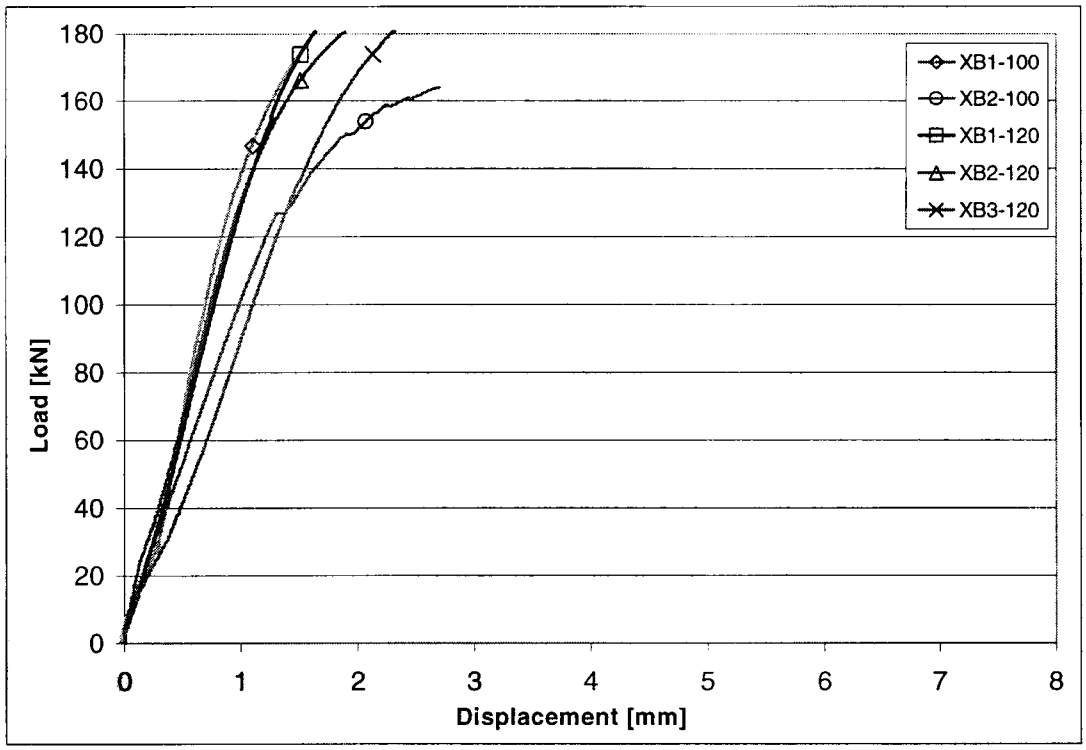

Figure 56: *Load-displacement curves of XB-combinations*

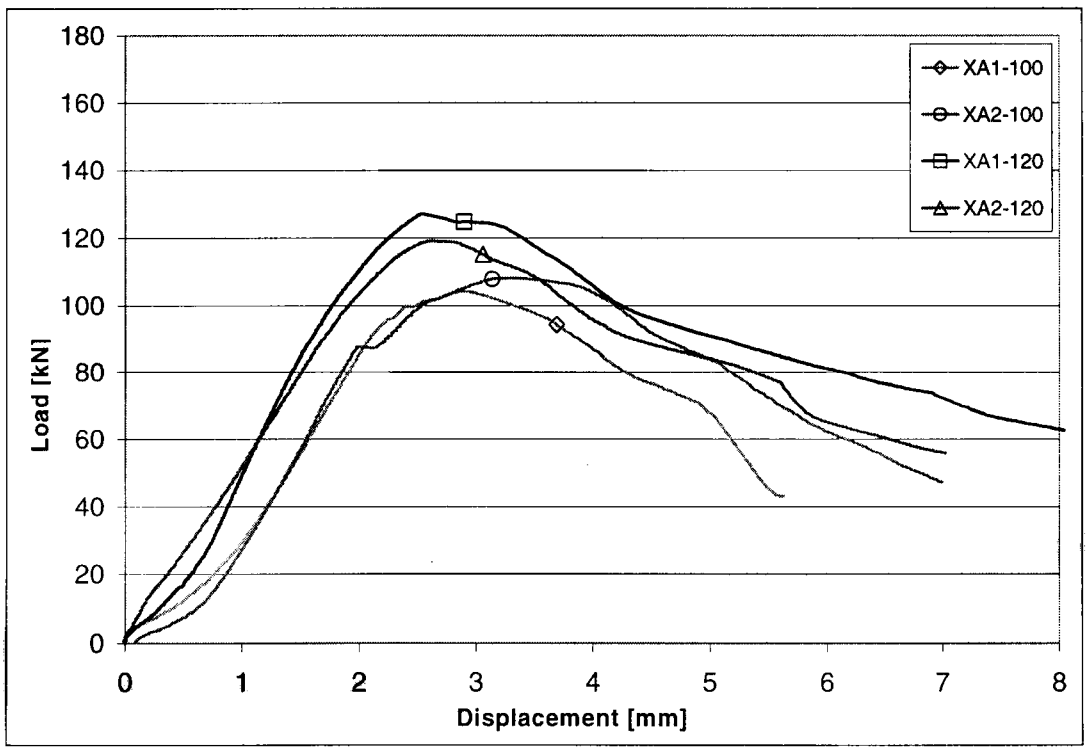

Figure 57: *Load-displacement curves of XA-combinations*

4.1.2 **Group II** (Douglas Fir & Microllam®LVL)

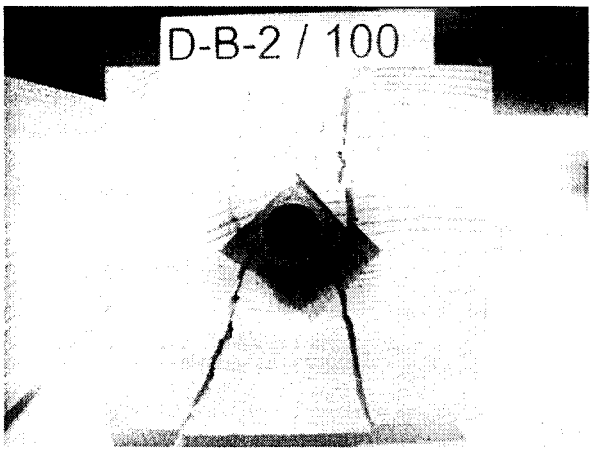

Figure 58: *Group II: Splitting along the rows of holes; a typical failure mechanism of connector type B combinations*

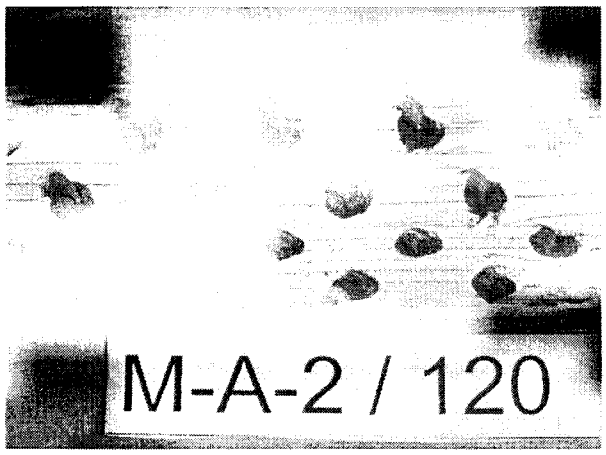

Figure 59: *Group II: Bearing and relatively large displacements due to shear failure of connector type A combinations*

Two major trends were observed in this group:

- Combinations with connector type A showed relatively ductile failure characteristics after reaching the maximum load with a comparatively low average ultimate load of 77kN for LVL and 93kN for Douglas Fir.
- Unlike type A specimens, connector type B combinations provided higher stiffness and ultimate strength, but typically failed in a very brittle and abrupt manner, providing an average ultimate load of 157kN for LVL and 169kN for Douglas Fir.

In general, severe splitting and shear failure along the rows of holes caused the sudden failure. In addition, Type A specimens sustained significant bearing and group tear-out.

The pins of failed type B connectors were deformed and showed cracks at the pin base (Figure 131f, page 107). For type A connectors no evidence of damage to the connector was observed.

Although two out of the ten type B specimens (DB1-120 and DB2-120) survived, severe cracking noises just before reaching the limit load and a delayed failure of DB2-120 15 seconds after the loading had stopped, indicated that 180kN is near the ultimate load.

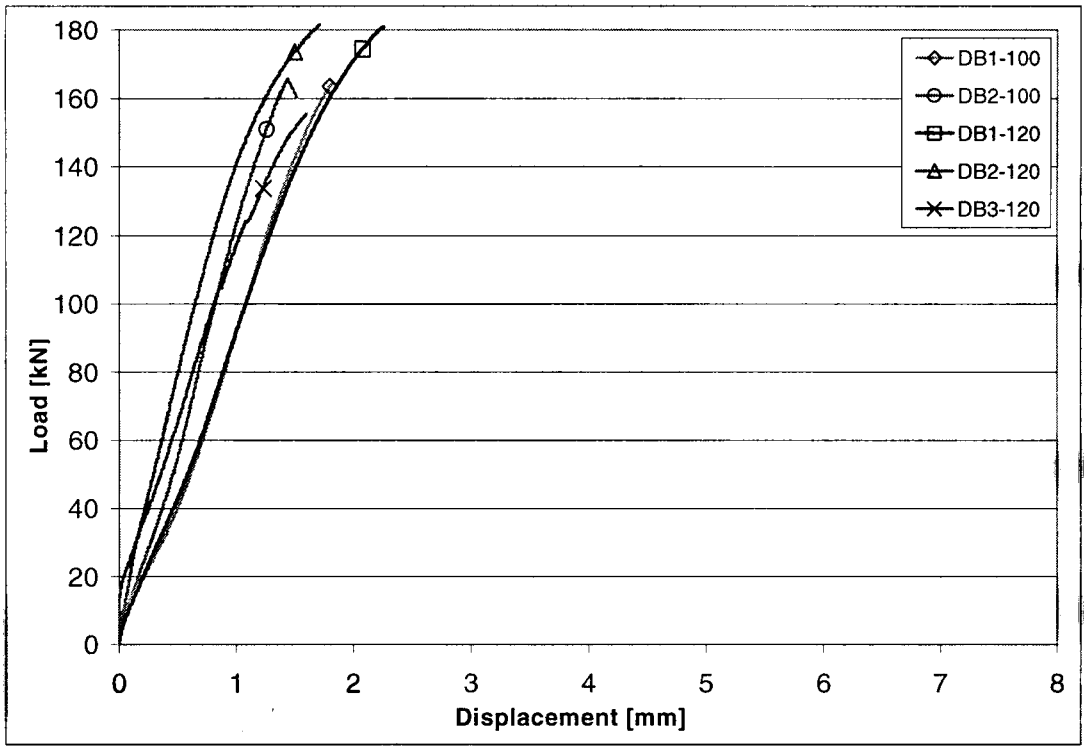

Figure 60: *Load-displacement curves of DB-combinations*

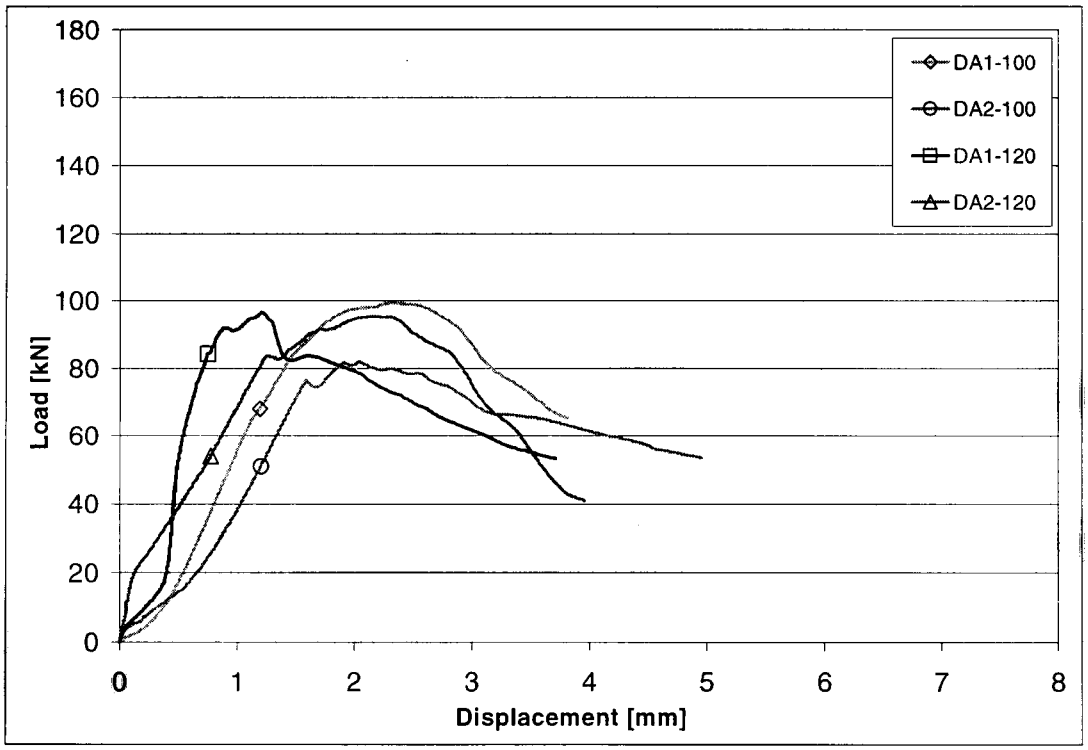

Figure 61: *Load-displacement curves of DA-combinations*

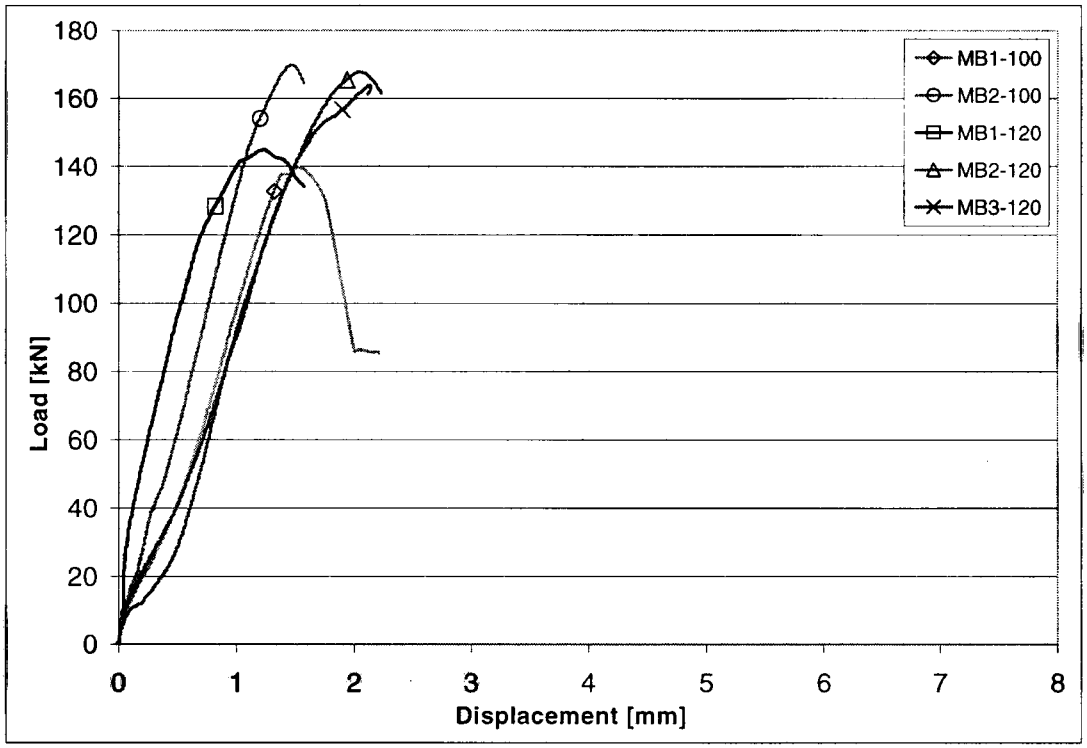

Figure 62: *Load-displacement curves of MB-combinations*

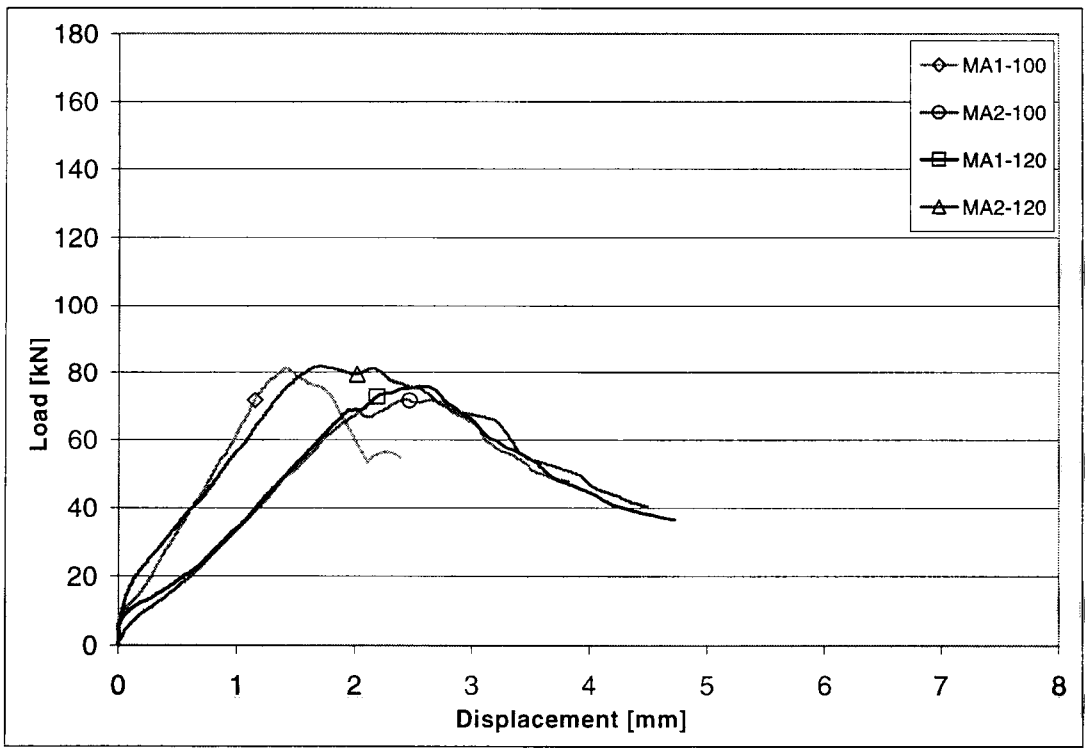

Figure 63: *Load-displacement curves of MA-combinations*

4.1.3 **Group III** (Parallam® PSL)

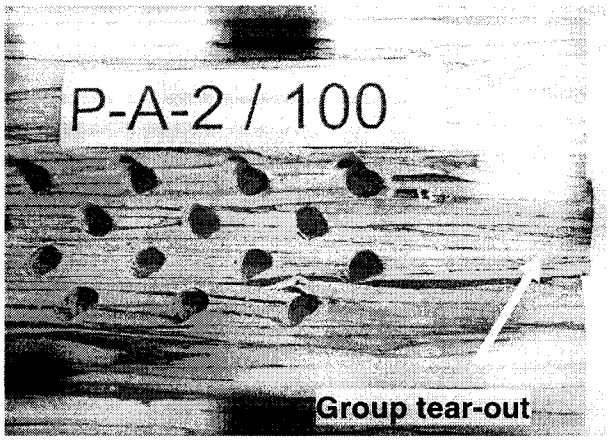

Figure 64: *Group III: Bearing and tear-out of connector type A combinations*

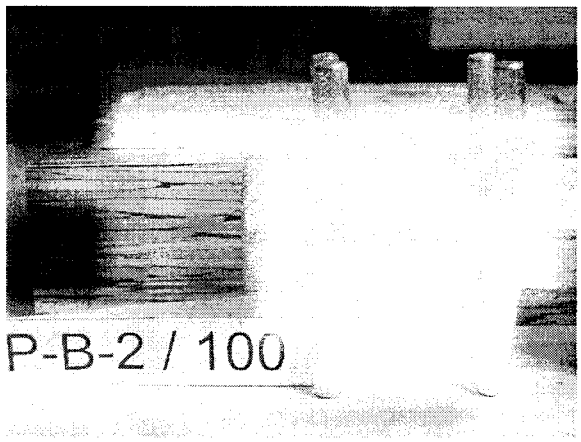

Figure 65: *Group III: Connector type B combinations with severe pin deformations or fracture*

As evident from the inconsistent performance for both type A and type B combinations, the connection's performance was governed by the local interaction of pins or spikes and the strand structure and was thus relatively random. The cavities between the strands seemed to act like pre-occurred damage to the wood structure. Therefore, an above average accumulation of these cavities in the area of a pin or spike hole led to premature crack propagation, resulting in splitting and a brittle failure mechanism. Investigating the connection region of type B members, it was found that specimens with a more interwoven strand layout performed in a more ductile manner, whereas members with strictly parallel alignment had failed in a brittle way. The advantageous interlocking of strands seemed to have less effect on type A connections.

In general, type A specimens failed due to severe bearing followed by shear-off along the rows of holes. Approaching the ultimate load level, often entire strand segments were torn-out (Figure 64). With heavy deformations and partially ripped-off pins, connection type B's typical failure mechanism was splitting along the rows of holes, dependent on aforementioned parameters resulting in very brittle or more ductile behavior.

The average ultimate loads determined for types A and B specimens were 94kN and 157kN, respectively.

Figure 66: *Load-displacement curves of PB-combinations*

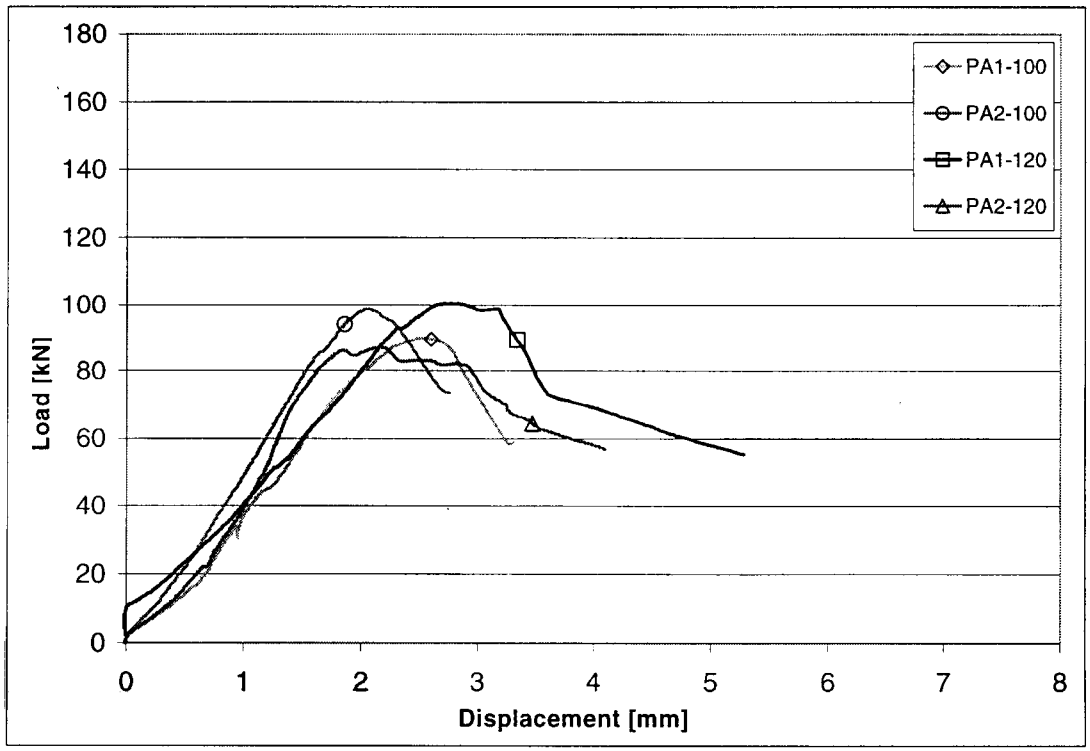

Figure 67: *Load-displacement curves of PA-combinations*

4.2 Test series II

As mentioned earlier, test series 2 consisted of a larger number of specimens with selected attributes. This provided a more representative statistical data base for those connection types that proved to be the most promising for practical applications. The following combinations were tested:

S-MB-100	***MB-100***
S-PB-100	***PB-100***
S-TB-100	***TB-100***
S-DB-100	***DB-100***

Due to a more detailed data set developed for each setup, the specimens were no longer grouped according to observed behavior, but evaluated in their individual connector and material categories.

LSL

Code	Max Load [kN]	cracking noises	failure	comments
(TB1-100)	177.6	> 120kN	brittle	failure due to bad glueline
(TB2-100)	180.0	> 145kN	no	failure of glueline, no connection failure
TB3-100	> 180.0	no	no	
TB4-100	> 180.0	> 170kN	no	
TB5-100	> 180.0	no	no	
TB6-100	> 180.0	> 170kN	no	
TB7-100	> 180.0	> 160kN	no	
TB8-100	> 180.0	no	no	
TB9-100	> 180.0	no	no	
TB10-100	> 180.0	> 170kN	no	
(S-TB1-100)	> 180.0	no	no	
S-TB2-100	> 180.0	no	no	
S-TB3-100	> 180.0	no	no	
S-TB4-100	> 180.0	> 160kN	no	
S-TB5-100	> 180.0	> 170kN	no	

Table 4: *Analyzed data of test series 2*

DG Fir

Code	Max Load [kN]	cracking noises	failure	comments
(DB1-100)	165.2	> 120kN	brittle	violent fail., row shear-out along rows of holes
(DB2-100)	165.8	> 110kN	brittle	violent failure, splitting, deformed pins
DB3-100	177.6	> 140kN	brittle	splitting, group tear-out
DB4-100	> 180.0	> 130kN	no	heavy cracking noises, close to failure
DB5-100	143.5	> 95kN	brittle	early cracking noises, splitting
DB6-100	130.9	> 110kN	brittle	abrupt failure, splitting
DB7-100	151.4	> 120kN	brittle	abrupt failure, splitting
DB8-100	> 180.0	> 150kN	no	heavy cracking noises
DB9-100	> 180.0	no	no	
DB10-100	> 180.0	> 170kN	no	
S-DB1-100	171.3	> 125kN	brittle	abrupt fail., splitting, partial net section fail.
S-DB2-100	173.3	> 130kN	brittle	abrupt failure, splitting, ripped-off pin
S-DB3-100	> 180.0	> 120kN	no	heavy crack. noises, close to failure
S-DB4-100	> 180.0	no	no	
S-DB5-100	170.5	> 90kN	brittle	violent failure, splitting

PSL

Code	Max Load [kN]	cracking noises	failure	comments
(PB1-100)	143.6	> 100kN	brittle	splitting, group tear-out, deformed pins
(PB2-100)	166.1	> 110kN	brittle	splitting, deformed pins
PB3-100	141.7	> 130kN	brittle	abrupt failure, splitting,
PB4-100	135.9	> 120kN	brittle	heavy cracking noises, violent failure, splitting, ripped-off pin
PB5-100	157.7	> 110kN	brittle	splitting, group tear-out
PB6-100	152.9	> 110kN	brittle	violent failure, splitting
PB7-100	166.1	> 150kN	brittle	splitting, strongly deform. pins
PB8-100	171.5	> 100kN	brittle	abrupt failure, splitting
PB9-100	145.5	> 130kN	brittle	abrupt failure, splitting, deform. pins, fissures at pin base
PB10-100	151.9	> 110kN	brittle	violent failure, splitting
S-PB1-100	160.5	> 90kN	brittle	splitting, group tear-out, deform. pins & fissures at pin base
S-PB2-100	166.4	> 120kN	brittle	abrupt failure, splitting
S-PB3-100	156.8	> 100kN	brittle	violent failure, splitting, row of pins ripped-off
S-PB4-100	171.2	> 130kN	brittle	violent failure, splitting, group tear-out
S-PB5-100	> 180.0	> 0kN	no	heavy crack. noises, close to failure

Table 4 (continued): *Analyzed data of test series 2*

LVL

Code	Max Load [kN]	cracking noises	failure	comments
(MB1-100)	139.9	> 70kN	brittle	splitting along rows of holes
(MB2-100)	169.7	> 100kN	brittle	splitting, group tear-out, deformed pins
MB3-100	142.8	> 80kN	brittle	abrupt failure, splitting, deformed pins
MB4-100	157.3	> 140kN	brittle	abrupt failure, splitting, 3 ripped-off pins, fissures at pin base
MB5-100	146.9	> 120kN	brittle	abrupt failure, splitting, partial row shear-out
MB6-100	147.6	> 130kN	brittle	abrupt failure, splitting, deformed pins
MB7-100	139.7	> 105kN	brittle	splitting, deformed pins
MB8-100	139.3	> 100kN	brittle	"slower" failure, splitting, deform. pins
MB9-100	147.6	> 120kN	brittle	abrupt failure, splitting, ripped-off row of pins
MB10-100	168.9	> 120kN	brittle	violent failure, splitting, ripped-off row of pins
S-MB1-100	157.1	> 110kN	brittle	abrupt failure, splitting
S-MB2-100	148.9	> 100kN	brittle	splitting, 2 ripped-off pins
S-MB3-100	168.9	> 120kN	brittle	splitting, deformed pins
S-MB4-100	175.6	> 70kN	brittle	violent failure, splitting, group tear-out
S-MB5-100	147.2	> 80kN	brittle	splitting, group tear-out

Table 4 (continued): *Analyzed data of test series 2*

4.2.1 Performance

4.2.1.1 TimberStrand® LSL

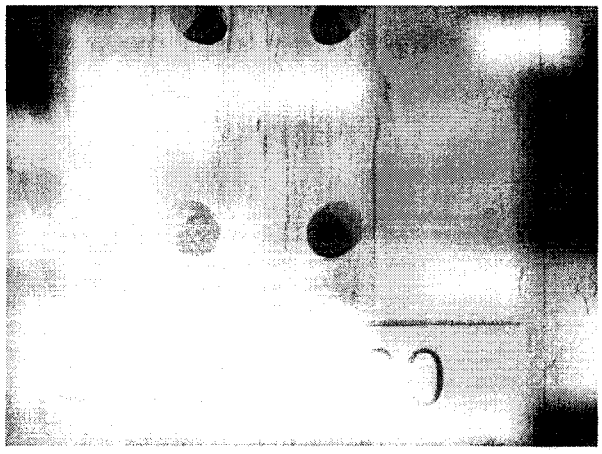

Figure 68: *LSL: No damage observed at the pin holes*

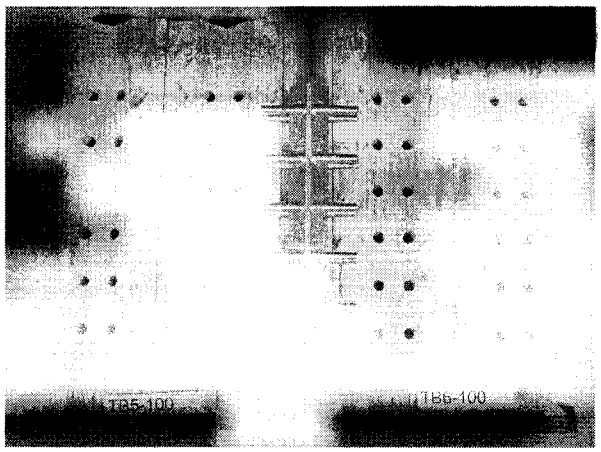

Figure 69: *LSL: No deformations of the connector*

Similar to the observations made in test series 1, in terms of ultimate strength, LSL outperformed all other materials. None of the 13 specimens were failed. At the limit load of 180kN the testing was stopped and the members were unloaded. For 6 specimens however, cracking noises were noticed around 160 to 170kN, indicating the beginning of

failure development. For the rest of the sample set no cracking noises or signs of distress were observed. Examining the connection area of the test members after cutting them open, it was found that neither the wood structure nor the connectors were damaged or deformed.

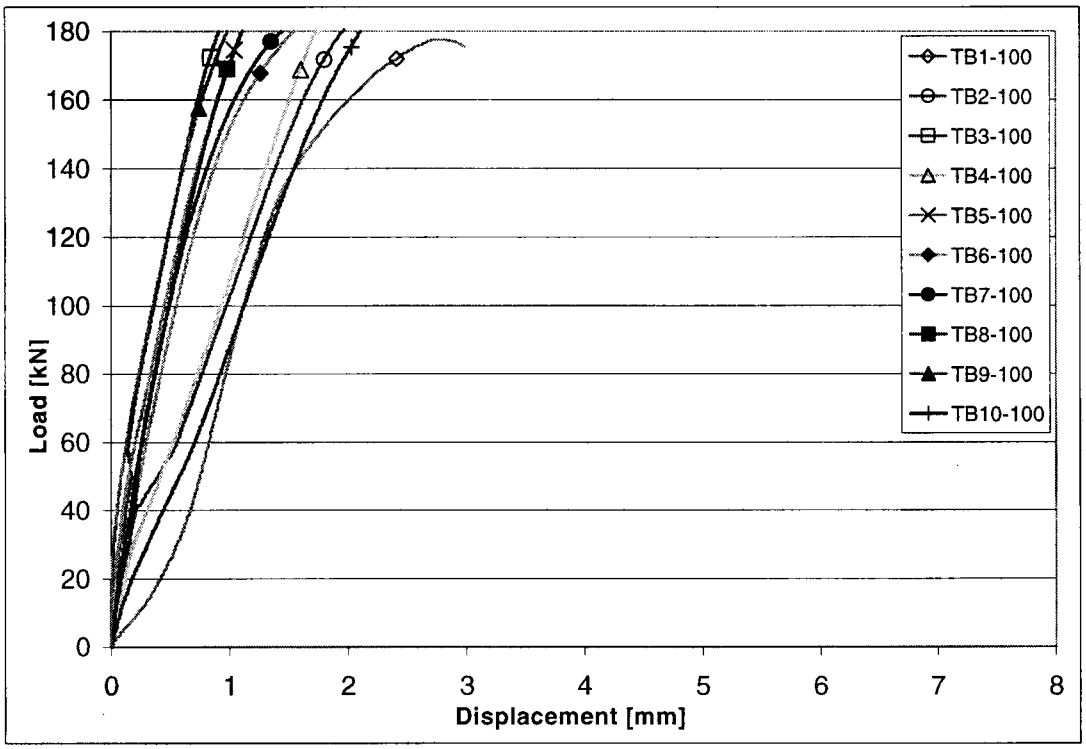

Figure 70: *Load-displacement curves of TB-combinations*

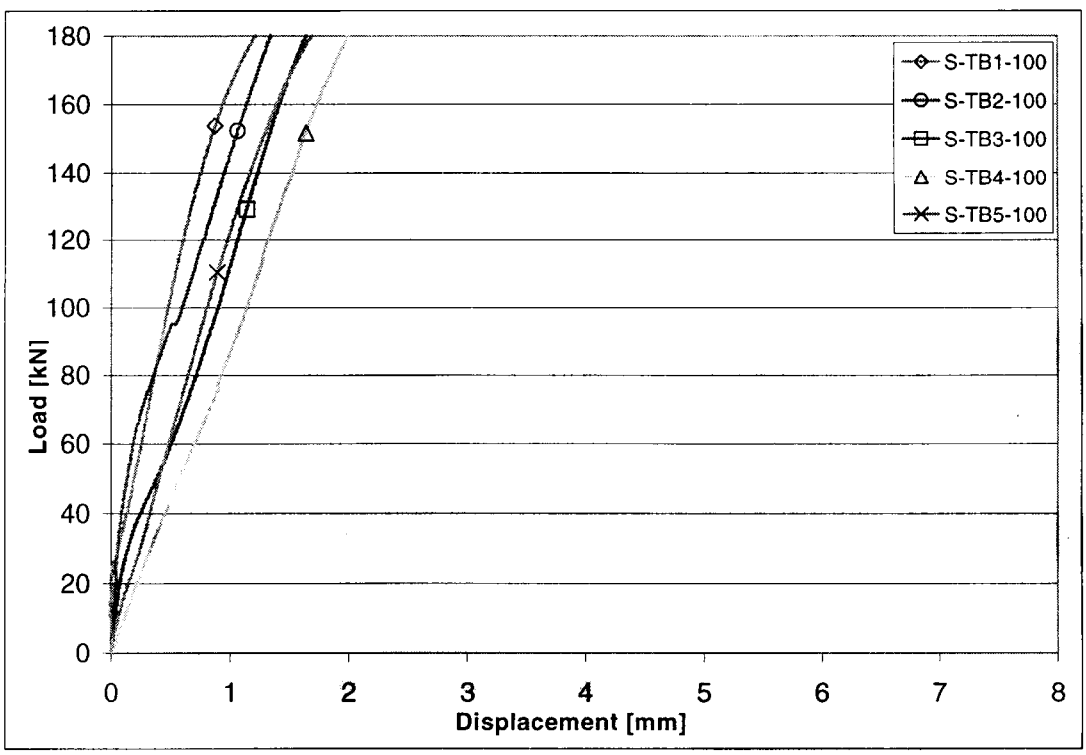

Figure 71: *Load-displacement curves of S-TB-combinations*

As listed in figures 70 and 71, it was evident that the alternative screw-bond of the timber halves did not have an apparent influence on the stiffness performance of the connection. Further evaluation of the test data (Sections 4.2.2 and 8.2) confirmed this.

4.2.1.2 Douglas Fir

Figure 72: DG fir: Splitting along rows of holes

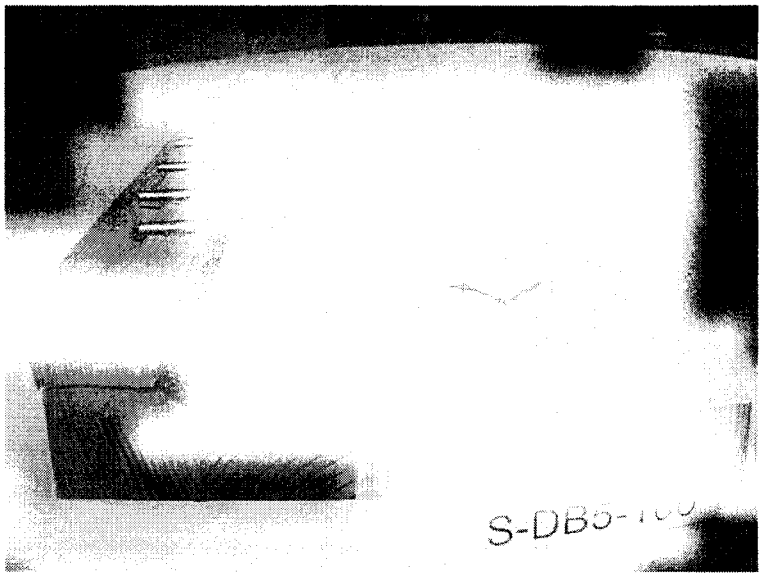

Figure 73: DG fir: Shear failure in the plane of the pins

Even though six of the 13 test specimens survived the 180kN load limit, for almost all Douglas Fir members heavy cracking noises were observed. Failure typically occurred very abruptly. Splitting along the rows of holes and shear-off along the plane of the pins caused extremely violent and brittle failures.

Comparing and analyzing screw-bonded and glued-laminated specimens, it was found that the alternative screw-lamination did not have a significant impact on the failure itself. Without exception, both types of lamination presented very similar failure mechanisms with failure in the plane of the pins. Investigating the failure areas of the screw-bonded specimens, no evidence was found that the screws influenced or contributed to the overall tensile strength and performance of the connection.

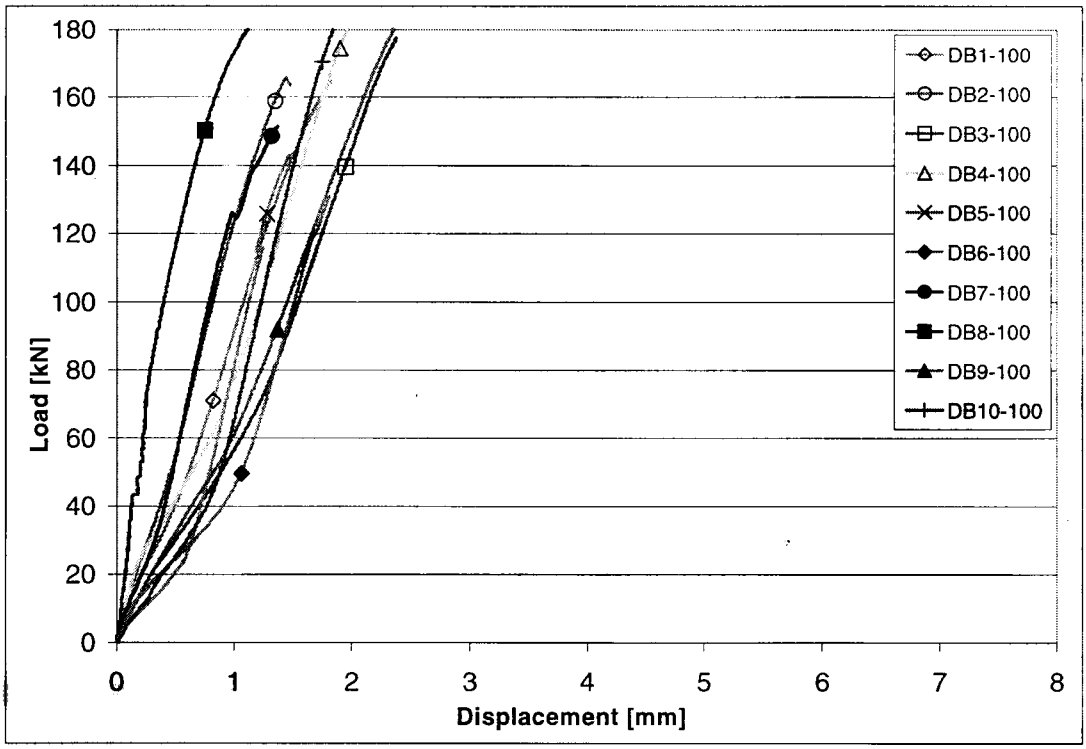

Figure 74: *Load-displacement curves of DB-combinations*

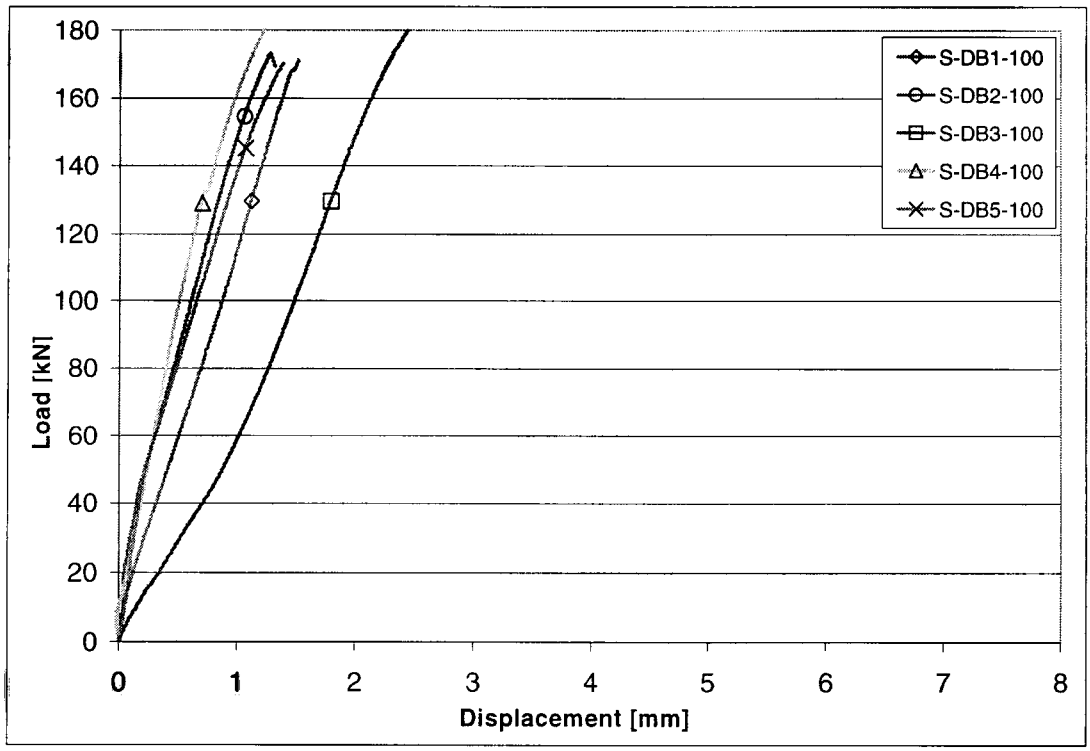

Figure 75: *Load-displacement curves of S-DB-combinations*

4.2.1.3 Parallam®PSL

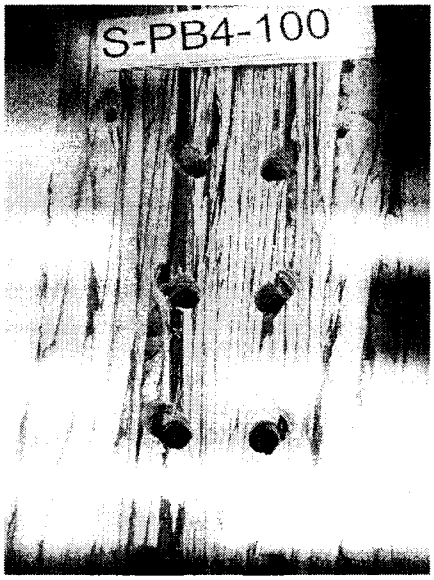

Figure 76: PSL: Splitting along the rows of holes

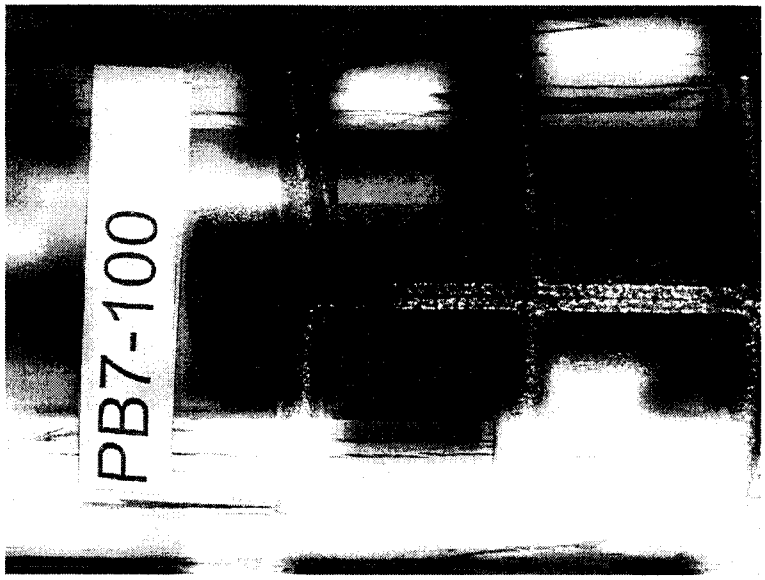

Figure 77: PSL: Deformation of the connector pins

Except for one specimen, member combinations with PSL failed due to splitting along the rows of holes before reaching the 180kN test limit. While loading the member, cracking noises indicated failure propagation, leading to a sudden but less violent failure. For most of the connectors strong deformations and fissures at the base of the pins were found; some pins were ripped-off. Similar to Douglas Fir specimens, glued-laminated and screw-bonded members performed similarly.

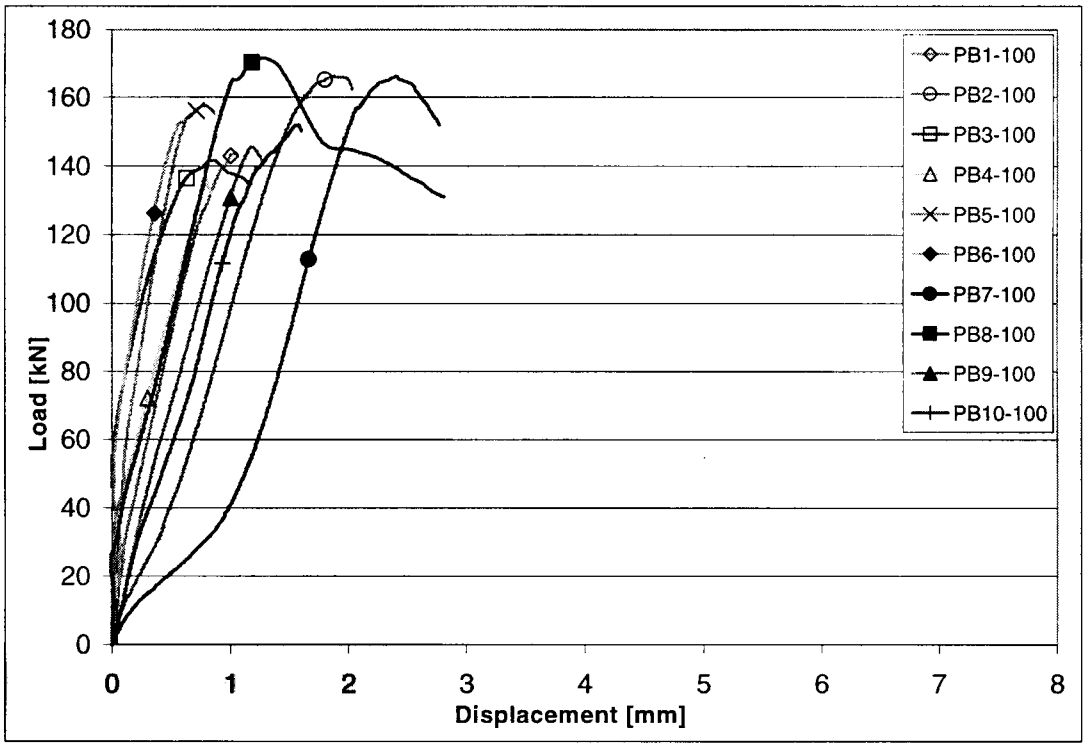

Figure 78: *Load-displacement curves of PB-combinations*

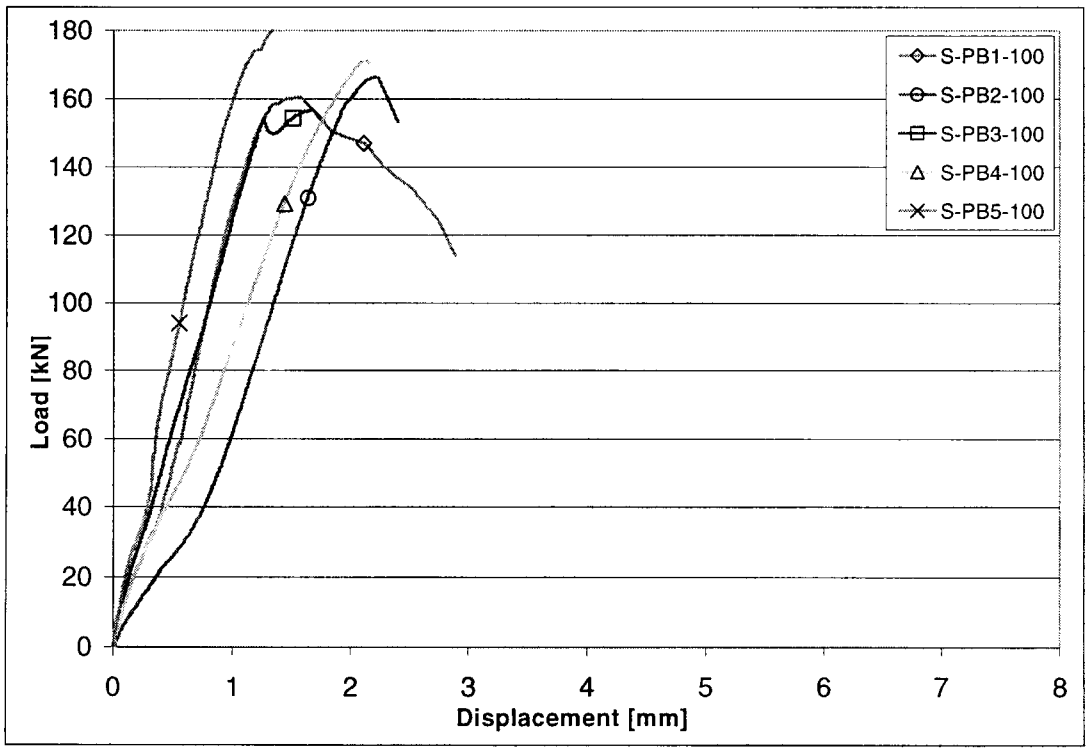

Figure 79: *Load-displacement curves of S-PB-combinations*

4.2.1.4 Microllam®LVL

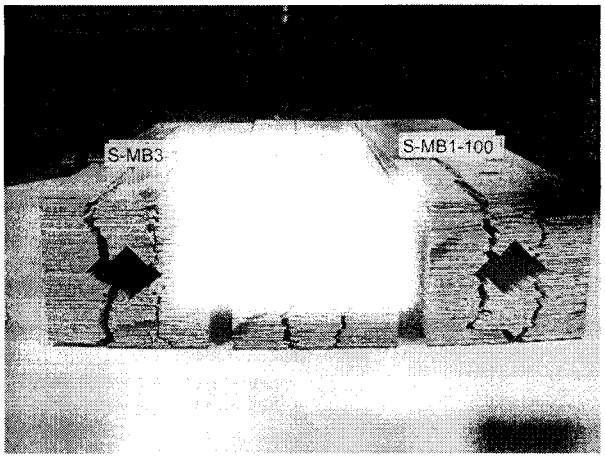

Figure 80: LVL: Splitting along rows of holes

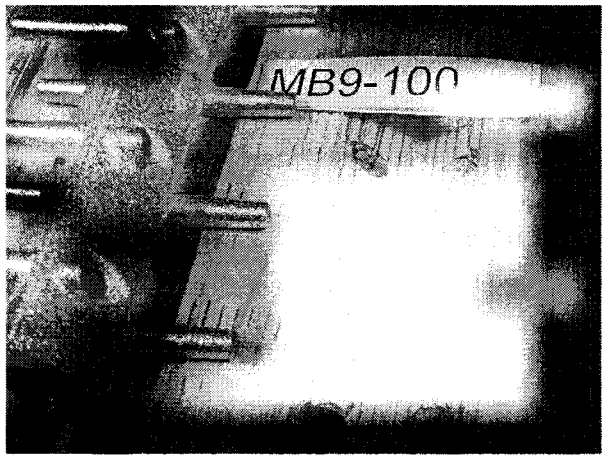

Figure 81: LVL: Ripped-off pins

Before reaching the limit load, all LVL specimens mostly failed due to splitting along the rows of holes. Similar to the observations made for Douglas Fir, the LVL combinations failed in an extremely violent and brittle manner. Typically, the connector pins were strongly deformed and partly ripped-off. Glued-laminated and screw-bonded members showed similar behavior.

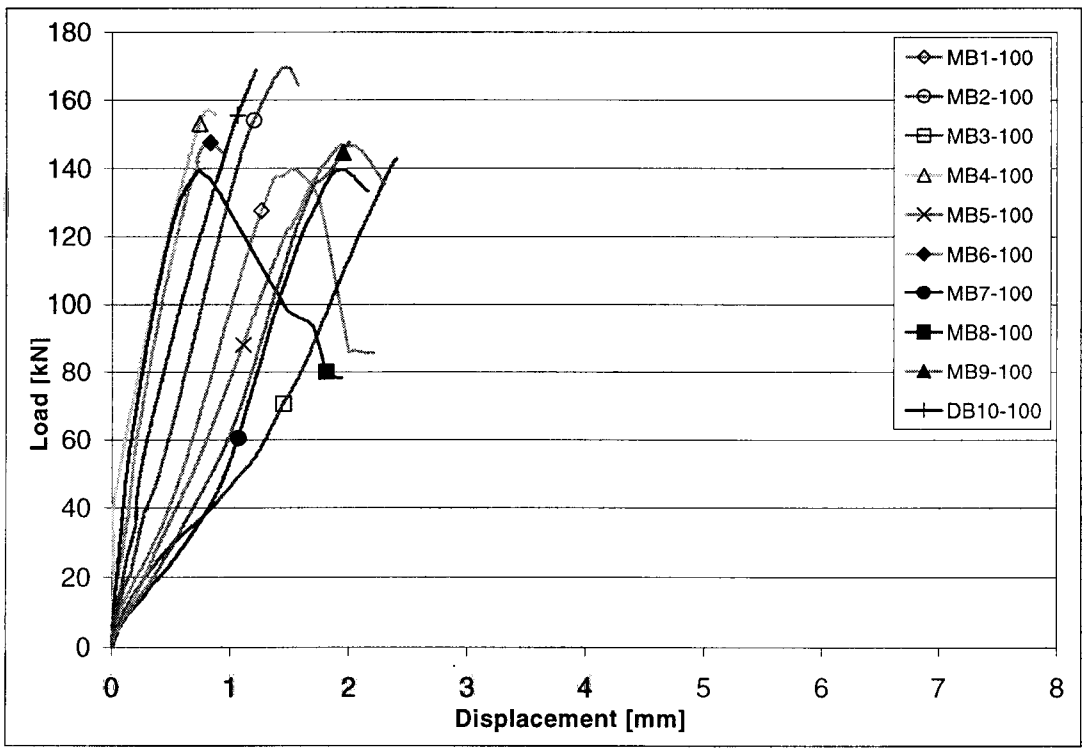

Figure 82: *Load-displacement curves of MB-combinations*

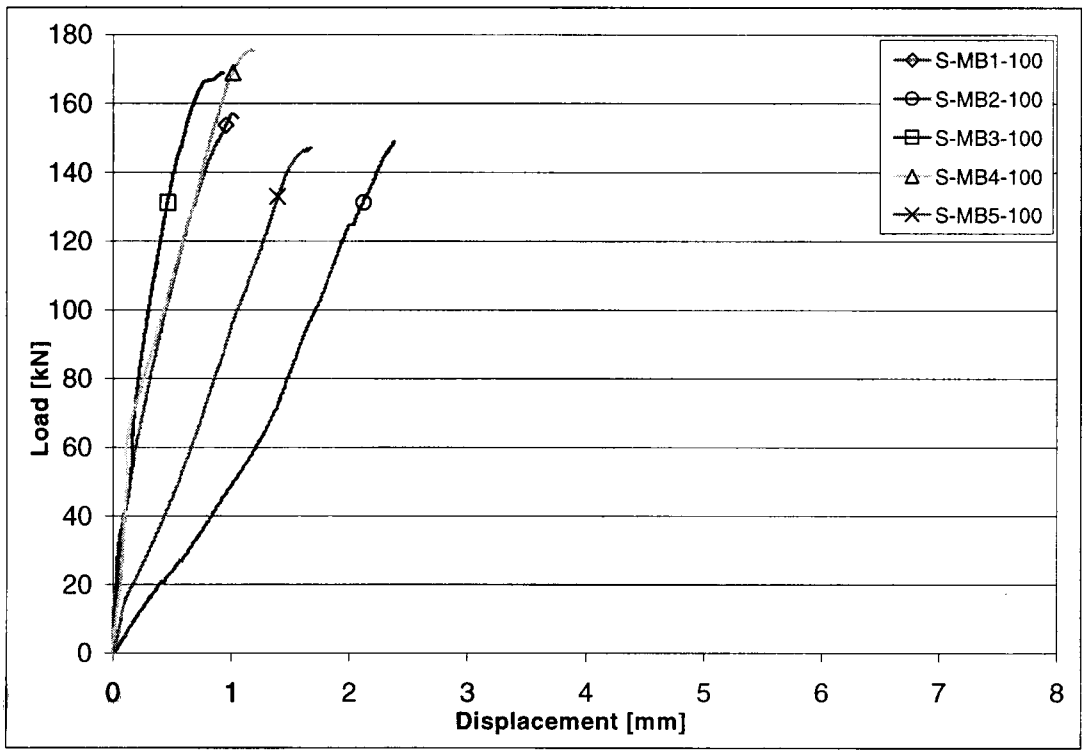

Figure 83: *Load-displacement curves of S-MB-combinations*

4.2.2 Strength and Stiffness

Since glued-laminated and screw-bonded test specimens performed similarly under tensile loading, it was decided to merge both sets of samples. Therefore by providing a larger sample size of 15 specimens, statistically more significant values for the characteristic strength and stiffness could be calculated.

Tables 5 and 6 display information on average ultimate strength and displacement for connector type B combinations. For specimens that were not failed, it was assumed that their ultimate load equated 180kN.

Ultimate Load [kN]

	LSL	DG Fir	PSL	LVL
min value	> 180.00	130.88	135.91	139.30
max value	> 180.00	> 180.00	> 180.00	175.62
mean	> 180.00	168.63	157.85	153.16
std dev		15.27	12.62	12.30
COV		9.1%	8.0%	8.0%

Table 5: *Statistics on ultimate load*

Displacement at ultimate load [mm]

	LSL	DG Fir	PSL	LVL
min value	0.91	1.12	0.6	0.72
max value	2.77	2.45	2.41	2.4
mean	1.57	1.71	1.43	1.49
std dev	0.50	0.43	0.56	0.57
COV	32.0%	25.1%	39.2%	38.3%

Table 6: *Statistics on displacement at ultimate load*

To determine the stiffness *S* of a connection, typically equation 4.1 is chosen to calculate the specific stiffness properties.

$$S = \frac{F_{40} - F_{10}}{d_{40} - d_{10}} \quad (4.1)$$

where:

S = Stiffness of the joint [N/mm]

F_{40} = Strength property at 40% of the ultimate load [N]

F_{10} = Strength property at 10% of the ultimate load [N]

d_{40} = Displacement at 40% of the ultimate load [mm]

d_{40} = Displacement at 10% of the ultimate load [mm]

Due to inconsistent stiffness performance at the beginning of the loading process, it was found that the 10%-40% approach does not precisely represent the actual stiffness of the connection. To provide more accurate values, stiffness was determined by using the 30%- and 70%-ultimate load points.

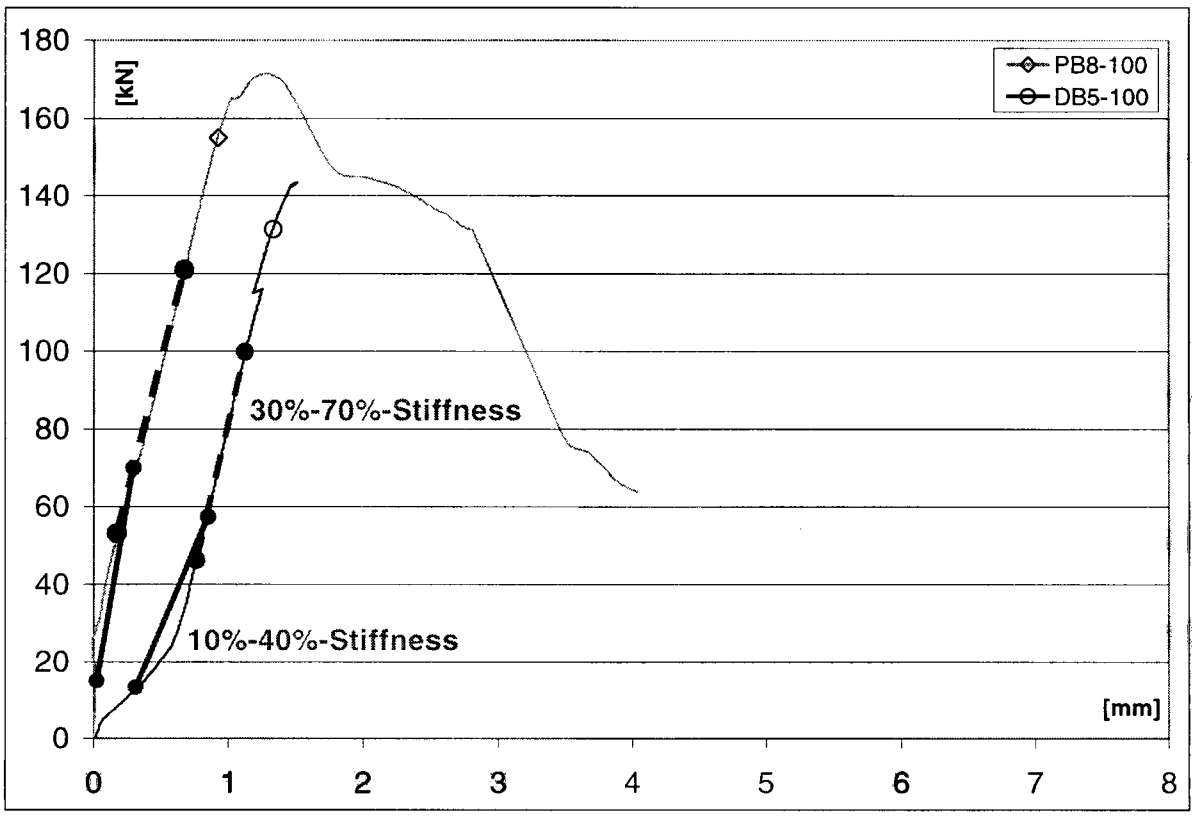

Figure 84: *Different approaches to determine the connection stiffness*

Figure 84 shows typical load-displacement curves of the test series, presenting a "softer" (DB5-100) as well as a "stiffer" behavior (PB8-100) at the beginning of the loading process. Comparing the dashed and solid straight lines indicating different stiffness, it is evident, that the 30/70-approach creates more realistic results than the 10/40-method.

For this reason the stiffness of the connection is determined as follows:

$$S = \frac{F_{70} - F_{30}}{d_{70} - d_{30}} \quad (4.2)$$

where:

S = Stiffness of the joint [N/mm]

F_{70} = Strength property at 70% of the ultimate load [N]

F_{30} = Strength property at 30% of the ultimate load [N]

d_{70} = Displacement at 70% of the ultimate load [mm]

d_{30} = Displacement at 30% of the ultimate load [mm]

Statistics on stiffness values calculated using both approaches are presented in table 7, showing that the 30/70 method generally results in a significantly lower variability of values and, except for Douglas Fir, a smaller average stiffness.

Stiffness [N/mm]

	S-TB / TB		S-DB / DB	
	10/40	**30/70**	**10/40**	**30/70**
min value	79,412	91,139	43,626	86,747
max value	360,000	200,000	300,000	318,797
mean	166,686	135,223	119,752	170,557
std dev	82,695	35,740	68,109	70,471
COV	49.6%	26.4%	56.9%	41.3%

	S-PB / PB		S-MB / MB	
	10/40	**30/70**	**10/40**	**30/70**
min value	53,581	96,454	39,678	62,105
max value	2,293,556	265,919	439,058	281,529
mean	351,768	154,228	186,075	140,235
std dev	592,150	52,960	145,808	61,473
COV	168.3%	34.3%	78.4%	43.8%

Table 7: *Statistics on different 10/40- and 30/70-connection stiffness*

Average ultimate strength and stiffness are elementary mechanical properties used to develop a basic understanding of the fasteners behavior. To model the characteristic connection strength, however, typically the lower 5th percentiles of the ultimate strengths have to be determined. Looking for the most accurate distribution to generate the 5th percentile values, a subroutine of the RELAN[6] software was used to fit Normal, Lognormal, 2P- and 3P-Weibull distributions to the ultimate strength data. The software calculated an overall data fitting error for each data set and developed a distribution function that fits a curve to all data points. Applying these fitted functions, the following formulas were used to calculate the 5th percentile values of the respective distributions:

Normal Distribution:

$$x_P = \mu - k\sigma \quad (4.3)$$

where:

x_P = Strength property at the 5th percentile [N]

μ = Mean value [N]

k = Factor related to percentile P, level of confidence and sample size (k = 1.645)

σ = Standard deviation [N]

Lognormal Distribution:

$$x_P = e^{z_p \cdot \sigma_{\ln} + \mu_{\ln}} \quad (4.4)$$

where:

x_P = Strength property at the 5th percentile [N]

$\mu_{\ln}$ = Log mean value

$\sigma_{\ln}$ = Log standard deviation

z_p = Standard normal number (z score) for a given percentile ($z_{p,\,0.05}$ = 1.645)

and

$$\sigma_{\ln} = \sqrt{\ln\left(1 + \frac{\sigma^2}{\mu^2}\right)} \quad (4.5)$$

$$\mu_{\ln} = \ln \mu - 0.5 \cdot \sigma_{\ln}^{\,2} \quad (4.6)$$

[6] RELAN: *REL*iabilty *AN*alysis software developed in the Department of Civil Engineering at UBC

where:

μ_{ln} = Log mean value

σ_{ln} = Log standard deviation

μ = Mean value [N]

σ = Standard deviation [N]

Weibull Distribution:

$$x_P = x_0 + m \cdot \left[-\ln\left(1-P\right)\right]^{\frac{1}{k}} \quad (4.7)$$

where:

x_P = Strength property at the 5th percentile [N]

x_0 = Location parameter (x_0 = 0 for a 2P-Weibull distribution)

m = Scale parameter

k = Shape parameter

P = Percentile value

Analyzing the data generated by RELAN, it was found that 3P-Weibull functions provided the best fit on the lower tail of the ultimate strength data set. Table 15 in section 8.2 presents detailed information on the different fitting errors and distribution functions computed by RELAN. With these fitted functions, the following 5th percentiles were calculated:

5th percentile strength [kN]

	Normal	Lognorm.	2P-Weib.	3P-Weib.
LSL				**(180.00)**
DG Fir	141.98	144.75	138.24	**138.24**
PSL	135.75	137.98	132.98	**135.64**
LVL	133.19	133.81	131.07	**137.48**

Table 8: *5th percentile strengths of respective distributions*

Accounting for the short term duration of loading (test specimens were typically failed in 5 to 7 minutes), the 5th percentile results were multiplied with a factor K_{DOL} to generate the characteristic values of maximum tensile capacity (Table 9).

$$T_k = x_P \cdot K_{DOL} \quad (4.8)$$

where:

x_P = Strength property at the 5th percentile [N]

K_{DOL} = Factor to account for short term loading (K_{DOL} = 0.8)

T_k = Characteristic value for the maximum tensile capacity [N]

Characteristic values of maximum tensile capacity [kN]

	Normal	Lognorm.	2P-Weib.	3P-Weib.
LSL				(144.00)
DG Fir	113.58	115.80	110.59	110.59
PSL	108.60	110.39	106.38	108.51
LVL	106.55	107.05	104.85	109.98

Table 9: *Characteristic values of maximum tensile capacity*

The RELAN data fitting subroutine was also used to compute the 5th percentile values of the connection stiffness. Similar to the results of the 5th percentile of the connection strength, 3P-Weibull distributions provided the most accurate data fit. The following tables present the complete set of results for all distributions and the 10/40- as well as the 30/70-method to determine the individual connection stiffness.

5th percentile stiffness [N/mm]

10/40	Normal	Lognorm.	2P-Weib.	3P-Weib.
LSL	54,615	62,809	51,169	74,200
DG Fir	35,270	41,227	34,229	45,758
PSL	41,946	41,710	37,687	73,608
LVL	25,140	30,231	18,292	38,402

Table 10: *5th percentile of 10/40-stiffness*

5th percentile stiffness [N/mm]

30/70	Normal	Lognorm.	2P-Weib.	3P-Weib.
LSL	77,658	82,623	74,769	85,913
DG Fir	71,800	78,982	68,820	88,012
PSL	84,626	86,900	80,860	101,784
LVL	52,888	60,378	52,027	63,571

Table 11: *5th percentile of 30/70-stiffness*

5. Discussion

5.1 Evaluation of test results

Appraising the findings of both tests series, with respect to member material and connector type, two major conclusions were reached:

1. Material:

Superior tensile strength and failure-free performance of type-B test members significantly distinguishes LSL from LVL, PSL and Douglas-Fir lumber. Assuming the 180kN upper bound limit as the capacity of the unfailed specimens, the latter three generally had 30% weaker characteristic strength properties accompanied by brittle failure modes under tensile loading of the joint. In combination with connector type A, LSL furthermore showed an advantageously ductile failure behavior, providing the highest average ultimate load value of all type A member setups.

Conclusion: LSL outperforms LVL, PSL and Douglas-Fir lumber.

2. Connector:

Connector type B combinations presented high characteristic tensile strength values and failed typically in splitting along the rows of holes with bending, and in some cases rupture of the pins, whereas type A member setups were primarily engaged in bearing and group tear-out of the wood, eventually failing in tension perpendicular to the strands or the veneer layers; Douglas Fir members typically failed in splitting of the wood. In addition, type A combinations presented a 60% lower average ultimate tensile strength.

Conclusion: Connector type B is stronger than type A, but causes abrupt and very brittle failures at high ultimate load levels.

Figure 85 shows all possible material/connector setups, indicating combinations with weak (white), stronger (light grey) and most beneficial (dark grey) tensile strength properties. Due to the promising performance of LSL-type A combinations in test series 1, this connection setup is specially indicated (light grey dot).

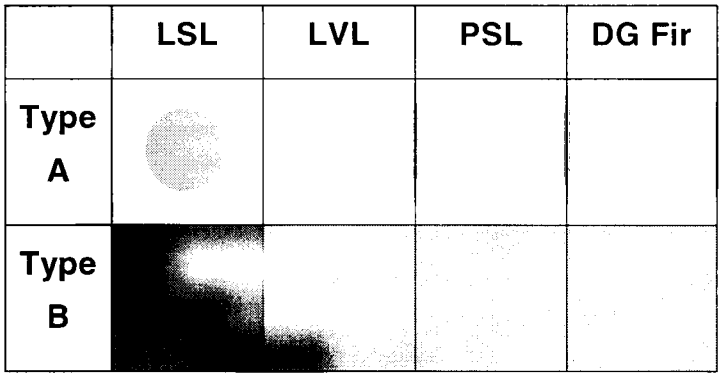

Figure 85: *Classification of member setups according to tensile performance*

The axial resistance of a dowel-type connection with multiple fasteners is primarily dependent on the dimension, the strength, the number, the spacing and the edge distances of the fasteners, as well as the mechanical properties and characteristics of the member material. In the case of the INDUO-connector, except for the loaded edge distance (set to 10d), all fastener related parameters are defined by the connector itself, leaving only the cross-section and the material of the member as variable factors. Thus, the tensile strength of the connection is directly dependent on the quality and strength of the member material.

Every wood or wood-based material features man-made and / or natural characteristics that influence the material and connection strength. When the applied load exceeds the capacity of the wood joint, failure typically initiates at the weakest spot of the connection. Solid wood with its non-homogeneous structure contains various weakening characteristics and 'natural defects' such as knots, checks and varying density (growth-rings, late-early wood) that present such weak points. To create a more uniform and less heterogeneous wood-based material, engineered wood products were developed, eliminating major wood defects and evenly distributing minor weakening characteristics over the entire volume of the member. In the manufacturing process, however, where the original fiber structure is partially destroyed, the recreated wood product shows man-made defects that likewise present undesired characteristics. A close look at the end grain of PSL (Figure 86a) reveals relatively large voids embedded in the strand structure (white circles). In addition, PSL strands and LVL plies feature little surface cracks (white box) that derive from the peeling and drying process during the veneer manufacture as

well as from bending while forming and pressing the strand mat into a billet (PSL manufacture).

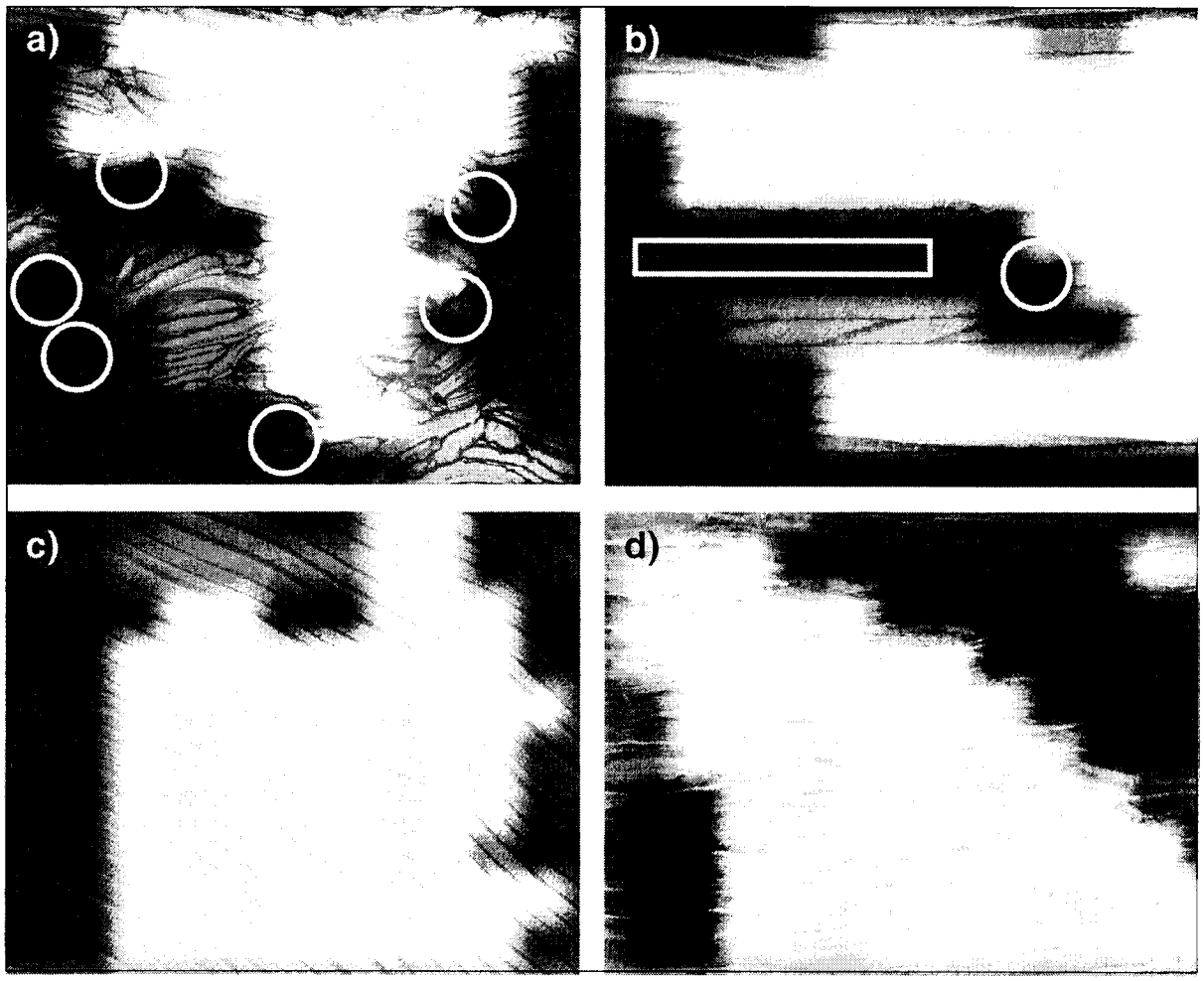

Figure 86: *Close-up of end grain: a) PSL; b) LVL; c) Douglas Fir; d) LSL*

LSL's advantageous connection strength properties originate from the high density (0.68g/cm^3 [7]) and uniformity of the material and its interwoven strand structure. In comparison to PSL, the end grain of LSL does not show any visible cavities (Figure 86d) or initial damage to strands, because the thin and flexible LSL strands overlap and bend without creating hollow spaces and surface cracks, thus reducing potential weak spots in the composite structure.

Providing a more cross-layered strand orientation than PSL, the interwoven fiber structure of LSL seems to act like inner reinforcement of the mainly parallel aligned composite. This material property is considered to be responsible for the fact that, in

[7] Density value provided by manufacturer TrusJoist

contrast to Douglas Fir, LVL and PSL, none of the LSL specimens failed in wood splitting along the rows of holes. In conclusion, LSL's performance is based on high material density and uniformity, accounting for a high embedding strength and the unique strand structure that reduces splitting of the material.

5.2 Comparison of characteristic strength values

For the most common fasteners used in contemporary wood construction, timber codes provide the necessary information to calculate and dimension all structural components related to the joint. For connection techniques that have not been introduced into the code, reliable design information has to be supplied by the manufacturer of the fastener. This data is typically generated in specific test series.

5.2.1 Connection Model

Due to the costly procedure for an official approval and certification of the INDUO-connector type A, in 2000 it was decided to modify the fastener shape so that it can be modeled and calculated as a "tight-fitting dowel connection with inside steel plate" according to DIN1052-1988 (Blaß 2001).

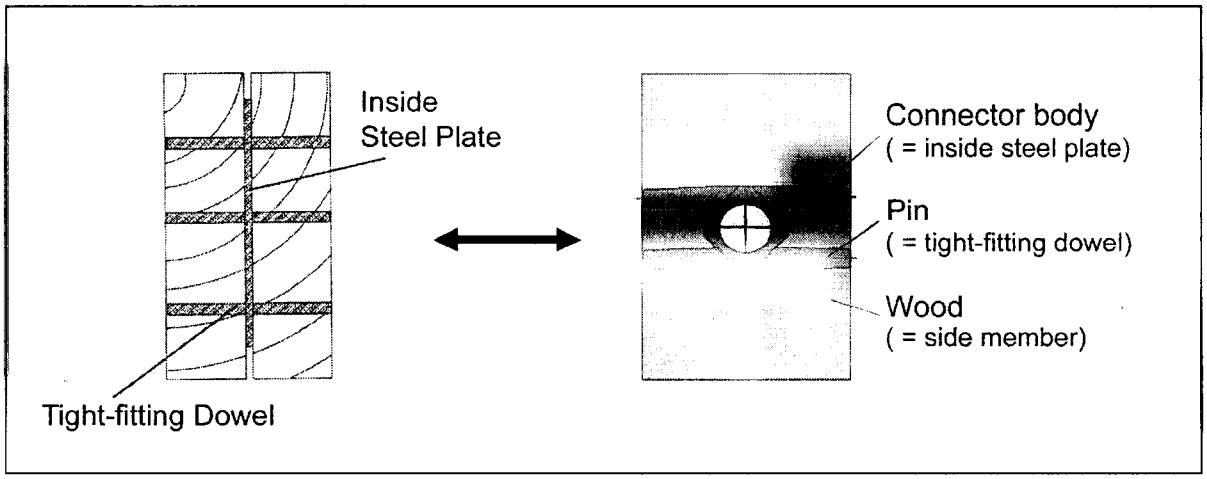

Figure 87: *Connection model*

With this connection model, the specific design strength for the tensile capacity of the INDUO-connector can be calculated according to any timber code, provided that the respective code includes dowel-type fasteners. The characteristic tensile strengths

derived from the results of test series 2 can then be compared and verified with corresponding values generated from code design strengths. Using the aforementioned connection model, in section 5.2.2 these design strength values will be determined according to the new German *DIN1052-2000 (Draft),* the European *EC5*, the Canadian *CSA 086.1* and the US-American *ASCE 16-95* timber code. All four codes are based on a *Limit States Design* philosophy, but vary in detail due to different safety approaches. With a step-by-step approximation of the different code results, the characteristic tensile strength for each design approach will be generated and compared with the data developed from the test series.

5.2.2 Determination of code design values

To create a uniform and comparable set of results, values for member dimensions, material properties, service conditions and duration of loading are defined as follows:

Connection Model:

Dowel-type connection with inside steel plate and wooden side members.

Number of dowel-type fasteners: 12

Number of shear planes per fastener: 2

Components of connection:

Side members: Wood or wood product:

Douglas Fir, No1. & better grade

LSL, 1.5E grade

LVL, 1.9E grade

PSL, 2.0E grade

Moisture content: MC < 19%

Cross-sectional area: 33 x 100mm

Main member: Inside steel plate, spherical cast iron of EN-GIS-500-7 grade defined in EN1563

Characteristic ultimate tensile strength: $f_{u,k}$ = 500 N/mm^2

Characteristic yield strength: $f_{y,k}$ = 320 N/mm^2

Cross-sectional area: 14 x 100mm

Fastener: Tight-fitting dowel[8] / bolt[9], spherical cast iron of EN-GIS-500-7 grade, defined in EN1563

Dimension of fastener: d = 8mm, l = 80mm

Service condition and duration of loading:

Duration of loading: Medium or standard term loading (1 week – 6 months)

Service conditions: Temperature: 20° centigrade

Relative humidity of the surrounding air: 65%, exceeding 85% only for a few weeks of the year

Connection is not exposed to any corrosives

Treatment: The wooden side members are not impregnated with any strength reducing chemicals

Spacing and distances of fasteners:

Parallel to grain direction: a_1 = 40.4mm □ 5.05d

Perpendicular to grain direction: a_2 = 25.0mm □ 3.13d

Loaded edge: a_3 = 80.0mm □ 10.0d

Unloaded edge: a_4 = 37.5mm □ 4.67d

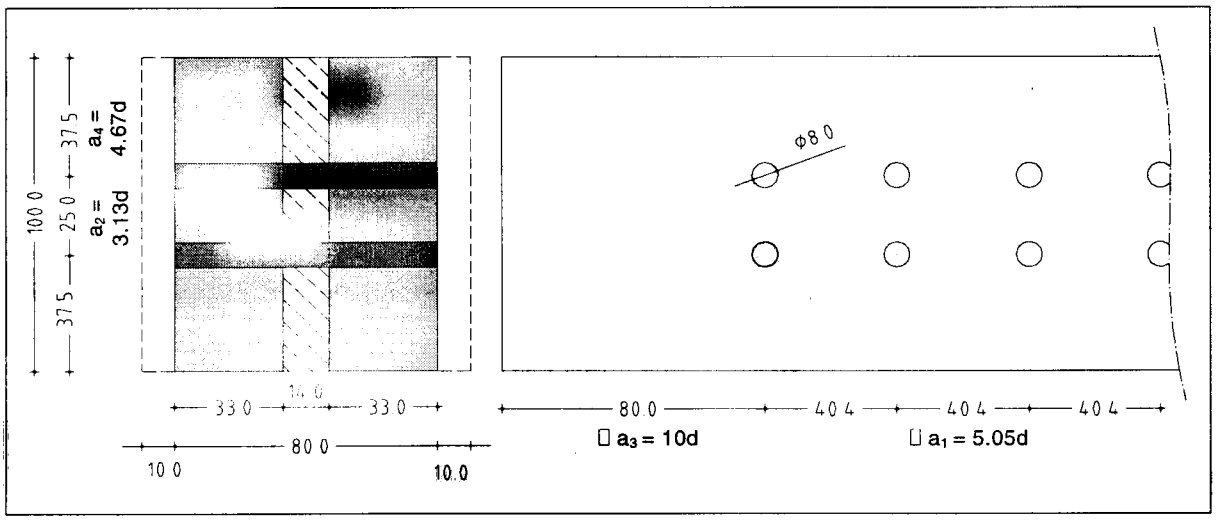

Figure 88: *Plan of connection*

[8] according to DIN1052-2000 and EC5
[9] according to CSA 086.1 and ASCE 16-95

Failure modes according to the European Yield Model:

EC5, CSA 086.1 and ASCE 16-95 use the *European Yield Model* (EYM) to describe typical failure modes occurring in dowel-type connections. Based on these failure models the codes provide equations to generate the nominal lateral strength resistances per shear plane and fastener. The failure modes are defined as follows:

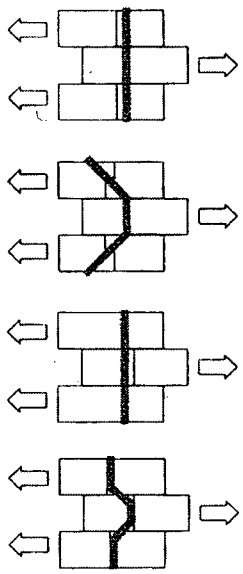

Failure mode I:
Bearing-dominated yield of the wood fibers in contact with the fastener

Failure mode II:
Fastener yield in bending at one plastic hinge point per shear plane and bearing-dominated yield of the wood fibers in contact with fastener

Failure mode III:
Bearing-dominated yield of the main member in contact with the fastener
(Not compatible with actual performance of INDUO-connector)

Failure mode IV:
Fastener yield in bending at two plastic hinge points per shear plane with limited localized crushing of wood fibers near the shear planes
(Not compatible with actual performance of INDUO-connector)

Figure 89: *Failure modes according to European Yield Model*

Since the failure modes III and IV do not represent the characteristic performance of the INDUO-connector and in addition neither of these failure types was observed in the test series, only mode I and II will be considered in the design calculations.

Each of the following sections (5.2.2.1 to 5.2.2.5) presents for the design procedure and the equations used to calculate the axial strength for dowel-type connections according to the respective timber code.

5.2.2.1 DIN1052-2000 (Draft)

$$F_d \leq R_d \quad (5.1)$$

$$R_d = R_k \cdot \frac{k_{mod}}{\gamma_m} \cdot n_{ef} \cdot n_r \cdot n_s \quad (5.2)$$

$$R_k = \sqrt{2} \cdot \sqrt{2 \cdot M_{y,k} \cdot f_{h,k} \cdot d} \quad (5.3)$$

provided that

$$t_{req} = 4 \cdot \sqrt{\frac{M_{y,k}}{f_{h,k} \cdot d}} \quad (5.4)$$

$$n_{ef} = \min \begin{cases} n \\ n^{0.9} \cdot \sqrt[4]{\frac{a_1}{10d}} \end{cases} \quad (5.5)$$

$$M_{y,k} = 0.26 \cdot f_{u,k} \cdot d^{2.7} \quad (5.6)$$

$$f_{h,k} = 0.082 \cdot (1 - 0.01 \cdot d) \cdot \rho_k \cdot k_a \quad (5.7)$$

$$k_a = \sqrt{\frac{a_1}{7d}} \quad (5.8)$$

where:

F_d = Design force [N]

R_d = Design value of the load-carrying capacity of the connection [N]

R_k = Characteristic load-carrying capacity per shear plane and fastener [N]

k_{mod} = Factor accounting for the effect of load duration and moisture content (k_{mod} =0.8)

γ_m = Partial factor for steel in timber connections (γ_m = 1.1)

n_{ef} = Effective number of fasteners in a row

n = Number of fasteners in a row

n_r = Effective number of fasteners in a row

n_r = Number of rows

n_s = Number of shear planes

a_1 = Fastener spacing in grain direction [mm]

d = Fastener diameter [mm]

$M_{y,k}$ = Characteristic fastener yield moment [Nmm]

$f_{h,k}$ = Characteristic embedding strength of the wood [N/mm^2]

t_{req} = Required minimum thickness of the wood side member ($t_{req} \geq l_1$ = 33mm)

l_1 = Embedding length of fastener in the wood side member [mm]

$f_{u,k}$ = Characteristic ultimate tensile strength of the fastener [N/mm^2]

ρ_k = Characteristic density of the wood [kg/m^3]

k_a = Reduction factor accounting for $a_1 < a_{1,req} = 7d$

5.2.2.2 EC5 (Eurocode 5)

$$F_d \leq R_d \quad (5.9)$$

$$R_d = R_{d,0} \cdot n \cdot n_r \cdot n_s \quad (5.10)$$

$$M_{y,k} = 0.8 \cdot f_{u,k} \cdot \frac{d^3}{6} \quad (5.13)$$

$$f_{h,k} = 0.082 \cdot (1 - 0.01 \cdot d) \cdot \rho_k \cdot k_a \quad (5.14)$$

$$k_a = \sqrt{\frac{a_1}{7d}} \quad (5.15)$$

The lesser $R_{d,0}$ of mode 1 and 2:

Failure mode I:

$$R_{d,0} = \frac{k_{mod}}{\gamma_{m,w}} \cdot f_{h,k} \cdot l_1 \cdot d \quad (5.11)$$

Failure mode II:

$$R_{d,0} = 1.1 \cdot \frac{k_{mod}}{\gamma_{m,w}} \cdot f_{h,k} \cdot l_1 \cdot d \cdot \left(\sqrt{2 + \frac{4 \cdot \frac{M_{y,k}}{\gamma_m}}{\frac{k_{mod}}{\gamma_{m,w}} \cdot f_{h,k} \cdot d \cdot l_1^2}} - 1 \right) \quad (5.12)$$

where:

F_d = Design force [N]

R_d = Design value of the load-carrying capacity of the connection [N]

$R_{d,0}$ = Design value of the load-carrying capacity per shear plane and fastener [N]

n = Number of fasteners in a row

n_r = Number of rows

n_s = Number of shear planes

k_{mod} = Factor accounting for the effect of load duration and moisture content (k_{mod} =0.8)

$\gamma_{m,w}$ = Partial factor for wood and wood composites ($\gamma_{m,w}$ = 1.3)

γ_m = Partial factor for steel in timber connections (γ_m = 1.1)

$f_{h,k}$ = Characteristic embedding strength of the wood [N/mm^2]

l_1 = Embedding length of fastener in wood side member [mm]

d = Fastener diameter [mm]

$M_{y,k}$ = Characteristic fastener yield moment [Nmm]

$f_{u,k}$ = Characteristic tensile strength of the fastener [N/mm^2]

ρ_k = Characteristic density of the wood [kg/m^3]

k_a = Reduction factor accounting for $a_1 < a_{1,req} = 7d$

5.2.2.3 CSA 086.1

$$F_d \leq P_r \quad (5.15)$$

$$P_r = \Phi \cdot P_u \cdot n_s \cdot n_r \cdot n_F \cdot J_F \quad (5.16)$$

The lesser p_u of mode 1 and 2:

Failure mode I:

$$p_u = 0.8 \cdot f_1 \cdot d \cdot l_1 \quad (5.17)$$

Failure mode II:

$$p_u = 0.8 \cdot f_1 \cdot d^2 \cdot \left(\sqrt{\frac{1}{6} \cdot \frac{f_2}{f_2 + f_1} \cdot \frac{f_y}{f_1}} + 0.2 \cdot \frac{l_1}{d} \right) \quad (5.18)$$

$$J_G = 0.33 \cdot \left(\frac{l_1}{d} \right)^{0.5} \cdot \left(\frac{s}{d} \right)^{0.2} \cdot n_F^{(-0.3)} \quad (5.19)$$

where:

P_r = Factored lateral strength of a bolted connection [N]

Φ = Resistance factor (Φ = 0.7)

P_u = $p_u \cdot (K_D \cdot K_{SF} \cdot K_T)$

p_u = Lateral strength resistance for loading in grain direction [N]

K_T = Fire-retardant treatment factor (K_T = 1.0)

K_{SF} = Service condition factor (K_{SF} = 1.0)

K_D = Load duration factor (K_T = 1.0)

n_s = Number of shear planes

n_r = Number of fastener rows

n_F = Number of fasteners in a row

J_F = $J_G \cdot J_L \cdot J_R$

J_L = Factor for loaded end distance (J_L = 1.0)

J_R = Factor for number of rows (J_L = 0.8)

J_G = Factor for two to maximum 12 fasteners in a row

l_1 = Embedding length of fastener in the wood side member [mm]

d = Fastener diameter [mm]

s = Fastener spacing in the row [mm]

f_1 = Embedding strength of the wood [N/mm^2] ($f_1 = 63 \cdot G \cdot (1-0.01d)$)

G = Mean oven-dry density

f_2 = Embedding strength of the inside steel member [N/mm^2] (set to f_2 = 10,000 N/mm^2 ≈ infinite embedding strength)

f_y = Yield strength of the steel fastener [N/mm^2]

5.2.2.4 ASCE 16-95

$$Z_u \leq \Phi_Z \cdot \lambda \cdot Z' \quad (5.20)$$

$$Z' = Z \cdot n_F \cdot C_g \cdot C_M \cdot C_T \cdot C_\Delta \quad (5.21)$$

$$C_g = \frac{n_r}{n_F}\left[\frac{m\cdot\left(1-m^{2n}\right)}{\left(1+R_{EA}\cdot m^n\right)\cdot(1+m)-1+m^{2n}}\right]\cdot\left(\frac{1+R_{EA}}{1-m}\right) \quad (5.24)$$

$$m = u - \sqrt{u^2-1} \quad (5.25)$$

$$u = 1+\gamma\cdot\frac{s}{2}\cdot\left(\frac{1}{E_m\cdot A_m}+\frac{1}{E_s\cdot A_s}\right) \quad (5.26)$$

The lesser Z of mode 1 and 2:

Failure mode I:

$$Z = 1.66\cdot d\cdot l_s\cdot f_{es} \quad (5.22)$$

Failure mode II:

$$Z = 2.08\cdot d\cdot l_s\cdot f_{em}\cdot\frac{k_3}{(2+R_e)} \quad (5.23)$$

$$k_3 = \sqrt{\frac{2\cdot(1+R_e)}{R_e}+\frac{2\cdot f_{y,b}\cdot(2+R_e)\cdot d^2}{3\cdot f_{em}\cdot l_s^2}}-1 \quad (5.27)$$

where:

Φ_Z = Resistance factor connections (Φ_Z = 0.65)

λ = Time-effect factor (λ = 0.80)

Z_u = Connection force due to factored loads [lbs]

Z' = Adjusted connection lateral resistance [lbs]

Z = Reference connection lateral resistance [lbs]

n_F = Total number of fasteners in the connection

n_r = Number of fastener rows

n = Number of fasteners in a row

C_g = Group action factor

C_M = Wet service factor (C_M = 1.0)

C_T = Temperature factor (C_T = 1.0)

C_Δ = Geometry factor (C_Δ = 1.0)

R_{EA} = the lesser of $\frac{E_s\cdot A_s}{E_m\cdot A_m}$ or $\frac{E_m\cdot A_m}{E_s\cdot A_s}$

E_s = Modulus of elasticity of wood side member [psi]

E_m = Modulus of elasticity of steel main member [psi]

A_s = Gross cross-sectional area of main member [in^2]

A_m = Sum of gross cross-sectional areas of side members [in^2]

γ = $270{,}000 \cdot d^{1.5}$ [lbs/in]

d = Fastener diameter [in]

s = Fastener spacing in grain direction [in]

l_s = Embedding length of fastener in side member [in]

f_{es} = Embedding strength of wood side member[10] [psi]

f_{em} = Embedding strength of main member [psi]
(set to 10,000 N/mm^2 = $1.45 \cdot 10^6$ psi ≈ infinite embedding strength)

R_e = f_{em} / f_{es}

$f_{y,b}$ = Dowel bending yield strength [psi]; ($f_{y,b}$ = 60,000 psi)

5.2.3. Characteristic strength values

To determine how realistic the connection model defined in section 5.2.1 describes the actual tensile capacity of the INDUO-connector, characteristic connection strengths derived from design values calculated according to sections 5.2.2.1-4 are compared with the characteristic values generated from test results.

The basic design equation for mechanical connections based on a Limit States Design approach is as follows:

$$D_C \leq R_C \quad (5.28) \qquad \longleftarrow \qquad R_C = \Phi \cdot r_C \quad (5.29)$$

where:

D_c = Design force applied to connection or 'Demand'

R_c = Factored strength of a mechanical connection or 'Resistance'

r_c = Reference strength of a mechanical connection

Φ = Resistance or modification factor

Equation 5.29 can be further modified by factoring out the group action factor that accounts for the effects of more than one fastener in a mechanical connection (Equation 5.30).

[10] *Table 8A*, LRFD Structural Connections Supplement of the Manual for Engineered Wood Construction, AF&PA / American Wood Council

$$R_C = \Phi \cdot k_G \cdot r_{C,k} \quad (5.30)$$

$$r_{C,k} = \frac{R_C}{\Phi \cdot k_G} \quad (5.31)$$

where:

R_c = Factored strength of a mechanical connection or 'Resistance'

$r_{c,k}$ = Specific characteristic strength value of a mechanical connection

k_G = Group action factor

Φ = Resistance or modification factor

Applying equation 5.30, Table 12 presents the stepwise approximation of the specific characteristic tensile strength value. Column IV, 'Adjustment of embedding strength', considers the relatively small wood embedding strength value provided in the Canadian code by adjusting it to the correspondent values of the other timber codes.

Based on two different test procedures (Figure 90), the embedding strength of wood and wood-based products is determined according to the American *ASTM D5764a-1997* and the European *EN 383-1993* test standards, respectively. In the timber design codes, however, the embedding strength values are calculated using the fastener diameter and the mean oven-dry density as variables and specific calibration factors that vary for each code. Although the US and Canadian embedment values are based on the same testing procedure, the Canadian embedment design values are significantly more conservative. To eliminate this discrepancy in the comparison with test results an adjustment factor has been applied in table 12, column IV.

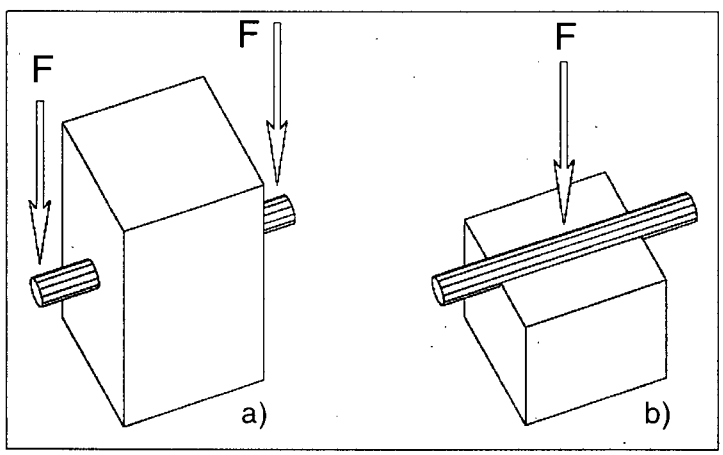

Figure 90: *Different test procedures to determine the embedding strength of wood and wood-based material; a), DIN EN 383-1993 b) ASTM D5764a-1997*

Similarly, the group reduction factor in the Canadian code is much more severe than in the other design codes. To allow for a more realistic comparison of the characteristic values the design strengths were modified in column II by eliminating the group action factors.

Cells featuring an 'arrow' indicate that due to code specifications the respective calibration step is not applicable.

LSL, 1.5E	Ratio I / V	Design strength (factored resistance)	No group reduction factor (1/ k_G)	No resistance / modification factor (1/ Φ)	Adjustment of embedding strength	Specific char. tensile strength value
[N]	I / V	I	II	III	IV	V
DIN 1052-2000	64%	80,108	113,682	125,050	→	**125,050**
EC5	81%	98,755	→	122,193	→	**122,193**
CSA 086.1	25%	26,076	60,215	86,022	105,373	**105,373**
ASCE 16-95	60%	76,108	82,299	126,613	→	**126,613**

Table 12: *Example showing a step-by-step approach to determine characteristic values for tensile capacity*

Due to different safety approaches of each timber code, the results for the design strength of the dowel-type connection model defined in section 5.2.1 vary significantly from each other. Especially, the Canadian timber code with a factored resistance of 26.1kN represents a very conservative design approach.

Comparison of characteristic strength values

i	*[kN]*	LSL	Ratio i / I	DG Fir	Ratio i / I	PSL	Ratio i / I	LVL	Ratio i / I
I	**Char. strength Test series 2**	**144.00**		**110.59**		**108.51**		**109.98**	
II	**DIN 1052-2000**	**125.05**	87%	**114.94**	104%	**116.11**	107%	**116.11**	106%
III	**EC5**	**122.19**	85%	**108.51**	98%	**110.04**	101%	**110.04**	100%
IV	**CSA 086.1**	**105.37**	73%	**91.94**	83%	**94.79**	87%	**94.79**	86%
V	**ASCE 16-95**	**126.61**	88%	**111.40**	101%	**112.92**	104%	**112.92**	103%

Table 13: *Comparison of characteristic connection strength values*

Comparing the characteristic strength values, Table 13 shows that overall the connection model used to determine the code design strengths reasonably represents the actual tensile strength properties of the INDUO-type B connector. Except for LSL, that features significantly lower code values, the characteristic strengths calculated for Douglas Fir, LVL and PSL show relatively small deviations from the values generated from the test series. The Canadian code generally provides the most conservative results, whereas DIN1052-2000 and ASCE 16-95 predict a slightly higher characteristic strength value (dark grey cells).

The European, Canadian and American timber codes assume that for dowel-type connections with multiple fastener configurations, providing sufficient spacing and loaded end distance of the fasteners, connection strength values according to the European Yield Model can be achieved. The characteristic performance of the INDUO-connection with predominantly brittle failure behavior therefore does not strictly comply with the failure modes defined by the EYM. For this reason, it is pointed out that the tight-fitting dowel model does not comprehensively describe the actual performance of the INDUO-fastener. Although it is implied that, for dowel type connections, the values given by the EYM provide reasonable estimate of load capacity, brittle failure modes are not explicitly considered. They are deemed to be avoided by the prescription of dowel spacing and end distance. From testing experience, however, it is evident that brittle failure modes often dictate the load capacity and it is thus recommended that appropriate design equations for brittle failure modes to be developed.

5.3 Evaluation of connection stiffness with structural model

Figures 91-93 show the *Thalkirchen Bridge* over the River Isar in Munich, Germany, built-up by a wooden space truss system, featuring Glulam beam elements with special steel connectors at both ends and spherical cast steel nodes with inside thread. The wood-to-steel joint of the beam is a tight-fitting dowel connection with inside steel plate. All elements were prefabricated in the shop and assembled on-site, simply connecting the beams and nodes with threaded bolts. Completed in 1991, it is still the only wooden highway bridge using a space truss system to support the road deck.

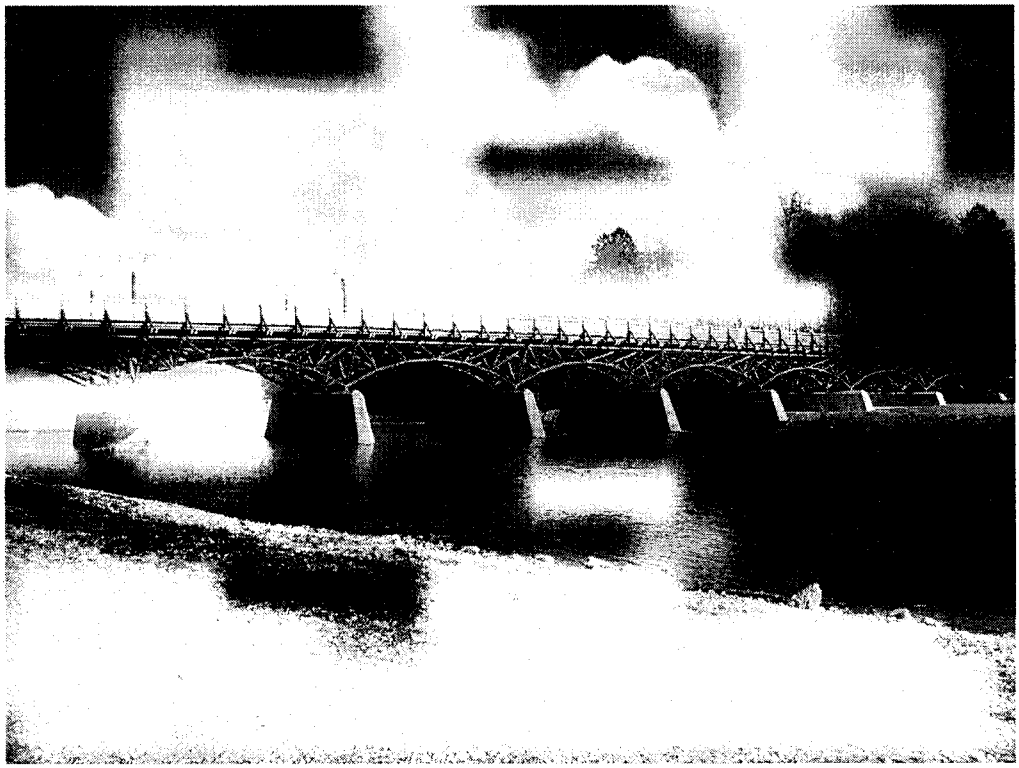

Figure 91: *Thalkirchen Bridge, Munich, Germany*

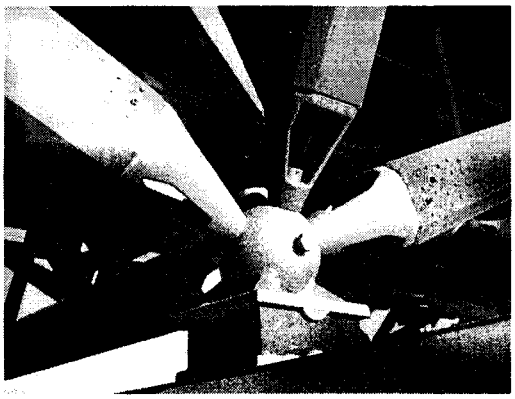

Figure 92: *Support with node and connected beams*

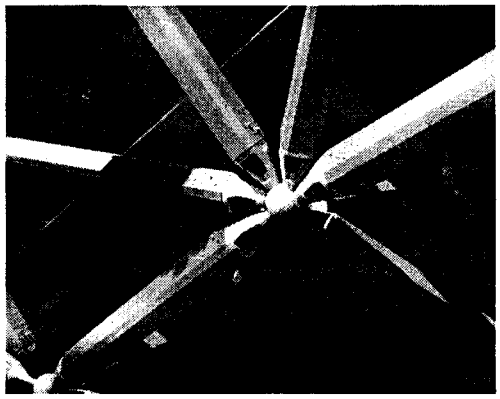

Figure 93: *Node in the truss system*

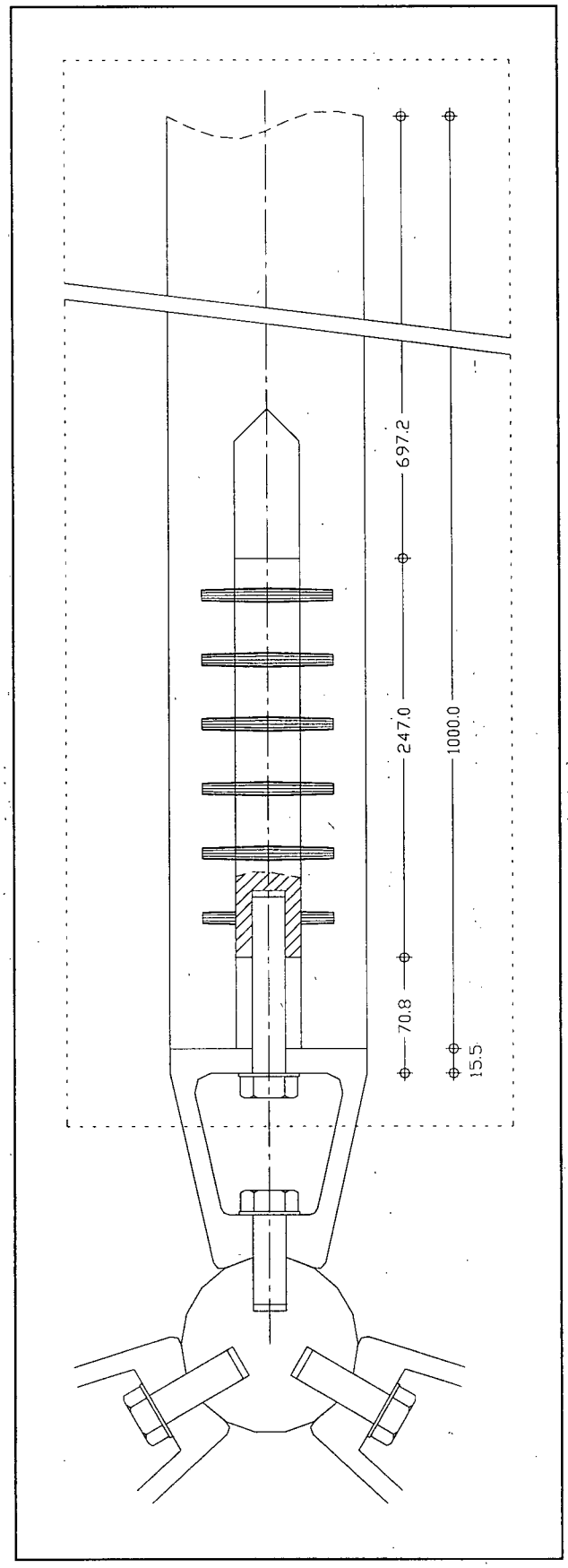

Figure 94: Connection setup of INDUO-connector in 3D-space truss beam

Being well suited for transferring high tensile loads, the INDUO-fastener can be applied in heavy-timber structures like the space truss system of the Thalkirchen Bridge. Compared to the dowel-joint that is exposed to the weather and an corrosive environment resulting from the use of road salt during winter time, the relatively small and compact INDUO-connector is sandwiched and protected in the wood member, providing a high tensile load capacity.

Figure 94 shows how the INDUO-connector could be applied as a substitute for the tight-fitting dowel connection used in the structure of the bridge. Table 14 presents a stiffness calculation of the proposed connection setup that shows the relatively small deformations under a tensile design load of 60kN.

Example: INDUO-connector applied in 3D-Truss beam

#	Component	Grade	l (mm)	As (mm^2)	MOE (N/mm^2)		Stiffness (N/mm)	Displacement (mm)
1.1	Wood member 120x120 (Beam half):	DG Fir, SS	1,000.0	14,400	12,000		172,800	0.347
1.2	Wood member 100x100 (Beam half):	DG Fir, SS	1,000.0	10,000	12,000		120,000	0.500
2	INDUO-connector:		247.0				100,140	0.599
3	Bolt M20:	10.9	70.8	245	210,000		726,695	0.083
4	*Bolt + Connector*		*317.8**				*88,012**	
5					**Total 100x100:**		**50,773**	**1.182**
6					**Total 120x120:**		**58,312**	**1.029**

Table 14: *Calculation example on stiffness and displacement of INDUO-connector in 3D-truss beam*
**) Values from test series of research project*

6 Conclusion and Recommendations

Conclusion

This research project produced comprehensive results on tensile strength, stiffness and failure performance of the INDUO-Heavy-Timber joint. Overall 99 specimens featuring member setups of different material-connector combinations were tested and evaluated. Furthermore, the results for the characteristic tensile strength were compared with values derived from international timber codes.

In conclusion, it can be said that the INDUO-connector type B, providing significantly higher tensile strength properties, outperforms the older type A version. In combination with TimberStrand®LSL connector type B presented the best test results in terms of tensile strength and failure performance. For Microllam®LVL, Parallam®PSL and Douglas-Fir lumber both connector types generally showed brittle failure mechanisms.

Investigating an alternative lamination method to connect the timber halves of the INDUO-members, it was found that screw-bonded and glued-laminated test specimens did not present different tensile strengths and failure modes.

The comparison of the characteristic tensile strength with numbers derived from design values of different international timber codes (Europe, Germany, Canada and USA) showed that the INDUO-connector type B can be modeled and calculated as "doweled or bolted connection with inside steel plate". While all four codes generally complied with the characteristic tensile strength properties generated from the test results, due to different safety approaches, the respective design values differed significantly from each other. Here, the Canadian code proved to be the most conservative and the European code the most progressive design approach.

Recommendations

After more than two years of research and comprehensive investigations, it can be said that the INDUO-connection meets most of the state-of-the-art performance requirements stated by Madsen (page 11). Presenting high strength and high stiffness properties, the INDUO-heavy-timber system is both easy to manufacture and erect and meets esthetic as well as fire protection demands due to the embedment of the connector in the timber member. In comparison with other mechanical fasteners, such as nails, bolts or steel

dowels, however, the undesirably brittle failure mechanisms of the INDUO-connection under tensile loading present a major disadvantage. Similar to the proposed use of glued-in rods with welded steel plates (page 12), it is therefore recommended to design the INDUO-connection in a way that failure will occur in the ductile steel bolt which joints the embedded connector and the adjacent structure.

Due to budgetary limits, this research project could only focus on one specific field of interest: The tensile performance of the INDUO-connection. Based on the experience and results gained during the project, future research on the performance and strength properties of the INDUO-connector should investigate the following:

Type of loading:

- Investigation of connection behavior under cycling loading; information for the design of dynamically loaded structures, e.g. caused by traffic, earthquake or wind.
- Transverse loading of INDUO-connection: Influence of different member materials on shear capacity.

Different member materials:

Tensile and transverse connection capacity of

- LVL with cross-plies (KertoQ of Finnforest)
- Other solid wood species (Hemlock, SPF, etc.)

Alternative lamination methods of timber halves using:

- Nails (smooth nails, annular ringed or helically threaded nails)
- Truss-plates

Alternative configuration of connector:

- Investigation of tensile strength and performance with a connector body made of mild steel (manufactured by point-welding steel dowels to steel connector body)
- Increasing number of load-bearing pins by serially connecting two (or 1½) type B connectors

7 List of References

American Society of Civil Engineers. (1996). "Standard for Load and Resistance Factor Design for Engineered Wood Construction - ASCE 16–95", *ASCE*, New York, NY, USA

American Society for Testing and Materials. (1996). "Standard Methods of Testing Small Clear Specimens of Timber - D143-83", *ASTM*, Philadelphia, PA, USA

American Society for Testing and Materials. (1996). "Standard Test Methods for Mechanical Fasteners in Wood - D1761-88", *ASTM*, Philadelphia, PA, USA

American Society for Testing and Materials. (1996). "Standard Test Methods for Specific Gravity of Wood and Wood-Base Materials - D2395-93", *ASTM*, Philadelphia, PA, USA

American Society for Testing and Materials. (1996). "Standard Specification for Evaluation of Structural Composite Lumber Products - ASTM D5456-93", *ASTM*, Philadelphia, PA, USA

American Society for Testing and Materials. (1996). "Standard Test Methods for Mechanical Fasteners in Wood - ASTM D1761-88", *ASTM*, Philadelphia, PA, USA

American Society for Testing and Materials. (1996). "Standard Test Methods for Bolted Connections in Wood and Wood-Base Materials - ASTM D5652-95", *ASTM*, Philadelphia, PA, USA

American Society for Testing and Materials. (1997). "Standard Test Method for Evaluating Dowel-Bearing Strength of Wood and Wood-Base Products - ASTM D5764a-97", *ASTM*, Philadelphia, PA, USA

Blaß, H.J. (2001). Expert's report: "Optimierung des INDUO-Verbundankers; Zusammenfassung der Gutachten / Typenstatik", *Ingenieurbüro Blaß & Eberhart*, Karlsruhe, Germany

Buchanan, A., Moss, P., Eistetter, S.. (2000). "Cement Grouted Steel Bars in Glulam", Proceedings, 6th World Conference on Timber Engineering, Whistler, BC

Canadian Standards Association. (1994). "Engineering Design in Wood (Limit States Design) - CAN/CSA-O86.1-94", *CSA*, Rexdale, Ontario, Canada

Canadian Wood Council. (1995). "Wood Design Manual 1995", *Canadian Wood Council,* Ottawa, Ontario, Canada

Canadian Wood Council. (1999). "Introduction to Wood Design", *Canadian Wood Council,* Ottawa, Ontario, Canada

Deutsches Institut für Bautechnik. (2002). "Bauaufsichtliche Zulassung Multi-Krallen-Dübel (MKD / SpikeTec) als Holzverbindungsmittel, Zulassungsnummer 1.9.1-193/01, Neuzulassung 11.03.2002", *DIBt*, Berlin, Germany

Deutsches Institut für Normung eV. (2000). "(Norm-Entwurf) DIN 1052-2000 - Entwurf, Berechnung und Bemessung von Holzbauwerken - Allgemeine Bemessungsregeln und Bemessungsregeln für den Hochbau", *Beuth Verlag*, Berlin, Germany

Deutsches Institut für Normung e.V.. (1988). "DIN 1052 (4/88) Teil 1 - Holzbauwerke, Berechnung und Ausführung". *Beuth-Verlag*, Berlin, Germany

Deutsches Institut für Normung e.V.. (1988). "DIN 1052 (4/88) Teil 2 - Holzbauwerke, Mechanische Verbindungen". *Beuth-Verlag*, Berlin, Germany

Deutsches Institut für Normung e.V.. (1994). "DIN V ENV 1995 Teil1-1 (06/94) - Eurocode 5: Entwurf, Berechnung und Bemessung von Holzbauwerken, Teil 1-1: Allgemeine Bemessungsregeln, Bemessungsregeln für den Hochbau", *Beuth-Verlag*, Berlin, Germany

European Committee for Standardization. (1993). "Eurocode No. 5: Design of Timber Structures, Part 1 - 1: General Rules und Rules for Buildings", *CEN*, Brussels, Belgium

European Committee for Standardization. (1997). "EN 1562 - Founding - Malleable Cast Irons; *CEN*, Brussels, Belgium

European Committee for Standardization. (1997). "EN 1563 - Founding - Spheroidal Graphit Cast Irons", *CEN*, Brussels, Belgium

European Committee for Standardization. (1993). "EN 383 - Timber structures; test methods; determination of embedding strength and foundation values for dowel type fasteners", *CEN*, Brussels, Belgium

Führer, W. (2002). Expert's report: "Enwicklung einer montagefreundlichen Werkzeuglösung für die rückwärtige INDUO-Verbundanker-Verschraubung", *RWTH Aachen*, Aachen, Germany

Güldenpfennig, J. (1997). Expert's report: "Stellungnahme zur Einhaltung der Anforderungen an einen genehmigungsfähigen Standsicherheitsnachweis von Einfamilienhäusern in Selbstbauweise unter Verwendung von Kreuzbalken mit INDUO-Verbundankern", *RWTH Aachen*, Aachen, Germany

Johansen, K.W.. (1949). "Theory of timber connections", *International Association of Bridge and Structural Engineering*, Bern, Switzerland

Kangas, J.. (2000). "Design of connections based on in V-form glued-in rods", Proceedings, 6th World Conference on Timber Engineering, Whistler, BC

Mischler, A., Prion, H., Lam, F.. (2000). "Load-carrying Behavior of Steel-to-Timber Dowel Connections", Proceedings, World Conference of Timber Engineering 2000, Whistler, BC

Madsen, B. .(1998). "Reliable timber connections.", North Vancouver, BC, Canada

National Research Council Canada. (1984), "CCMC Evaluation Report, CCMC 08675-R - Microllam™ LVL", *Canadian Construction Materials Centre,* Ottawa, Ontario, Canada

National Research Council Canada. (1986), "CCMC Evaluation Report, CCMC 11161-R-Parallam® PSL", *Canadian Construction Materials Centre,* Ottawa, Ontario, Canada

National Research Council Canada. (1994), "CCMC Evaluation Report, CMC 12627-R-TimberStrand® LSL", *Canadian Construction Materials Centre,* Ottawa, Ontario, Canada

Riberholt, H.. (1988). "Glued bolts in Glulam", *Dept of Structural Engineering, Technical University of Denmark*, Lyngby, Denmark

Schneider, Klaus-Jürgen (1998). "Bautabellen für Ingenieure", *Werner Verlag,* Düsseldorf, Germany

Schreyer, A., Bathon, L., Prion, H.G.L.. (2000). "Determination of the Capacities of a new Composite Timber-Steel Connector System", Proceedings, 6th World Conference on Timber Engineering, Whistler, BC

Smith, I., Foliente, G.. (2002). "Load and Resistance Factor Design of Timber Joints: International Practice and Future Direction", Journal of Structural Engineering, Vol. 128, No.1

Turkovskij, S. B.. (1991). "Use of Glued-in Bars for Reinforcement of Wood Structures", Proceedings, 1991 Timber Engineering Conference, London, UK

Wisconsin Department of Commerce, Safety & Buildings Division. (2002). Building Products Evaluation, Evaluation # 200216-O, "Bertsche System - Concealed Forged Steel Heavy Timber Connection System", *Wisconsin Department of Commerce,* Madison, WI; USA

8 Appendices

8.1 Photographic documentation

8.1.1 Manufacturing steps of test specimen

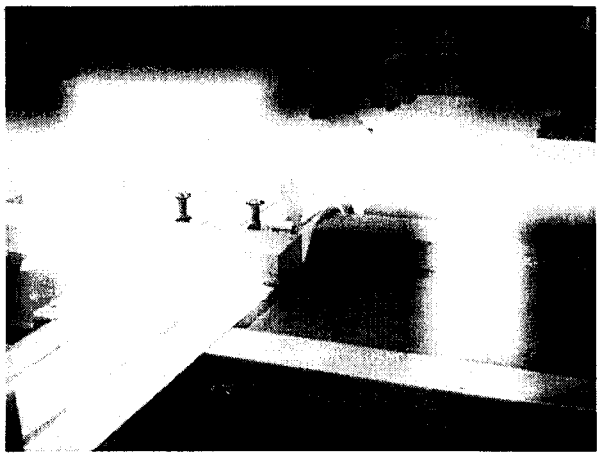

Figure 95: *Cutting timber members to rough dimensions (Sliding Table Saw)*

Figure 96: *Planing of timber members to final width and thickness (4-Sided Planer)*

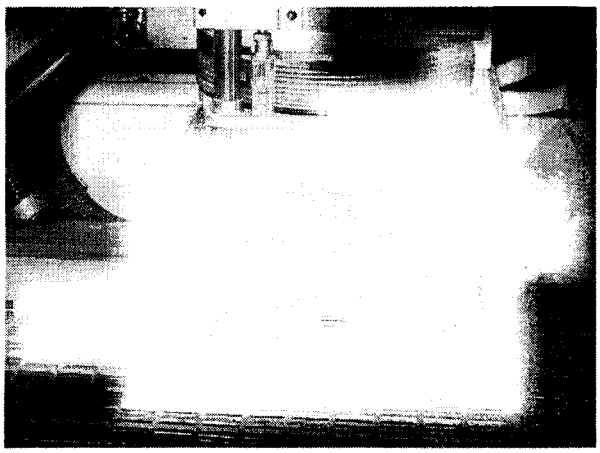

Figure 97: *Machining of rows of holes and V-groove by means of CNC-router*

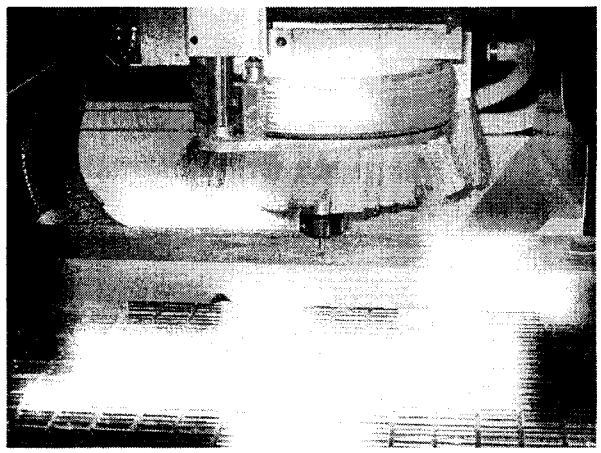

Figure 98: *Machining of circular grooves (CNC-router)*

Figure 99: *INDUO-connector ready to be embedded in machined timber halves*

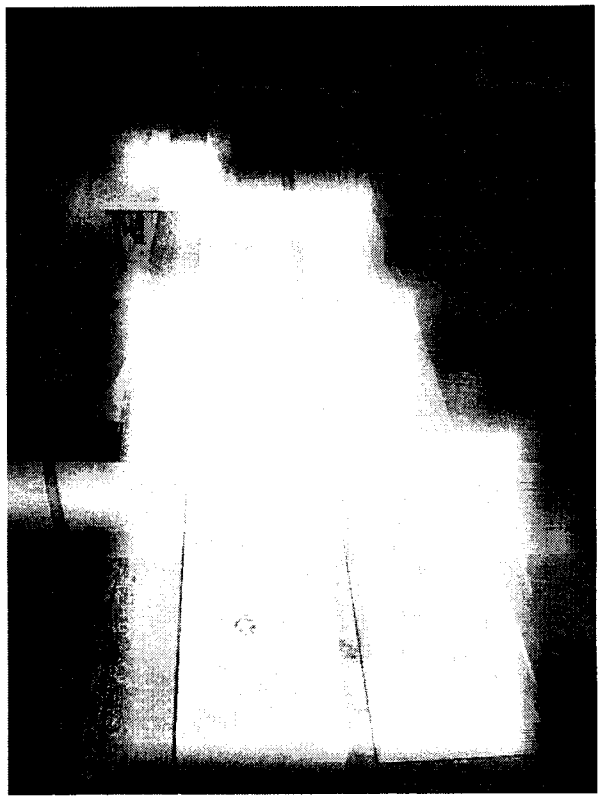

Figure 100: *Circular grooves to accommodate Steel Side Plates*

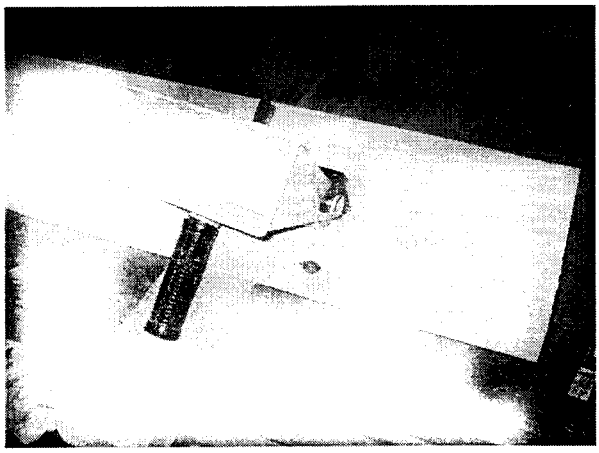

Figure 101: *Applying PVA-construction glue to both inside faces of the timber halves*

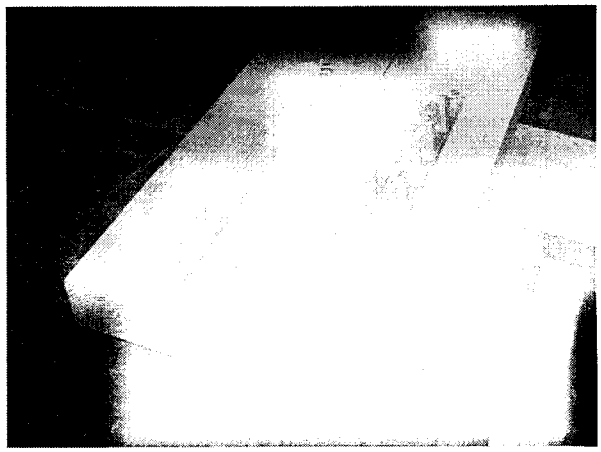

Figure 102: *Inserting the connector in V-groove*

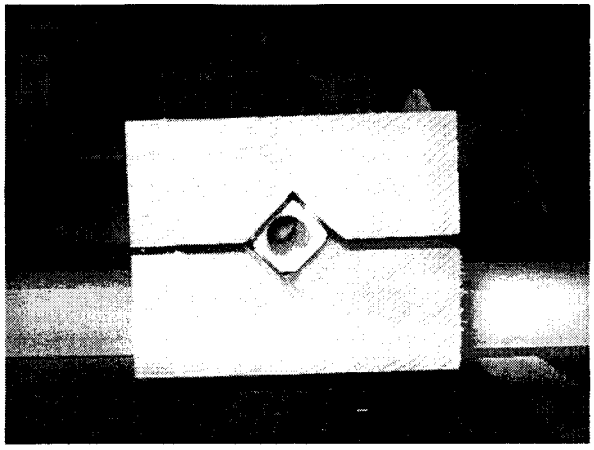

Figure 103: *Joining of both timber halves enclosing the connector*

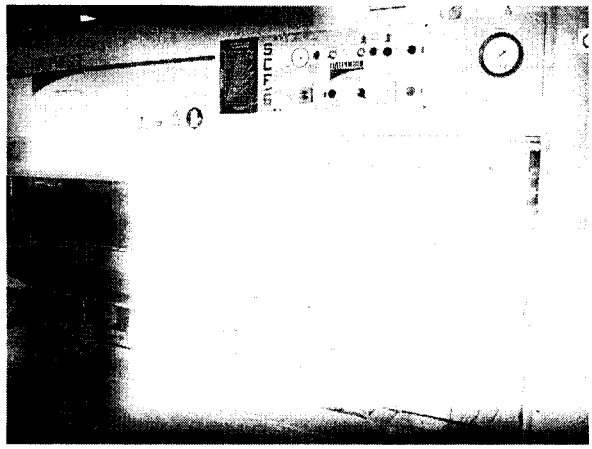

Figure 104: *Inserting the composite member into hydraulic press; Pressing time: 30 minutes*

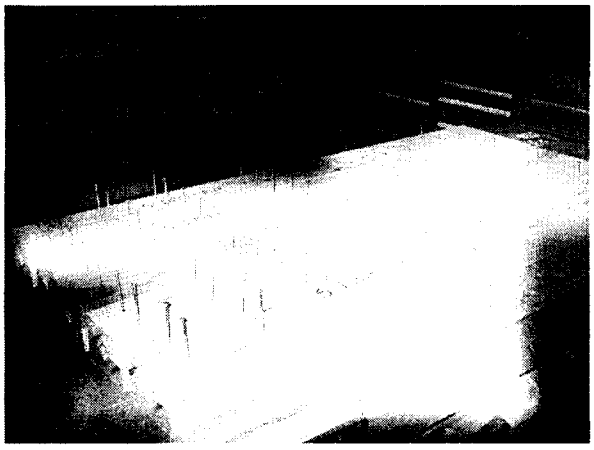

Figure 105: *Alternative connection of timber halves with regular wood-screws 6x10*

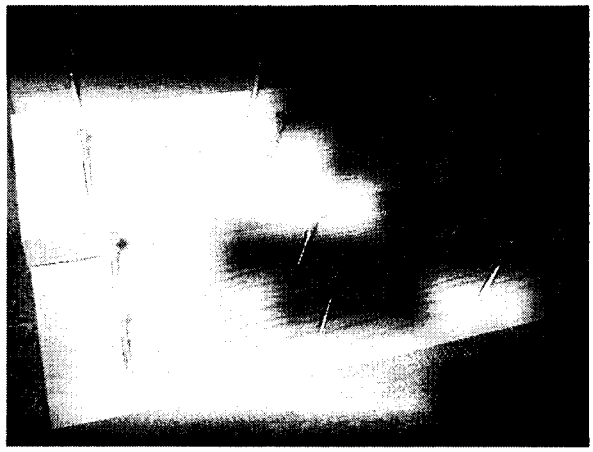

Figure 106: *Setup of screws*

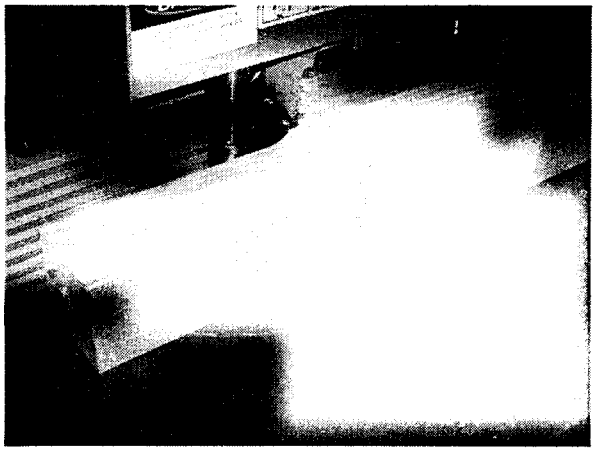

Figure 107: *Tapering of the test member to squared cross-section 100x100 and 120x120mm respectively (NC-shaper)*

8.1.2 Test procedure

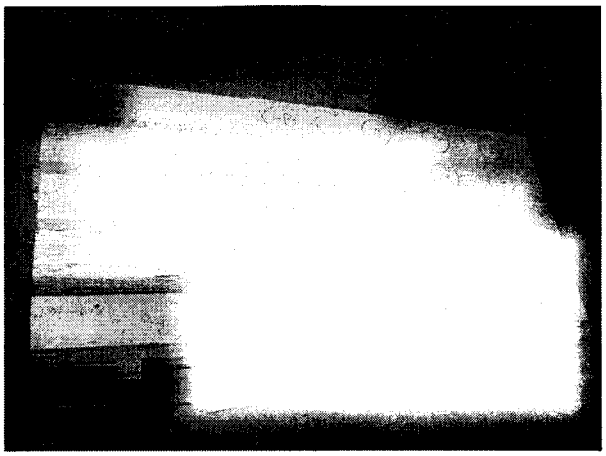

Figure 108: *Specimen ready to be tested*

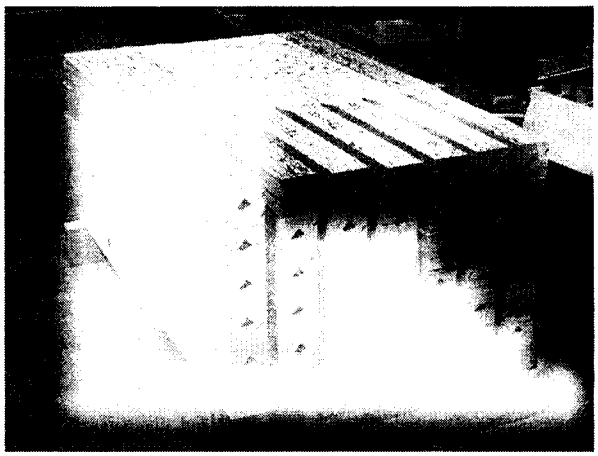

Figure 109: *Stacked members of different connector-material setups before testing*

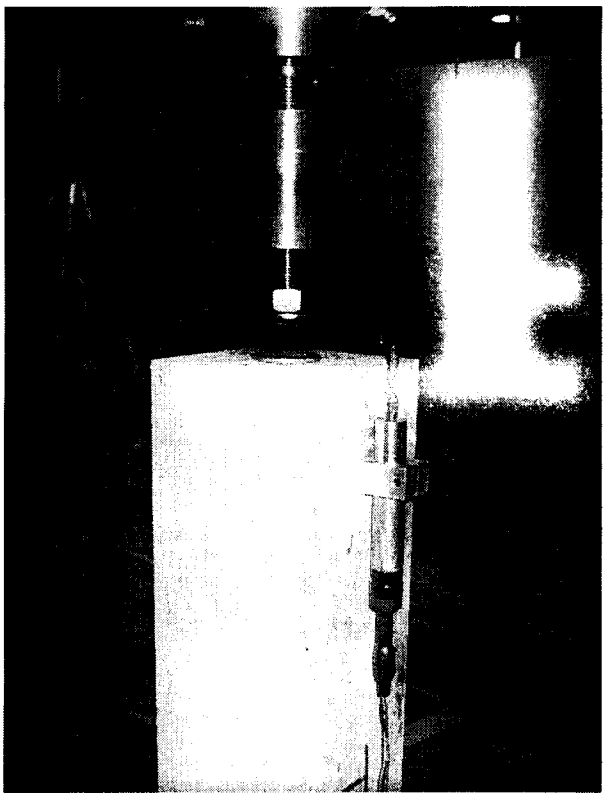

Figure 110: *Specimen connected to upper machine support*

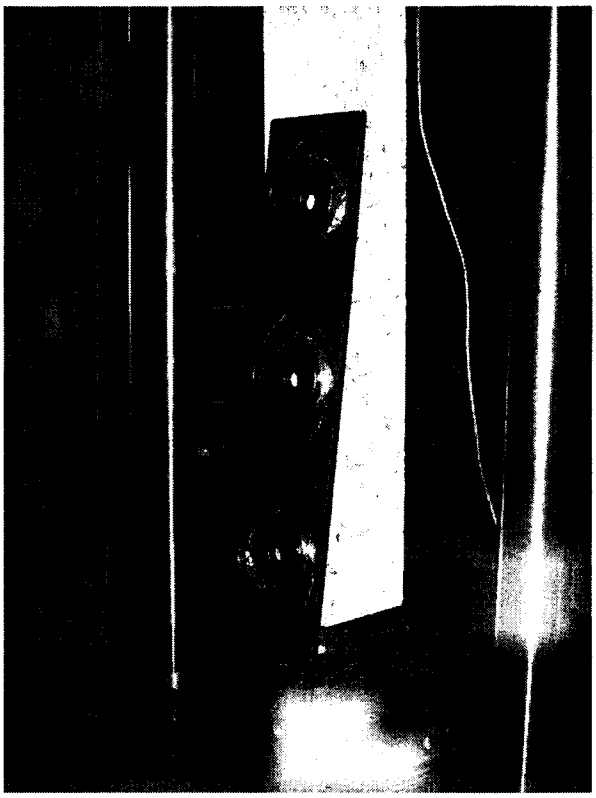

Figure 111: *Steel Side Plates transfer applied load from the lower machine support to test member*

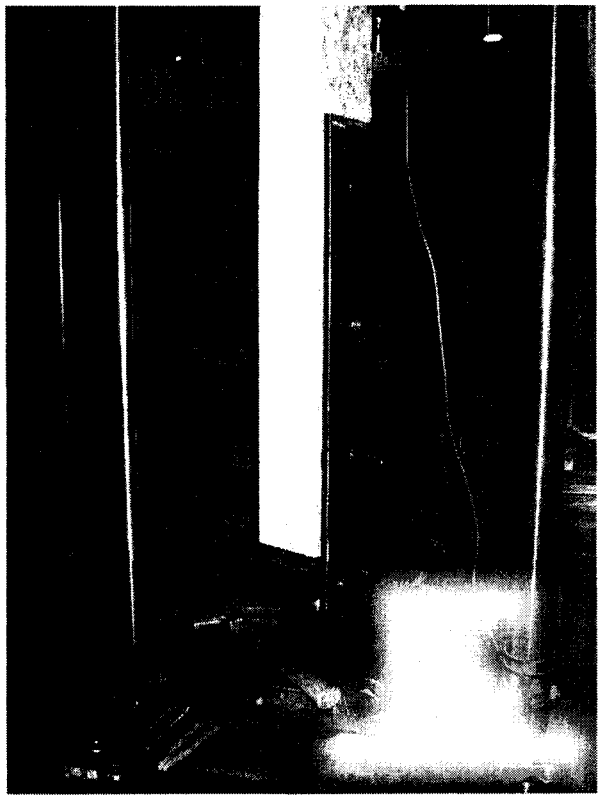

Figure 112: *Assembly of Steel Side Plates with 7/8-inch bolts*

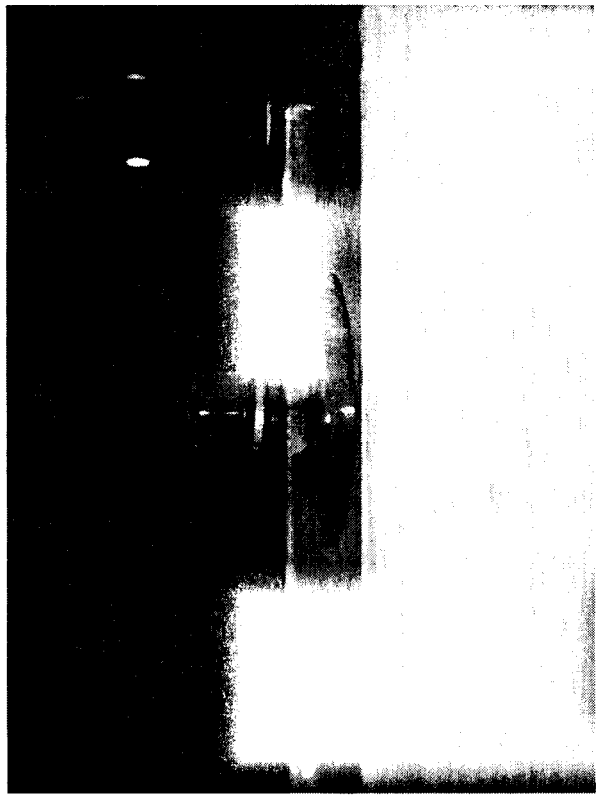

Figure 113: *Close-up of steel rings sliding into circular groove*

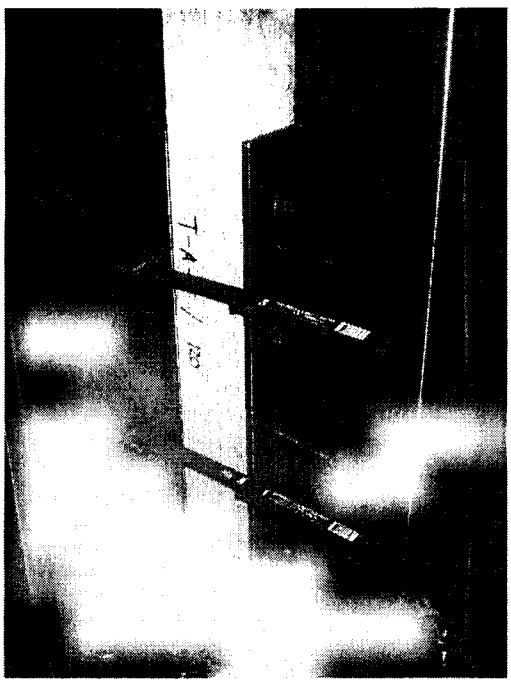

Figure 114: *Steel Side Plates are pressed into grooves by means of regular clamps*

Figure 115: *Components of lower coupling: Distance plates and two 1-inch bolts*

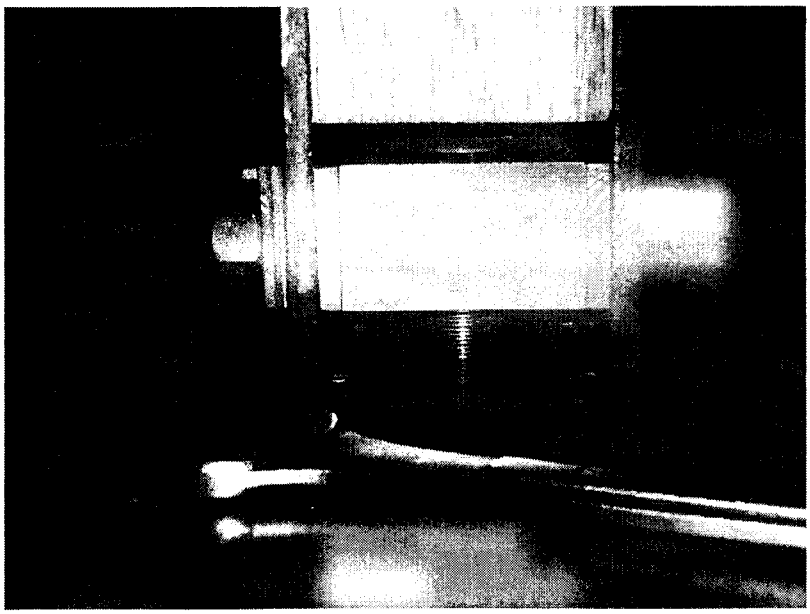

Figure 116:
Lower coupling fastened

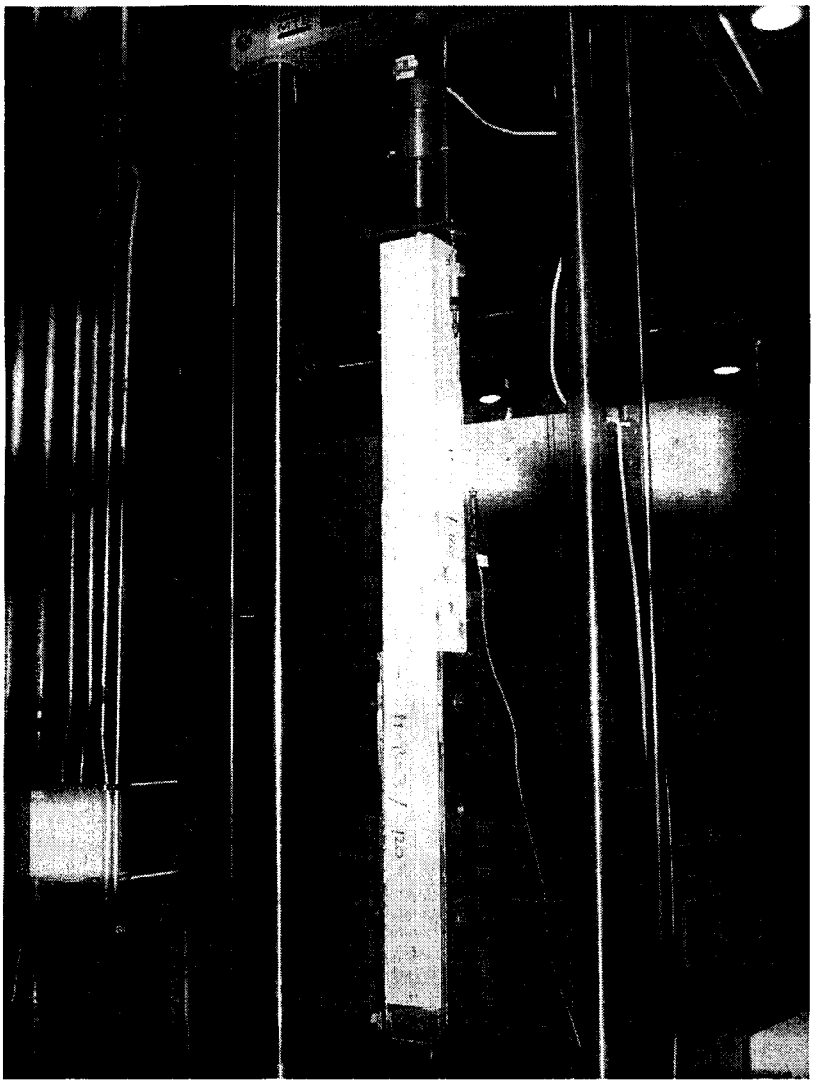

Figure 117: *Specimen connected to test apparatus, ready to be tested*

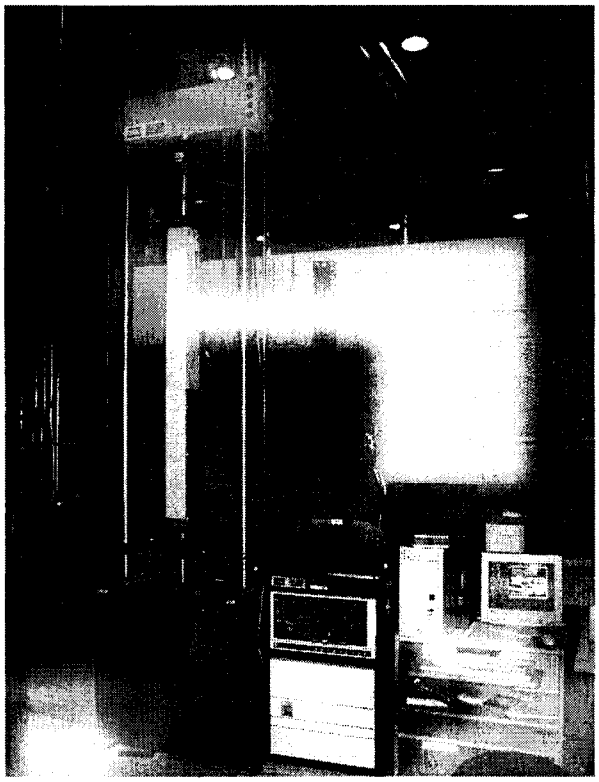

Figure 118: Test apparatus consisting of test machine, control unit and PC

Figure 119:** Unloading of **heavy test member by means of a "mobile gallow"

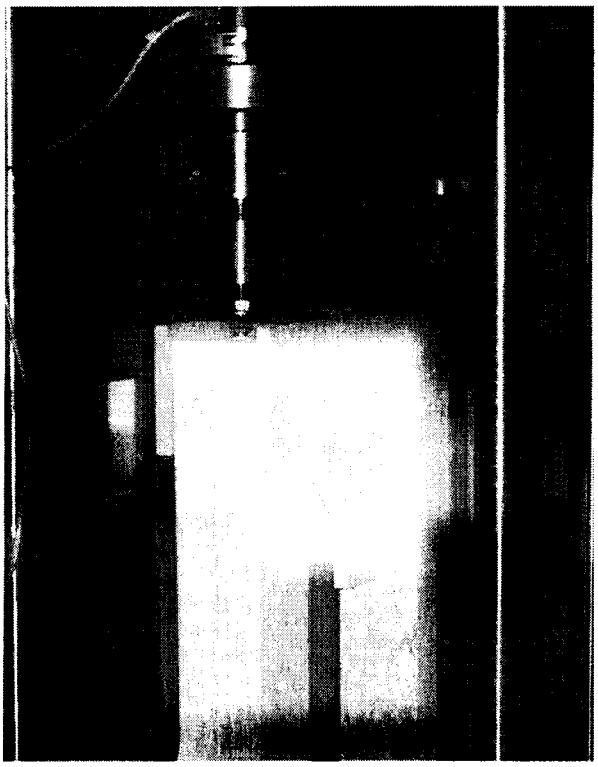

***Figure 120:** Gallow in place to support the test member after being uncoupled*

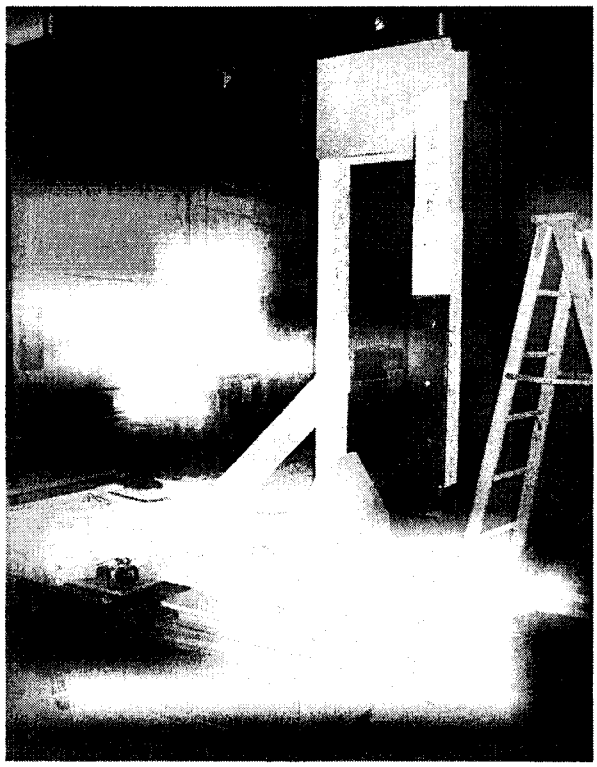

***Figure 121:** Disassembling of upper and lower couplings*

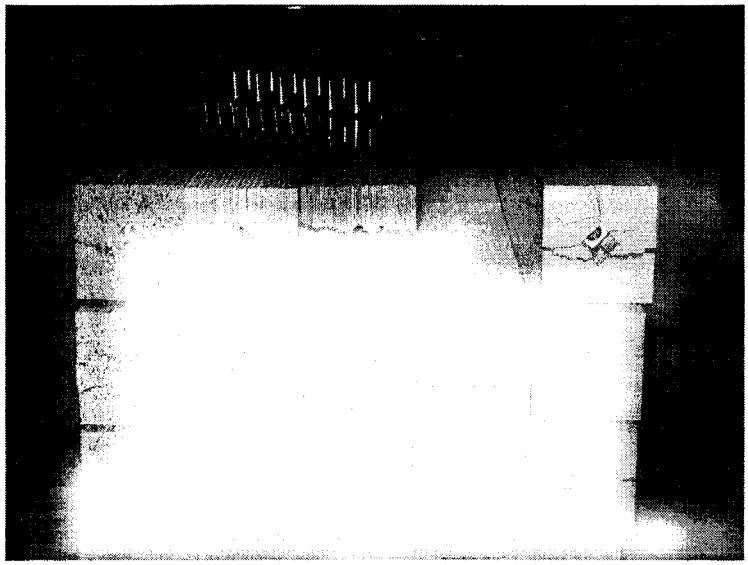

Figure 122:
Tested type A and B specimens, 120x120mm, test series 1

Figure 123:
Tested type A and B specimens, 100x100mm, test series 1

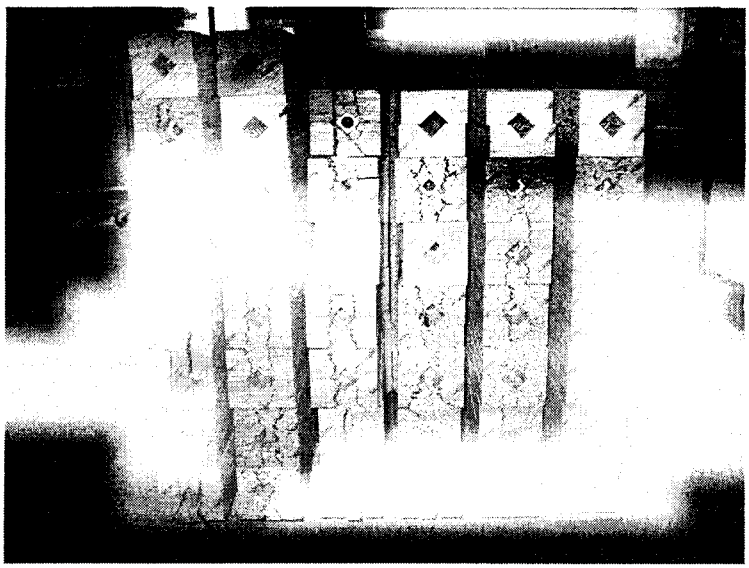

Figure 124:
Tested connector-type-B specimens, 100x100mm, test series 2

8.1.3 Failure modes

TimberStrand®LSL

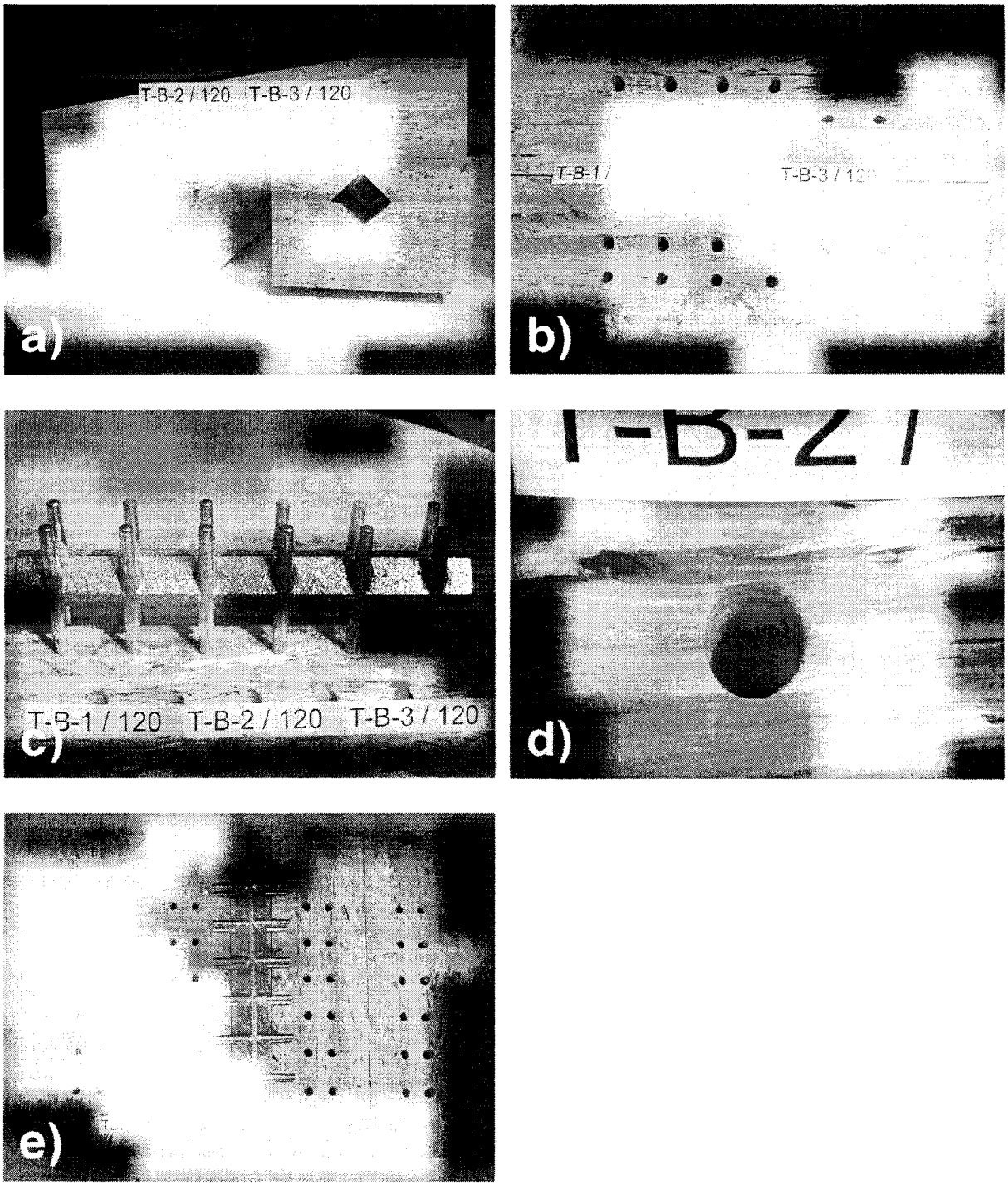

Figures125a-e: *No failure observed with TB-member setups*

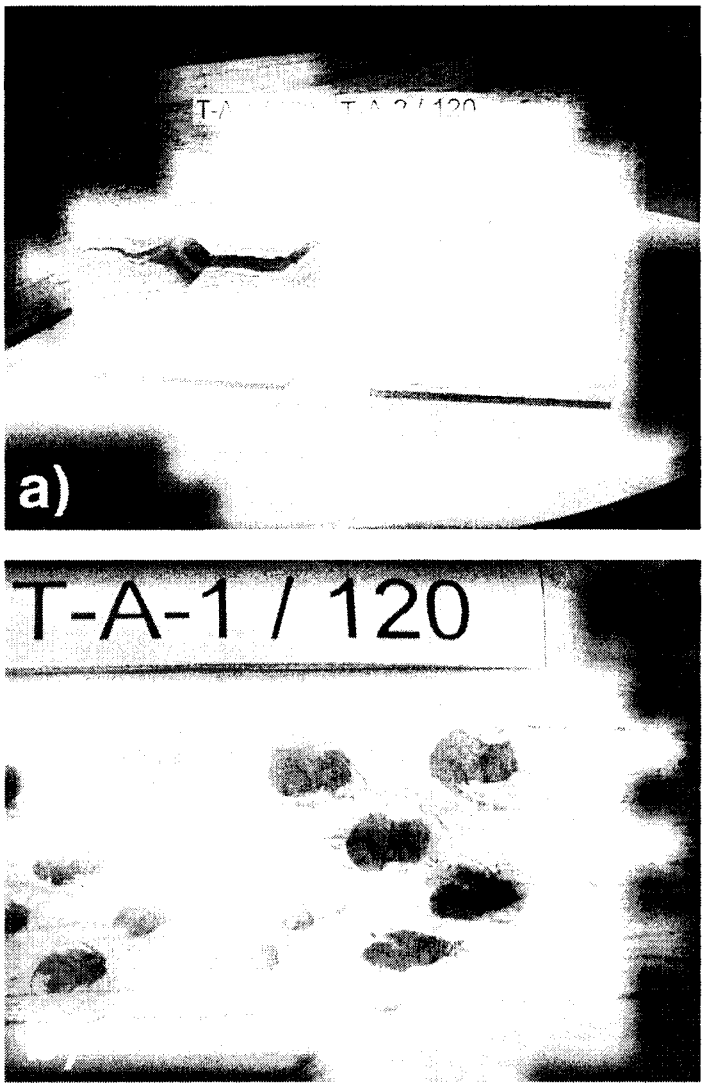

Figures126a-b: *Failure modes observed with TA-member setups*

Douglas-Fir plywood ("X-LVL")

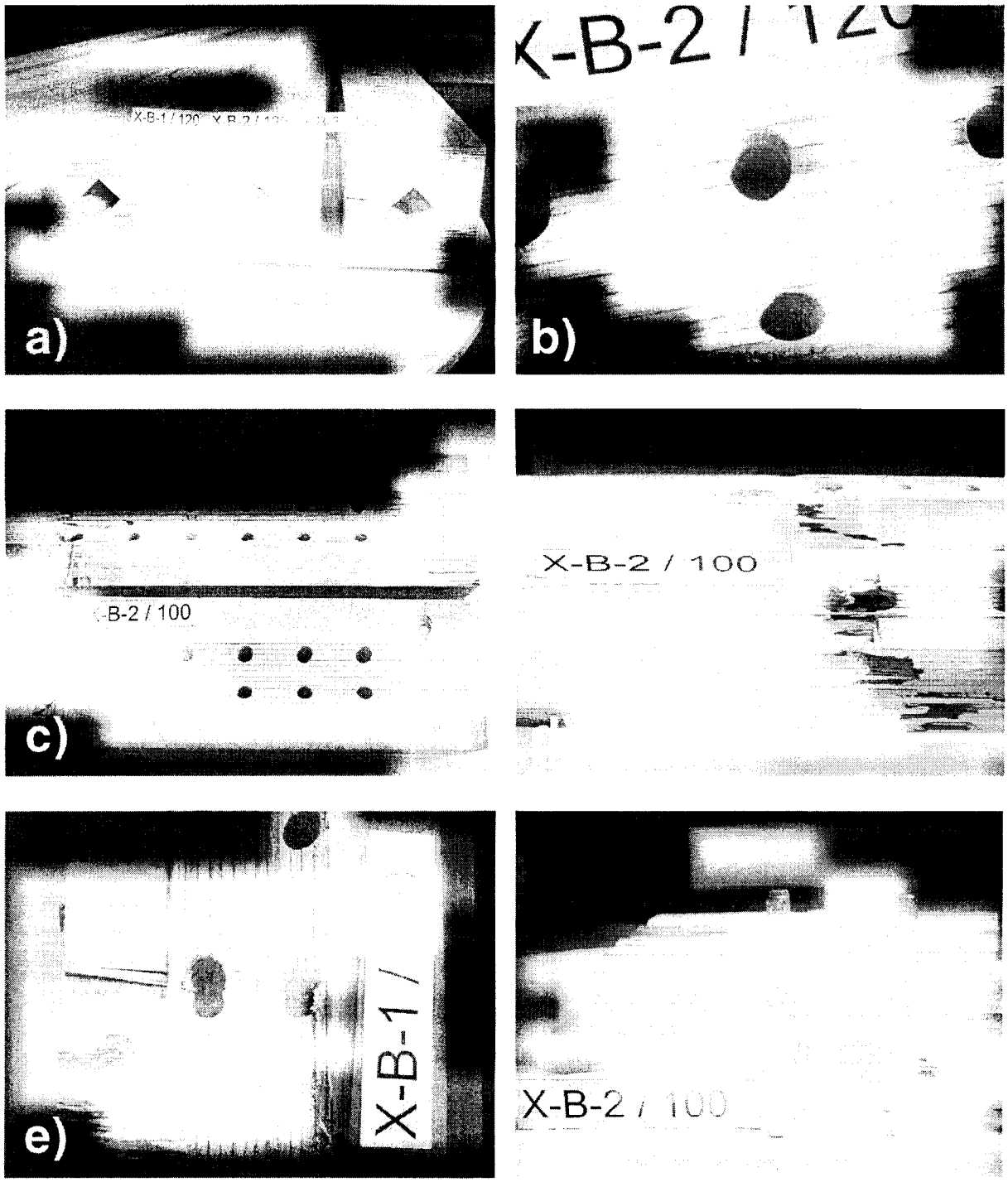

Figures 127a-f: *Failure modes observed with XB-member setups*

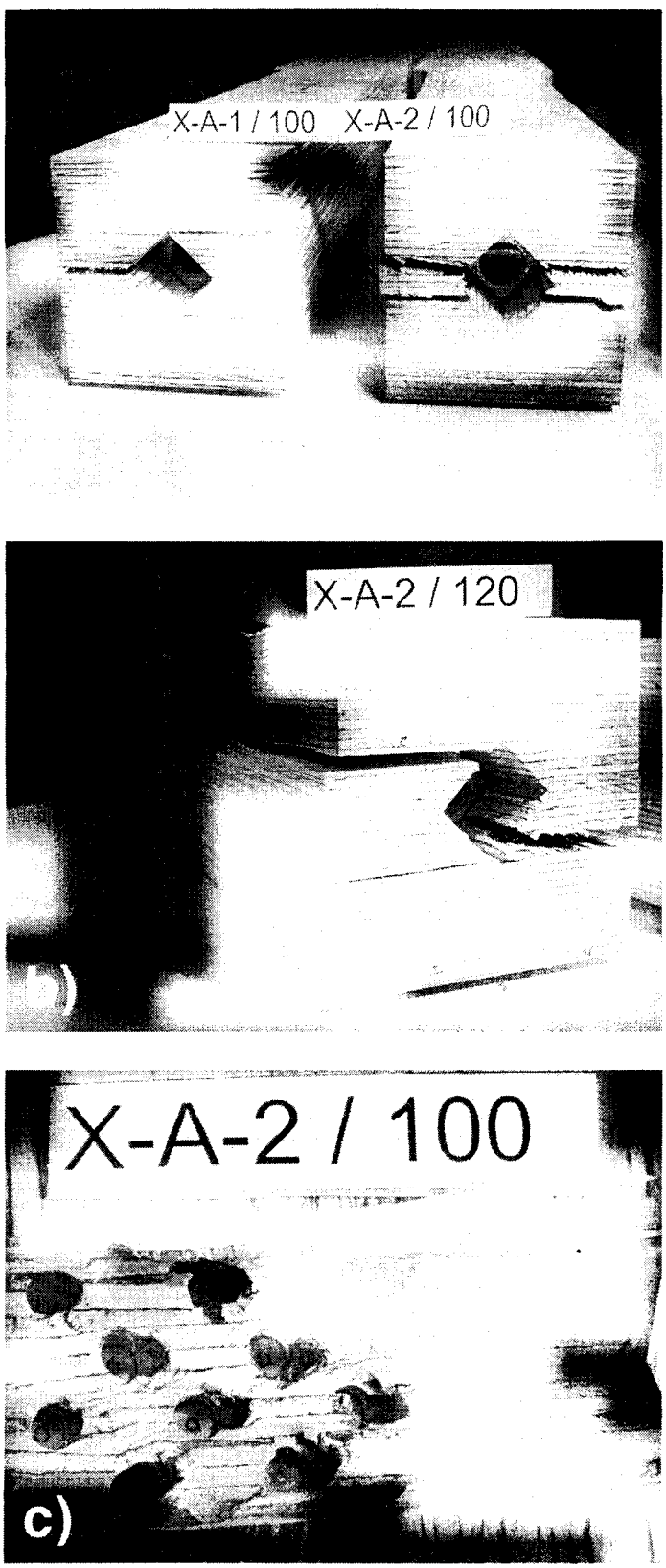

Figures 128a-c: *Failure modes observed with XA-member setups*

Douglas Fir

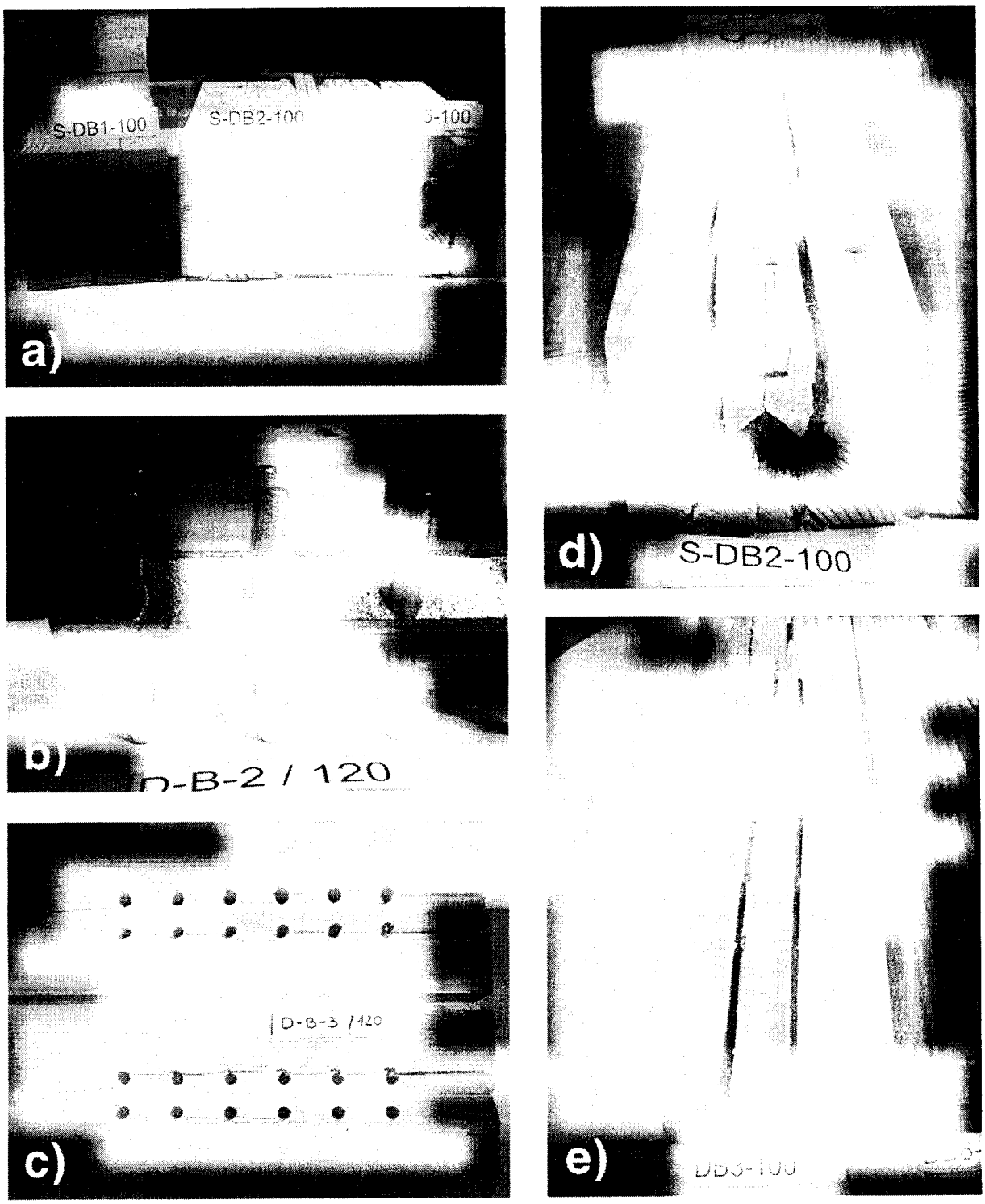

Figures 129a-g: *Failure modes observed with DB-member setups*

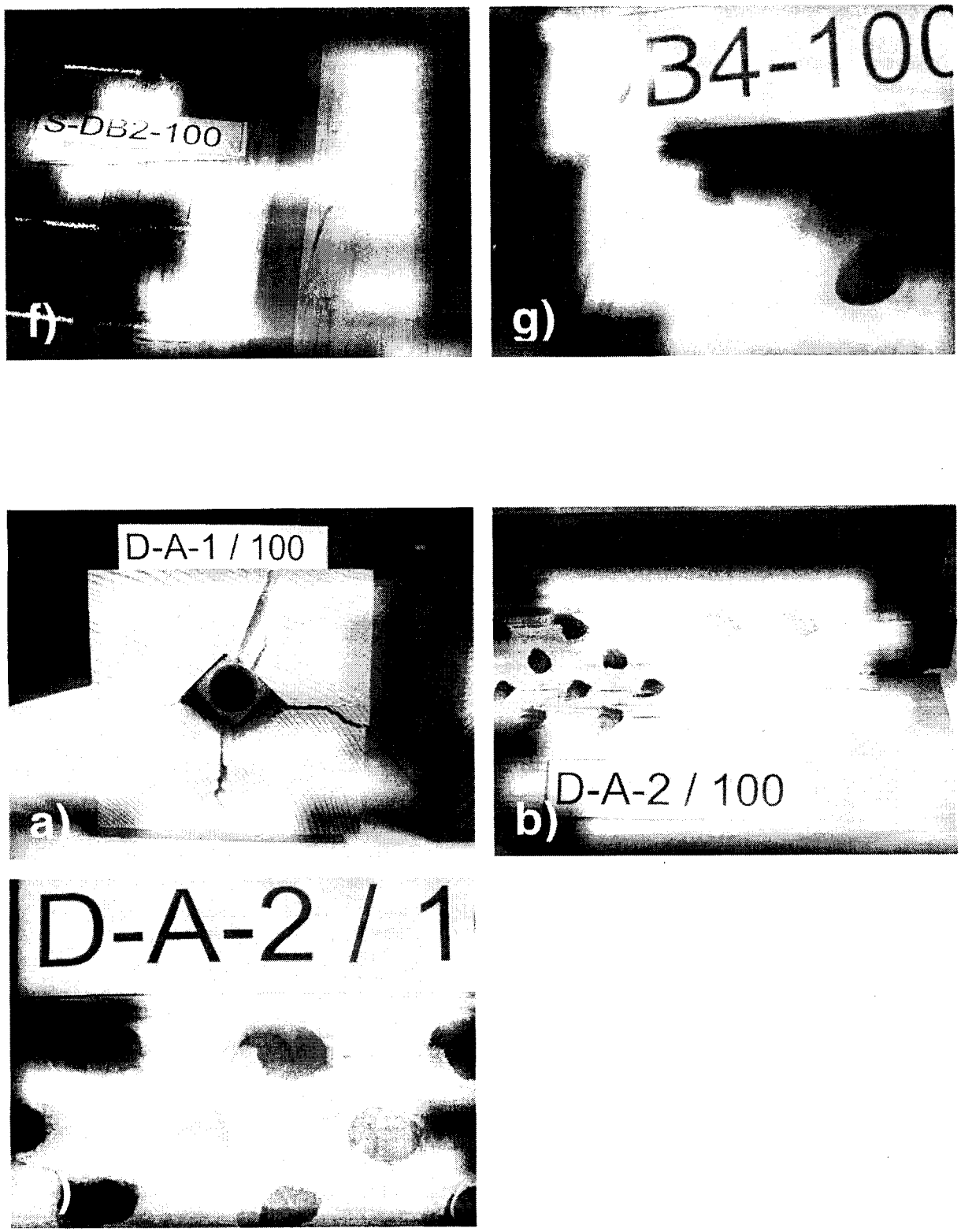

Figures 130a-c: *Failure modes observed with DA-member setups*

Microllam®LVL

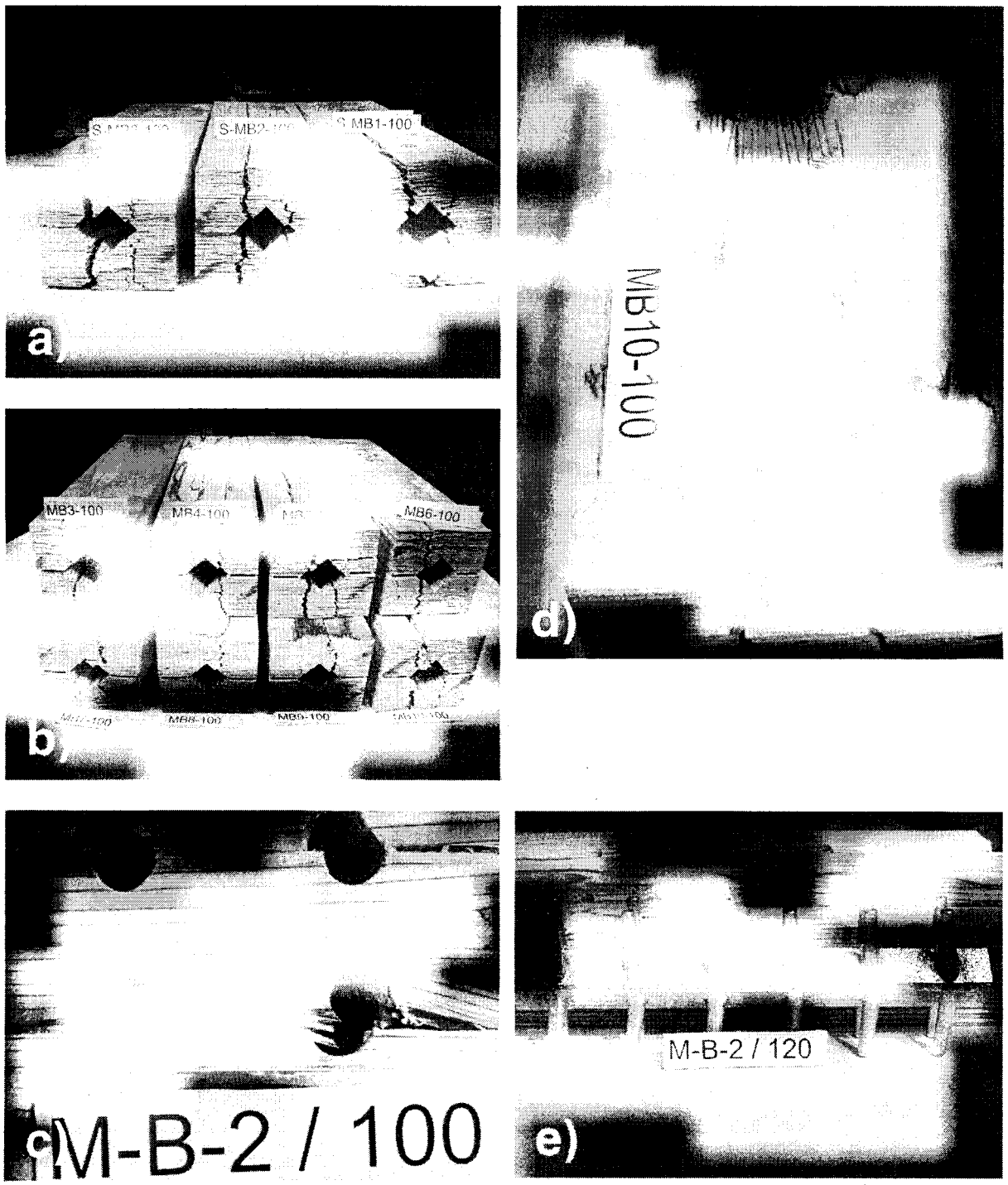

Figures 131a-g: *Failure modes observed with MB-member setups*

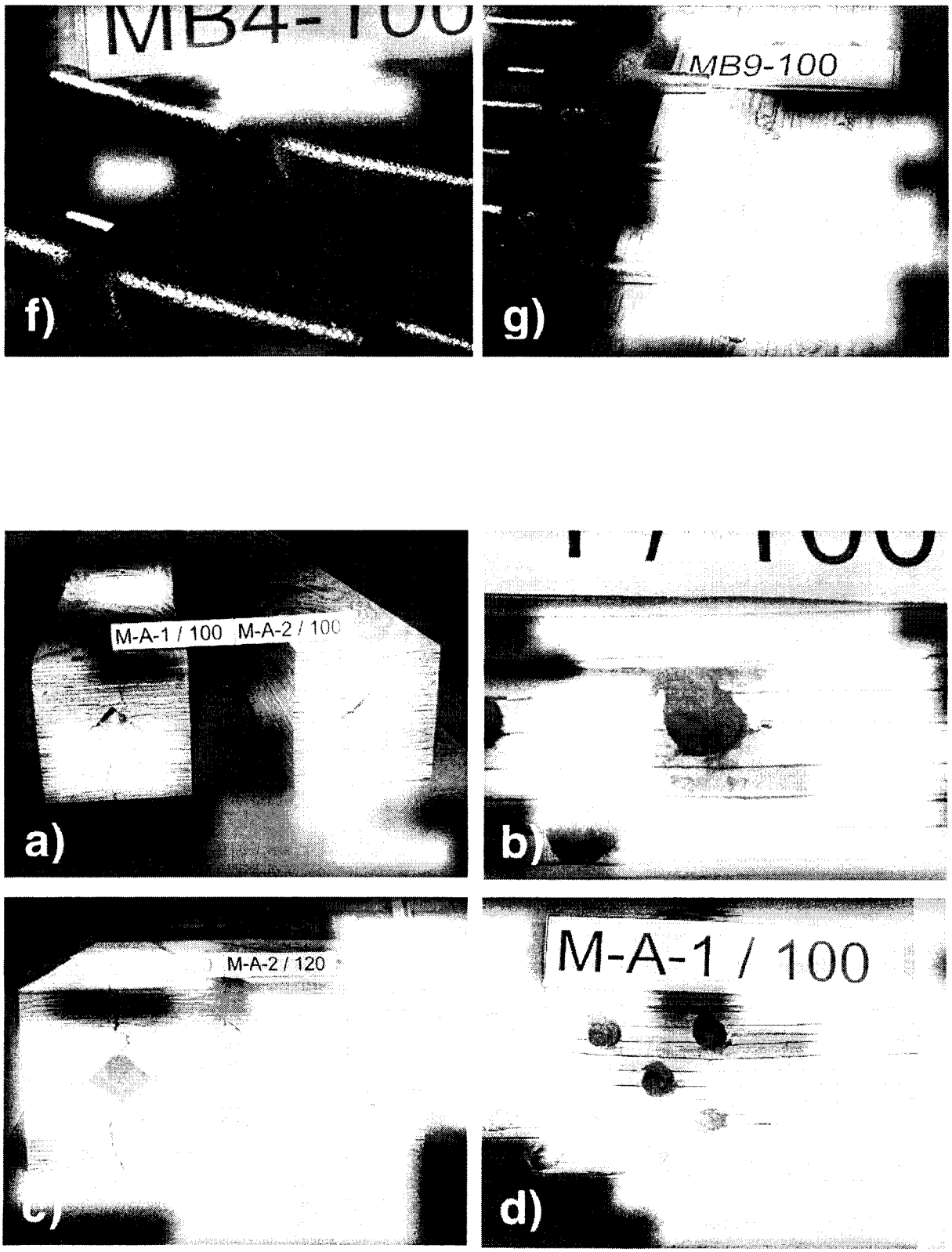

Figures 132a-d: *Failure modes observed with MA-member setups*

Parallam®PSL

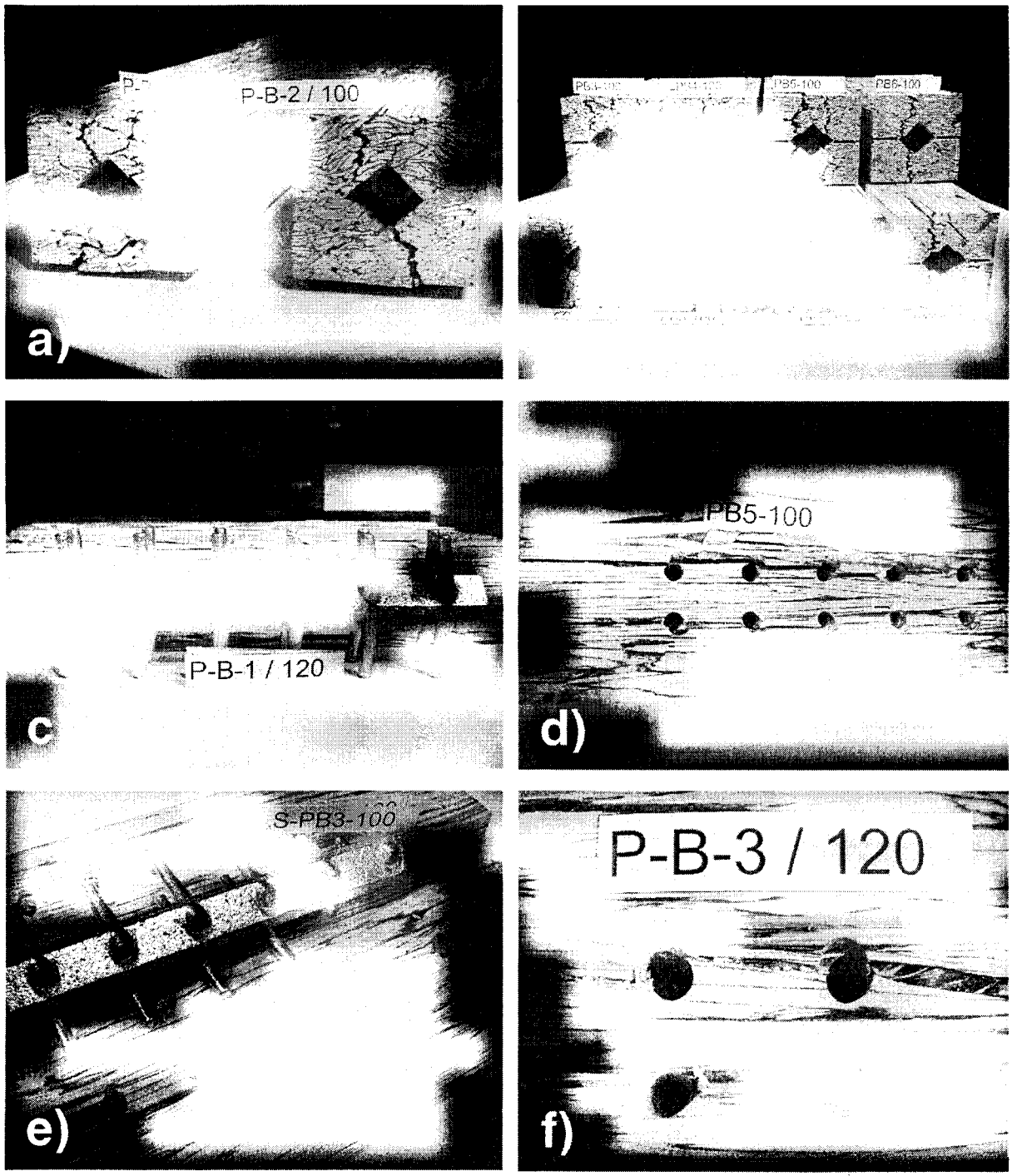

Figures 133a-f: *Failure modes observed with PB-member setups*

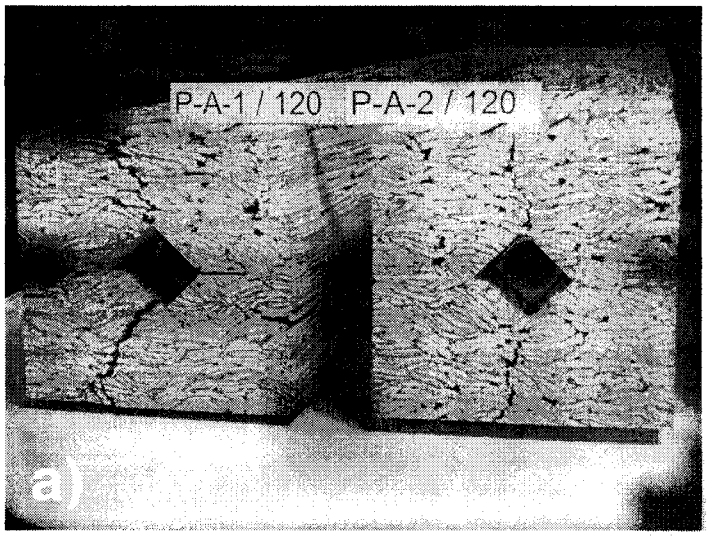

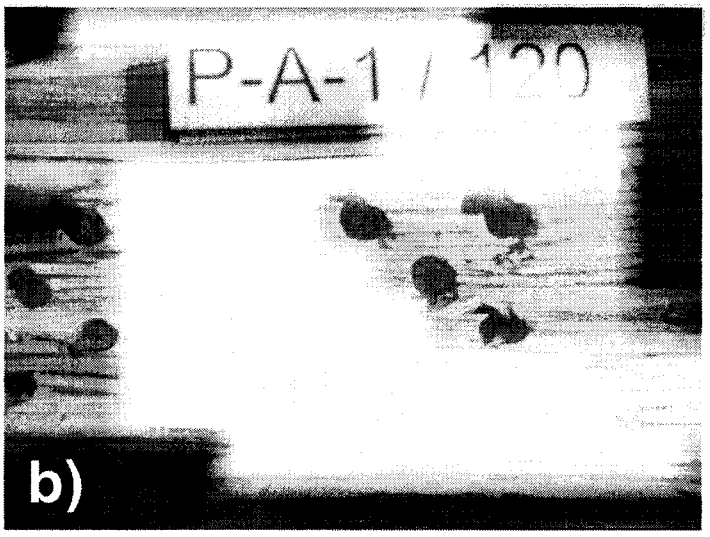

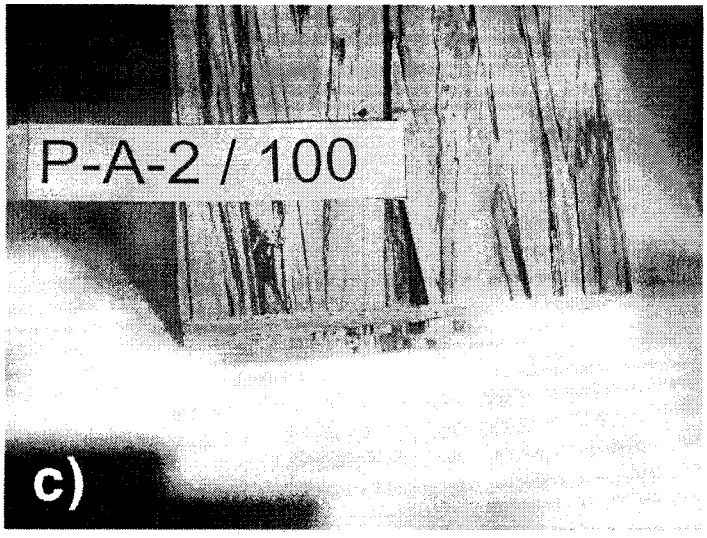

Figures 134a-c:
Failure modes observed with PA-member setups

8.2 Calculations

RELAN Data Fitting (Error of Distribution Fit)

	Normal	Lognorm.	2P-Weib.	3P-Weib.
DG Fir	0.0278	0.0333	0.0154	0.0154
PSL	0.0016	0.0019	0.0029	0.0014
LVL	0.0095	0.0082	0.0161	0.0051

Parameters of Fitted Distribution

	Normal		Lognorm.		2P-Weib.			3P-Weib.		
	mean	std. dev.	mean	std. dev.	loc	m	k	loc	m	k
DG Fir	168.078	15.867	168.066	15.315	0	174.962	12.608	0.000	174.962	12.608
PSL	157.821	13.419	157.920	13.489	0	163.278	14.469	113.000	49.602	3.787
LVL	152.956	12.017	153.083	12.320	0	157.642	16.089	134.655	20.841	1.485

5th percentile strength [kN]

	Normal	Lognorm.	2P-Weib.	3P-Weib.
LSL				(180.00)
DG Fir	141.98	144.75	138.24	138.24
PSL	135.75	137.98	132.98	135.64
LVL	133.19	133.81	131.07	137.48

Characteristic value of maximum tensile capacity [kN]

	Normal	Lognorm.	2P-Weib.	3P-Weib.
LSL				(144.00)
DG Fir	113.58	115.80	110.59	110.59
PSL	108.60	110.39	106.38	108.51
LVL	106.55	107.05	104.85	109.98

Table 15: *RELAN data fitting of strength data set*

RELAN Data Fitting (Error of Distribution Fit)

10/40	Normal	Lognorm.	2P-Weib.	3P-Weib.
LSL	0.5306	0.2042	0.3935	0.1346
DG Fir	0.3923	0.0656	0.2408	0.0547
PSL	1.8531	1.1627	1.5708	0.6728
LVL	2.1072	0.6898	1.0657	0.4833

Parameters of Fitted Distribution

10/40	Normal		Lognorm.		2P-Weib.			3P-Weib.		
	mean	std. dev.	mean	std. dev.	loc	m	k	loc	m	k
LSL	152,205	59,325	166,861	91,702	0	179,855	2.3629	68,005	103,262	1.0557
DG Fir	109,185	44,933	121,628	74,088	0	129,734	2.2292	39,332	86,376	1.1431
PSL	149,511	65,389	211,144	197,957	0	192,074	1.8238	73,562	93,711	0.3895
LVL	121,317	58,466	182,918	193,393	0	182,318	1.2918	34,438	138,028	0.8366

5th percentile stiffness [N/mm]

10/40	Normal	Lognorm.	2P-Weib.	3P-Weib.
LSL	54,615	62,809	51,169	74,200
DG Fir	35,270	41,227	34,229	45,758
PSL	41,946	41,710	37,687	73,608
LVL	25,140	30,231	18,292	38,402

Characteristic value of maximum stiffness (10/40)

10/40	Normal	Lognormal	2P-Weibull	3P-Weibull
LSL	43,692	50,248	40,935	59,360
DG Fir	28,216	32,981	27,383	36,606
PSL	33,557	33,368	30,149	58,886
LVL	20,112	24,185	14,634	30,721

RELAN Data Fitting (Error of Distribution Fit)

30/70	Normal	Lognorm.	2P-Weib.	3P-Weib.
LSL	0.1106	0.0791	0.1229	0.0666
DG Fir	0.2077	0.0050	0.1789	0.0228
PSL	0.2076	0.1145	0.2321	0.0493
LVL	0.1732	0.0267	0.1251	0.0255

Parameters of Fitted Distribution

30/70	Normal		Lognorm.		2P-Weib.			3P-Weib.		
	mean	std. dev.	mean	std. dev.	loc	m	k	loc	m	k
LSL	133,047	33,671	134,782	37,716	0	145,792	4.4479	74,887	67,382	1.6409
DG Fir	163,499	55,744	171,960	75,428	0	185,950	2.9882	79,608	99,783	1.2004
PSL	148,250	38,677	152,587	48,879	0	162,911	4.2402	99,326	55,783	0.9514
LVL	134,873	49,839	142,501	68,877	0	154,646	2.7265	52,263	98,391	1.3729

5th percentile stiffness [N/mm]

30/70	Normal	Lognorm.	2P-Weib.	3P-Weib.
LSL	77,658	82,623	74,769	85,913
DG Fir	71,800	78,982	68,820	88,012
PSL	84,626	86,900	80,860	101,784
LVL	52,888	60,378	52,027	63,571

Table 16: *RELAN data fitting of stiffness data set*

PSL, 2.0E	Design strength (factored resistance)	No group reduction factor ("Kg" = 1)	No resistance / modification factor ("PHI" = 1)	Adjustment of embedding strength	Characteristic value for tensile capacity
DIN 1052-2000	74,378	105,551	116,106	→	116,106
EC5	89,323	→	110,039	→	110,039
CSA 086.1	23,528	54,332	77,617	94,795	94,795
ASCE 16-95	69,257	73,400	112,923	→	112,923

		Metric units	Imperial units (inch, lbs, psi)
Charact. tensile strength of wood (N/mm²):	F t	15.5	2,250
MOE of wood (N/mm²):	E	13,790	2,000,000
Equivalent spec. gravity of wood (g/cm³)	p SG	0.50	0.50
Embedding length main member (mm):	L2	14.0	0.551
Embedding length side member (mm):	L1	33.0	1.299
Pin diameter (mm):	d	8.0	0.315
Spacing axial (mm):	a1	40.4	1.591
Spacing perp.(mm):	a2	25.0	0.984
End distance loaded edge (mm):	a3	80.0	3.150
Edge distance (mm)	a4	37.5	1.476

DIN 1052-2000

Factor accounting for DOL and MC:	k mod	0.8
Partial factor for steel in timber connections:	gamma m	1.1
Charact. ultim. tensile strength of steel dowel (N/mm²):	f u,k	500
Charact. yield moment of steel dowel (Nmm):	M y,k	35,669
Charact. embedding strength wood (N/mm²):	f h,0,k	37.72
Charact. embedding strength mod (N/mm²):	f h,k	32.04
Modification factor spacing / emb. strength:	k a	0.85
Factor for effective n:	n ef	4.23
Charact. Load-carrying capacity per shear plane, per fastener (N):	R k	6,047

EC5

Factor accounting for DOL and MC:	k mod	0.8
Partial factor for wood and wood composites:	gamma m,w	1.3
Partial factor for steel in timber connections:	gamma m	1.1
Charact. ultim. tensile strength of steel dowel (N/mm²):	f u,k	500
Charact. yield moment of steel dowel (Nmm):	M y,k	34,133
Charact. embedding strength wood (N/mm²):	f h,0,k	37.72
Charact. embedding strength mod (N/mm²):	f h,k	32.04
Modification factor spacing / emb. strength:	k a	0.85
Factor for effective n:	n ef = n	6
Failure Mode I Design value of the load-carrying capacity per shear plane, per fastener (N):	R d	5,205
Failure Mode II Design value of the load-carrying capacity per shear plane, per fastener (N):	R d	3,722
Failure Mode II Lateral resistance per shear plane, per fastener (gamma m =1) (N):	R d	4,585

CSA 086.1

Resistance factor:	PHI	0.7	
Embedding strength wood (N/mm²):	f 1	29.0	
Specific gravity / mean oven-dry density (g/cm³):	G	0.5	
Embedding strength steel main member (~ infinite) (N/mm²):	f 2	10000	
Bolt yield strength (N/mm²):	f y	320	
Number of shear planes:	n s	2	
Number of fasteners:	n F	12	
Factor for 2 to 12 fasteners in a row:	J G	0.54	
Factor for laoded end distance:	J L	1.00	
Factor for number of rows:	J R	0.80	
JG * JL * JR =	J F	0.43	
		f 1 = 28.4	*f 1 = 36.97*
Failure Mode I Lateral resistance per shear plane, per fastener (N):	p U	6,121	8,155
Failure Mode II Lateral resistance per shear plane, per fastener (N):	p U	3,234	3,950
KD = KT = KST = 1	p U = P U		
f 1 =	38.61		

ASCE 16-95

Resistance Factor Connection:	PHI z	0.65	
Time effect factor:	lamda	0.80	
Dowel bending yield strength (psi):	F yb	60,000	
L m (in):	L 2	0.55	
L s (in):	L 1	1.30	
Embedding strength steel main member (~ infinite) (psi):	F em	1,450,000	
Embedding strength wood side member (psi):	F es	5,600	
L m / L s =	R t	0.42	
F em / F es =	R e	258.93	
		Imperial units	*Metric units (N)*
Failure mode I: Nominal lateral design value for a single fastener (lbs):	Z I	3,804	16,921
Failure mode II: Nominal lateral design value for a single fastener (lbs):	Z II	2,644	11,763
Factor failure mode II:	k 3	0.56	
MC factor:	C m	1	
Temperature factor:	C t	1	
Group action factor:	C g	0.944	
MOE steel (psi):	E m	30,458,000	
MOE wood (psi):	E s	2,000,000	
R EA	R EA	0.155	
X-section main member (in²):	A m	2.170	
X-section side members (in²):	A s	5.115	
spacing (in):	s	1.590	
Slip modulus in dowel-type wood-to-steel connections:	gamma	47,725	
	u	1.004	
	m	0.912	
Number of fasteners in a row:	n	6	
Number of fast. rows:	n r	2	
Tot. number of fast.:	n F	12	

Table 17: *Calculation of characteristic strength values; PSL*

Douglas Fir, No 1 & better	Design strength (factored resistance)	No group reduction factor ("Kg" = 1)	No resistance / modification factor ("PHI" = 1)	Adjustment of embedding strength	Charactersitic value for tensile capacity
DIN 1052-2000	73,630	104,490	114,939	→	114,939
EC5	88,137	→	108,513	→	108,513
CSA 086.1	23,203	53,582	76,546	91,941	91,941
ASCE 16-95	67,042	72,409	111,398	→	111,398

		Metric units	Imperial units (inch, lbs, psi)
Charact. tensile strength of wood (N/mm²):	F t	8.1	1,175
MOE of wood (N/mm²):	E	10,500	1,522,896
Density of wood (g/cm³):	p	0.49	0.49
Embedding length main member (mm):	L2	14.0	0.551
Embedding length side member (mm):	L1	33.0	1.299
Pin diameter (mm):	d	8.0	0.315
Spacing axial (mm):	a1	40.4	1.591
Spacing perp.(mm):	a2	25.0	0.984
End distance loaded edge (mm):	a3	80.0	3.150
Edge distance (mm)	a4	37.5	1.476

DIN 1052-2000

Factor accounting for DOL and MC:	k mod	0.8
Partial factor for steel in timber connections:	gamma m	1.1
Charact. ultim. tensile strength of steel dowel (N/mm²):	f u,k	500
Charact. yield moment of steel dowel (Nmm):	M y,k	35,669
Charact. embedding strength wood (N/mm²):	f h,0,k	36.97
Charact. embedding strength mod (N/mm²):	f h,k	31.40
Modification factor spacing / emb. strength:	k a	0.85
Factor for effective n:	n ef	4.23
Charact. Load-carrying capacity per shear plane, per fastener (N):	R k	5,986

EC5

Factor accounting for DOL and MC:	k mod	0.8
Partial factor for wood and wood composites:	gamma m,w	1.3
Partial factor for steel in timber connections:	gamma m	1.1
Charact. ultim. tensile strength of steel dowel (N/mm²):	f u,k	500
Charact. yield moment of steel dowel (Nmm):	M y,k	34,133
Charact. embedding strength wood (N/mm²):	f h,0,k	36.97
Charact. embedding strength mod (N/mm²):	f h,k	31.40
Modification factor spacing / emb. strength:	k a	0.85
Factor for effective n:	n ef = n	6
Failure Mode I Design value of the load-carrying capacity per shear plane, per fastener (N):	R d	5,101
Failure Mode II Design value of the load-carrying capacity per shear plane, per fastener (N):	R d	3,672
Failure Mode II Lateral resistance per shear plane, per fastener (gamma m =1) (N):	R d	4,521

CSA 086.1

Resistance factor:	PHI	0.7	
Embedding strength wood (N/mm²):	f 1	28.4	
Specific gravity / mean oven-dry density (g/cm³):	G	0.49	
Embedding strength steel main member (~ infinite) (N/mm²):	f 2	10000	
Bolt yield strength (N/mm²):	f y	320	
Number of shear planes:	n s	2	
Number of fasteners:	n F	12	
Factor for 2 to 12 fasteners in a row:	J G	0.54	
Factor for laoded end distance:	J L	1.00	
Factor for number of rows:	J R	0.80	
JG * JL * JR =	J F	0.43	
		f 1 = 28.4	f 1 = 36.97
Failure Mode I Lateral resistance per shear plane, per fastener (N):	p U	5,998	7,808
Failure Mode II Lateral resistance per shear plane, per fastener (N):	p U	3,189	3,831
KD = KT = KST = 1	p U = P U		
f 1 =	36.97		

ASCE 16-95

Resistance Factor Connection:	PHI z	0.65	
Time effect factor:	lamda	0.80	
Dowel bending yield strength (psi):	F yb	60,000	
L m (in):	L 2	0.55	
L s (in):	L 1	1.30	
Embedding strength steel main member (~ infinite) (psi):	F em	1,450,000	
Embedding strength wood side member (psi):	F es	5,500	
L m / L s =	R t	0.42	
F em / F es =	R e	263.64	
		Imperial units	Metric units (N)
Failure mode I: Nominal lateral design value for a single fastener (lbs):	Z I	3,736	16,619
Failure mode II: Nominal lateral design value for a single fastener (lbs):	Z II	2,609	11,604
Factor failure mode II:	k 3	0.56	
MC factor:	C m	1	
Temperature factor:	C t	1	
Group action factor:	C g	0.926	
MOE steel (psi):	E m	30,458,000	
MOE wood (psi):	E s	1,522,896	
R EA	R EA	0.118	
X-section main member (in²):	A m	2.170	
X-section side members (in²):	A s	5.115	
spacing (in):	s	1.590	
Slip modulus in dowel-type wood-to-steel connections:	gamma	47,725	
	u	1.005	
	m	0.901	
Number of fasteners in a row:	n	6	
Number of fast. rows:	n r	2	
Tot. number of fast.:	n F	12	

Table 18: *Calculation of characteristic strength values; Douglas Fir*

LVL, 1.9E	Design strength (factored resistance)	No group reduction factor ("Kg" = 1)	No resistance / modification factor ("PHI" = 1)	Adjustment of embedding strength	Charactersitic value for tensile capacity
DIN 1052-2000	74,378	105,551	116,106	→	116,106
EC5	89,323	→	110,039	→	110,039
CSA 086.1	23,528	54,332	77,617	94,795	94,795
ASCE 16-95	69,034	73,400	112,923	→	112,923

		Metric units	Imperial units (inch, lbs, psi)
Charact. tensile strength of wood (N/mm²):	F t	12.4	1,805
MOE of wood (N/mm²):	E	13,100	1,900,000
Equivalent spec. gravity of wood (g/cm³)	p SG	0.50	0.50
Embedding length main member (mm):	L2	14.0	0.551
Embedding length side member (mm):	L1	33.0	1.299
Pin diameter (mm):	d	8.0	0.315
Spacing axial (mm):	a1	40.4	1.591
Spacing perp.(mm):	a2	25.0	0.984
End distance loaded edge (mm):	a3	80.0	3.150
Edge distance (mm)	a4	37.5	1.476

DIN 1052-2000

Factor accounting for DOL and MC:	k mod	0.8
Partial factor for steel in timber connections:	gamma m	1.1
Charact. ultim. tensile strength of steel dowel (N/mm²):	f u,k	500
Charact. yield moment of steel dowel (Nmm):	M y,k	35,669
Charact. embedding strength wood (N/mm²):	f h,0,k	37.72
Charact. embedding strength mod (N/mm²):	f h,k	32.04
Modification factor spacing / emb. strength:	k a	0.85
Factor for effective n:	n ef	4.23
Charact. Load-carrying capacity per shear plane, per fastener (N):	R k	6,047

EC5

Factor accounting for DOL and MC:	k mod	0.8
Partial factor for wood and wood composites:	gamma m,w	1.3
Partial factor for steel in timber connections:	gamma m	1.1
Charact. ultim. tensile strength of steel dowel (N/mm²):	f u,k	500
Charact. yield moment of steel dowel (Nmm):	M y,k	34,133
Charact. embedding strength wood (N/mm²):	f h,0,k	37.72
Charact. embedding strength mod (N/mm²):	f h,k	32.04
Modification factor spacing / emb. strength:	k a	0.85
Factor for effective n:	n ef = n	6
Failure Mode I Design value of the load-carrying capacity per shear plane, per fastener (N):	R d	5,205
Failure Mode II Design value of the load-carrying capacity per shear plane, per fastener (N):	R d	3,722
Failure Mode II Lateral resistance per shear plane, per fastener (gamma m =1) (N):	R d	4,585

CSA 086.1

Resistance factor:	PHI	0.7	
-			
Embedding strength wood (N/mm²):	f 1	29.0	
Specific gravity / mean oven-dry density (g/cm³):	G	0.5	
Embedding strength steel main member (~ infinite) (N/mm²):	f 2	10000	
Bolt yield strength (N/mm²):	f y	320	
Number of shear planes:	n s	2	
Number of fasteners:	n F	12	
Factor for 2 to 12 fasteners in a row:	J G	0.54	
Factor for loaded end distance:	J L	1.00	
Factor for number of rows:	J R	0.80	
JG * JL * JR =	J F	0.43	
		f 1 = 28.4	*f 1 = 36.97*
Failure Mode I Lateral resistance per shear plane, per fastener (N):	p U	6,121	8,155
Failure Mode II Lateral resistance per shear plane, per fastener (N):	p U	3,234	3,950
KD = KT = KST = 1	p U = P U		
f 1 =	38.61		

ASCE 16-95

Resistance Factor Connection:	PHI z	0.65	
Time effect factor:	lamda	0.80	
Dowel bending yield strength (psi):	F yb	60,000	
L m (in):	L 2	0.55	
L s (in):	L 1	1.30	
Embedding strength steel main member (~ infinite) (psi):	F em	1,450,000	
Embedding strength wood side member (psi):	F es	5,600	
L m / L s =	R t	0.42	
F em / F es =	R e	258.93	
		Imperial units	*Metric units (N)*
Failure mode I: Nominal lateral design value for a single fastener (lbs):	Z I	3,804	16,921
Failure mode II: Nominal lateral design value for a single fastener (lbs):	Z II	2,644	11,763
Factor failure mode II:	k 3	0.56	
MC factor:	C m	1	
Temperature factor:	C t	1	
Group action factor:	C g	0.941	
MOE steel (psi):	E m	30,458,000	
MOE wood (psi):	E s	1,900,000	
R EA	R EA	0.147	
X-section main member (in²):	A m	2.170	
X-section side members (in²):	A s	5.115	
spacing (in):	s	1.590	
Slip modulus in dowel-type wood-to-steel connections:	gamma	47,725	
	u	1.004	
	m	0.910	
Number of fasteners in a row:	n	6	
Number of fast. rows:	n r	2	
Tot. number of fast.:	n F	12	

Table 19: *Calculation of characteristic strength values; LVL*

LSL, 1.5E	Ratio I / V	Design strength (factored resistance)	No group reduction factor ("Kg" = 1)	No resistance / modification factor ("PHI" = 1)	Adjustment of embedding strength	Charactersitic value for tensile capacity
	I / V	I	II	III	IV	V
DIN 1052-2000	64%	80,108	113,682	125,050	→	125,050
EC5	81%	98,755	→	122,193	→	122,193
CSA 086.1	25%	26,076	60,215	86,022	105,373	105,373
ASCE 16-95	60%	76,108	82,299	126,613	→	126,613

		Metric units	Imperial units (inch, lbs, psi)
Charact. tensile strength of wood (N/mm²):	F t	13.4	1,950
MOE of wood (N/mm²):	E	10,342	1,500,000
Equivalent spec. gravity of wood (g/cm³)	p SG	0.58	0.58
Embedding length main member (mm):	L2	14.0	0.551
Embedding length side member (mm):	L1	33.0	1.299
Pin diameter (mm):	d	8.0	0.315
Spacing axial (mm):	a1	40.4	1.591
Spacing perp.(mm):	a2	25.0	0.984
End distance loaded edge (mm):	a3	80.0	3.150
Edge distance (mm)	a4	37.5	1.476

DIN 1052-2000

Factor accounting for DOL and MC:	k mod	0.8
Partial factor for steel in timber connections:	gamma m	1.1
Charact. ultim. tensile strength of steel dowel (N/mm²):	f u,k	500
Charact. yield moment of steel dowel (Nmm):	M y,k	35,669
Charact. embedding strength wood (N/mm²):	f h,0,k	43.76
Charact. embedding strength mod (N/mm²):	f h,k	37.16
Modification factor spacing / emb. strength:	k a	0.85
Factor for effective n:	n ef	4.23
Charact. Load-carrying capacity per shear plane, per fastener (N):	R k	6,513

EC5

Factor accounting for DOL and MC:	k mod	0.8
Partial factor for wood and wood composites:	gamma m,v	1.3
Partial factor for steel in timber connections:	gamma m	1.1
Charact. ultim. tensile strength of steel dowel (N/mm²):	f u,k	500
Charact. yield moment of steel dowel (Nmm):	M y,k	34,133
Charact. embedding strength wood (N/mm²):	f h,0,k	43.76
Charact. embedding strength mod (N/mm²):	f h,k	37.16
Modification factor spacing / emb. strength:	k a	0.85
Factor for effective n:	n ef = n	6
Failure Mode I Design value of the load-carrying capacity per shear plane, per fastener (N):	R d	6,038
Failure Mode II Design value of the load-carrying capacity per shear plane, per fastener (N):	R d	4,115
Failure Mode II Lateral resistance per shear plane, per fastener (gamma m =1) (N):	R d	5,091

CSA 086.1

Resistance factor:	PHI	0.7	
Embedding strength wood (N/mm²):	f 1	33.6	
Specific gravity / mean oven-dry density (g/cm³):	G	0.58	
Embedding strength steel main member (~ infinite) (N/mm²):	f 2	10000	
Bolt yield strength (N/mm²):	f y	320	
Number of shear planes:	n s	2	
Number of fasteners:	n F	12	
Factor for 2 to 12 fasteners in a row:	J G	0.54	
Factor for laoded end distance:	J L	1.00	
Factor for number of rows:	J R	0.80	
JG * JL * JR =	J F	0.43	
		f 1 = 28.4	*f 1 = 36.97*
Failure Mode I Lateral resistance per shear plane, per fastener (N):	p U	7,100	9,465
Failure Mode II Lateral resistance per shear plane, per fastener (N):	p U	3,584	4,391
KD = KT = KST = 1	p U = P U		
f 1 =	44.82		

ASCE 16-95

Resistance Factor Connection:	PHI z	0.65	
Time effect factor:	lamda	0.80	
Dowel bending yield strength (psi):	F yb	60,000	
L m (in):	L 2	0.55	
L s (in):	L 1	1.30	
Embedding strength steel main member (~ infinite) (psi):	F em	1,450,000	
Embedding strength wood side member (psi):	F es	6,500	
L m / L s =	R t	0.42	
F em / F es =	R e	223.08	
		Imperial units	*Metric units (N)*
Failure mode I: Nominal lateral design value for a single fastener (lbs):	Z I	4,415	19,640
Failure mode II: Nominal lateral design value for a single fastener (lbs):	Z II	2,965	13,189
Factor failure mode II:	k 3	0.54	
MC factor:	C m	1	
Temperature factor:	C t	1	
Group action factor:	C g	0.925	
MOE steel (psi):	E m	30,458,000	
MOE wood (psi):	E s	1,500,000	
R EA	R EA	0.116	
X-section main member (in²):	A m	2.170	
X-section side members (in²):	A s	5.115	
spacing (in):	s	1.590	
Slip modulus in dowel-type wood-to-steel connections:	gamma	47,725	
	u	1.006	
	m	0.900	
Number of fasteners in a row:	n	6	
Number of fast. rows:	n r	2	
Tot. number of fast.:	n F	12	

Table 20: *Calculation of characteristic strength values; LSL*